Grumman Tribody Concept featured on the 1978 company calendar. The basis for this idea will be explained below.

10. Supersonic Aerodynamics

10.1 Introduction

There have actually only been a few truly supersonic airplanes. This means airplanes that can *cruise* supersonically. Before the F-22, classic "supersonic" fighters used brute force (afterburners) and had extremely limited duration. As an example, consider the two defined supersonic missions for the F-14A:

F-14A Supersonic Missions

CAP (Combat Air Patrol)

- 150 miles subsonic cruise to station
- Loiter
- Accel, M = 0.7 to 1.35, then dash 25 nm
  - 4 1/2 minutes and 50 nm total
- Then, must head home, or to a tanker!

DLI (Deck Launch Intercept)

- Energy climb to 35K ft, M = 1.5 (4 minutes)
- 6 minutes at M = 1.5 (out 125-130 nm)
- 2 minutes Combat (slows down fast)

After 12 minutes, must head home or to a tanker.

In this chapter we will explain the key supersonic aerodynamics issues facing the configuration aerodynamicist. We will start by reviewing the most significant airplanes that had substantial sustained supersonic capability. We will then examine the key physical underpinnings of supersonic gas dynamics and their implications for configuration design. Examples are presented showing applications of modern CFD and the application of MDO. We will see that developing a practical supersonic airplane is extremely demanding and requires careful integration of the various contributing technologies. Finally we discuss contemporary efforts to develop new supersonic airplanes.

10.2 Supersonic "Cruise" Airplanes

The supersonic capability described above is typical of most of the so-called supersonic fighters, and obviously the supersonic performance is limited. The following list represents my selection

of the previous manned supersonic aircraft. It is a very short list. It is important for aerodynamic designers to be familiar with these airplanes. The *L/D*s given below are for supersonic flight.

- •1956: the B-58 (L/D_{max} = 4.5) Convair, 1st flight Nov. 1956,
  - –In 1962: Mach 2 for 30 minutes
- •1962: the A-12 (SR-71 in '64) (L/D_{max} = 6.6), Lockheed, 1st flight April 1962 (A-12), the 1st SR-71 flight was in Dec. 1964
  - –1st supersonic flight, May 4, 1962
  - –1st flight to exceed Mach 3, July 20, 1963
- •1964: the XB-70 (L/D_{max} = 7.2) North American Aviation, 1st flight Sept. 1964
  - – 1st Mach 3 flight Oct. 1965, In 1966: flew Mach 3 for 33 minutes
- •1968: the TU-144, Tupolev
  - –1st flight: Dec. 31, 1968
- •1969: the Concorde (L/D_{max} = 7.4) Aérospatiale/BAC design
  - –1st flight, March 2, 1969, 1st Mach 2 flt., Nov. 4, 1970)*
- •1990: the YF-22 and YF-23 (supercruisers)
  - –YF-23: Northrop led team, 1st flt. Aug. 27, 1990
  - –YF-22: Lockheed led team, 1st flt. Sept. 29, 1990, F-22 1st flt. Sept. 7, 1997

Note the low *L/D* values associated with supersonic flight. Nevertheless, these airplanes were all remarkable.

10.2.1 The B-58

The B-58 is shown in Figure 10-1. It is a strikingly attractive design. It followed the Convair approach of using a conically cambered delta wing in the tradition of the F-102 (1st flight 1953) and F-106 (1st flight 1956) airplanes from the same company.

Today B-58s can be seen at numerous museums, notably the Museum of the Air Force in Dayton, Ohio, and the Pima Air & Space Museum outside of Tucson, Arizona.

The B-58 had a three-man crew and weighed around 160,000 pounds, of which over 100,000 pounds was fuel! The structural weight fraction was an amazingly low 14%. To achieve the required aerodynamic performance the wings were thin, 4.08% at the tip and 3.46% at the root. In 1962 the B-58 flew 1300 mph for 30 minutes and 43 seconds, thus being the first airplane to fly over 2000 km/hr for 30 minutes, and was able to claim the Bleriot prize. It also set a record flying from Los Angeles to New York in 2 hours and 57 seconds (for comparison the SR-71 later made the trip in 68 minutes). The required static margin for longitudinal stability was 3%, but greater than 3% was required for directional stability to handle the engine out case. An ARI (Aileron-Rudder Interconnect) was used to cancel the yawing moment due to aileron deflection. The plane was powered by four pylon mounted GE J-79 engines, making it an extremely loud airplane.

One of the curious features was the use of a "double bubble" attached pod below the fuselage. The outer pod carried fuel and was jettisoned when empty. The inner pod was in fact the nuclear bomb.

* The last flights of the Concordes occurred on October 24, 2003.

The best paper to read on the B-58 is by Erickson.[1] The airplane had a poor safety record. In part this was because the tires were very small to allow the gear to fit in the fuselage. The takeoff and landing speeds were high, and the tires sometimes blew up. It was also very difficult to maintain.

Figure 10-1. The B-58 in flight.

10.2.2 The SR-71 Family

This is probably the most amazing design achievement ever made in aeronautics. Figure 10-2 shows this familiar airplane. The SR-71's predecessor, the A-12, first flew in 1962, while the SR-71's first flight occurred in 1964. It served for many years after having been developed in complete secrecy. The definitive paper on the aerodynamics of the SR-71 (on "the edge" between supersonic and hypersonic flight) was written by Ben Rich,[2] who later went on to be a key member of the team that developed the F-117 stealth "fighter". It is impossible to provide a better description of the plane than the one given by Rich. Aerodynamic heating was also an important consideration on the design. It was powered by two Pratt J-58 turboramjet engines.

The SR-71 had a crew of two. Its wing area was 1800 sq ft, the span was 55 ft 7 in, and the MTOGW was 172,000 lb. Its last military flight was in 1990. NASA operated SR-71 sporadically until 1999.

Another good description is available in the AIAA book by Peter Merlin.[3] That book comes with a DVD that has a wealth of information including flight manuals, photos and videos.

Figure 10-2. The SR-71.

10.2.3 The XB-70

The XB-70[4] is shown in Figures 10-3 and 10-4. The airplane was intended to be a Mach 3 intercontinental bomber. However, the successful development of ICBMs meant there was no longer a need for the plane, instead it became a research airplane. Two were built. It was a large airplane with a wing area of 6297 sq ft, a span of 105 ft, and a MTOGW of 542,000 lb. In May 1966 the XB-70 flew at Mach 3 for 33 minutes. It had six GE YJ93 engines.

It only reached Mach 3 a few times. This was in part because the second airplane was destroyed in a mid-air collision with an F-104 in June of 1966 during a publicity photo flight for General Electric. Joe Walker, the pilot of the F-104, was killed (XB-70 pilot Carl Cross also died, Al White survived) To increase directional stability and minimize the aerodynamic center shift the XB-70 deflected its wingtips down in supersonic flight. This is shown in Fig. 10-4. Only the second airplane had the full wingtip deflection capability.

Although it was also said to have increased aerodynamic efficiency through the use of "compression lift" on the lower surface, this could have been achieved by mild wing camber. Note that the canard is essentially a foreplane, acting as a trimmer. It also had a very high base drag associated with the propulsion installation in the transonic flight regime.

The remaining XB-70 is on display at the National Museum of the Air Force in Dayton, Ohio. It was flown to Dayton in February 1969.

Figure 10-3. The XB-70 on takeoff. Note the large delta wing. The canard is essentially a trimmer.

Figure 10-4. This figure shows the XB-70 flying with its wing tips deflected down.

10.2.4 The TU-144

The Tupolev TU-144 was a Soviet Union contemporary of the Concorde. It flew before the Concorde, on December 31, 1968. Fifteen were built. It was similar in configuration to the Concorde with the notable exception that it had a retractable "mustache" canard (as well as the drooping nose used by the Concorde). It also had a braking parachute, very unusual for a commercial airplane. The program suffered when a TU-144 crashed during a demonstration flight at the Paris Airshow in June 1973. Although it made a number of operational flights, it wasn't practical and the program ended. It was resurrected during the US HSCT program in the 1990s when it was used by NASA as a testbed for supersonic flight research. The TU-144 is cited as having a wing area of 5450 sq ft, a span of 94.4 ft, and a max TOGW of 455,950 lb.

10.2.5 The Concorde

The development of the Concorde, together with a discussion of the Russian SST effort and the aborted attempt by the US, is described in a wonderful paper by Poisson-Quinton[5] (that paper includes data showing how the TU-144 used the "mustache" canard). The AIAA published a case study on the Concorde[6] that provided a description of its aerodynamic design. Figure 10-5 is a photo from the Smithsonian web site that shows the Concorde planform. The Concorde has a wing area of 3856 sq ft, a span of 84 ft, and a max TOGW of 412,000 lb. The aerodynamic design of the wing is described in a paper by Wilde and Cormery.[7] To allow the slender wing configuration to land and takeoff at an acceptable angle of attack the Concorde took advantage of vortex lift as well as ground effects. During the years that the Concorde was in service I saw it frequently, both flying over Long Island on its was to Kennedy Airport, taxiing around Kennedy and also at London Heathrow. Compared to the other planes it was small, and the wing was extremely thin. One of the most notable aspects of its flight was how loud it was. If it had flown over my house more than once a day it would have been very annoying, even to me (and I lived about 35 miles from the airport).

Figure 10-5 The Concorde (from the Smithsonian website)

10.2.6 The F-22 (YF-23)

During the late 1970s and the 1980s the US Air Force studied the requirements for a new fighter. A key requirement was found to be "supercruise" wherein the airplane could fly supersonically without the use of the afterburner. This decreases fuel burn and allowed for significantly longer supersonic range than previous fighter aircraft. Stealth was also important, but not publicly discussed. The fighter requirement became official as the ATF (Advanced Tactical Fighter) in 1981. In 1986 teams led by Northrop (YF-23) and Lockheed (YF-22) won awards to build demonstrators. In 1991, after the flight demonstrations were completed, Lockheed was awarded the contract for the F-22. This process is described in detail in the AIAA book by Aronstein, Hirschberg and Piccirillo.[8] A description the F-22 aircraft was given in the 1992 Wright Brothers Lecture by Sherman Mullin.[9] A photo of the F-22 is shown in Figure10-6.

Figure 10-6. The Lockheed F-22 (from the web)

10.3 The Challenge for Airplane Design

From this small number of actual supersonic cruising airplanes, we see that supersonic flight is a challenge. We can get some insight from the range equation:

$$R = \frac{V\left(\frac{L}{D}\right)}{sfc} \ln\left(\frac{W_{initial}}{W_{final}}\right) \qquad (10\text{-}1)$$

Here we have to counterbalance the reduction in *L/D* as shown above for these airplanes with an increase in *V* (recall that subsonic transport *L*/*D*s should be between 18 and 20). However, we

always incur the extra cost of supersonic wave drag. We also need to be able to fly without afterburner to keep the *sfc* low. This is difficult because modern transonic transports use high bypass ratio engines. The large engine/nacelle diameters are not possible at supersonic speeds, the drag would be unacceptable. Thus we have numerous challenges for economical supersonic flight.

The basic physics of the flowfield change between sub- and super-sonic flow. This is illustrated in the figure originally presented by von Kármán [10] in Figure 10-7.

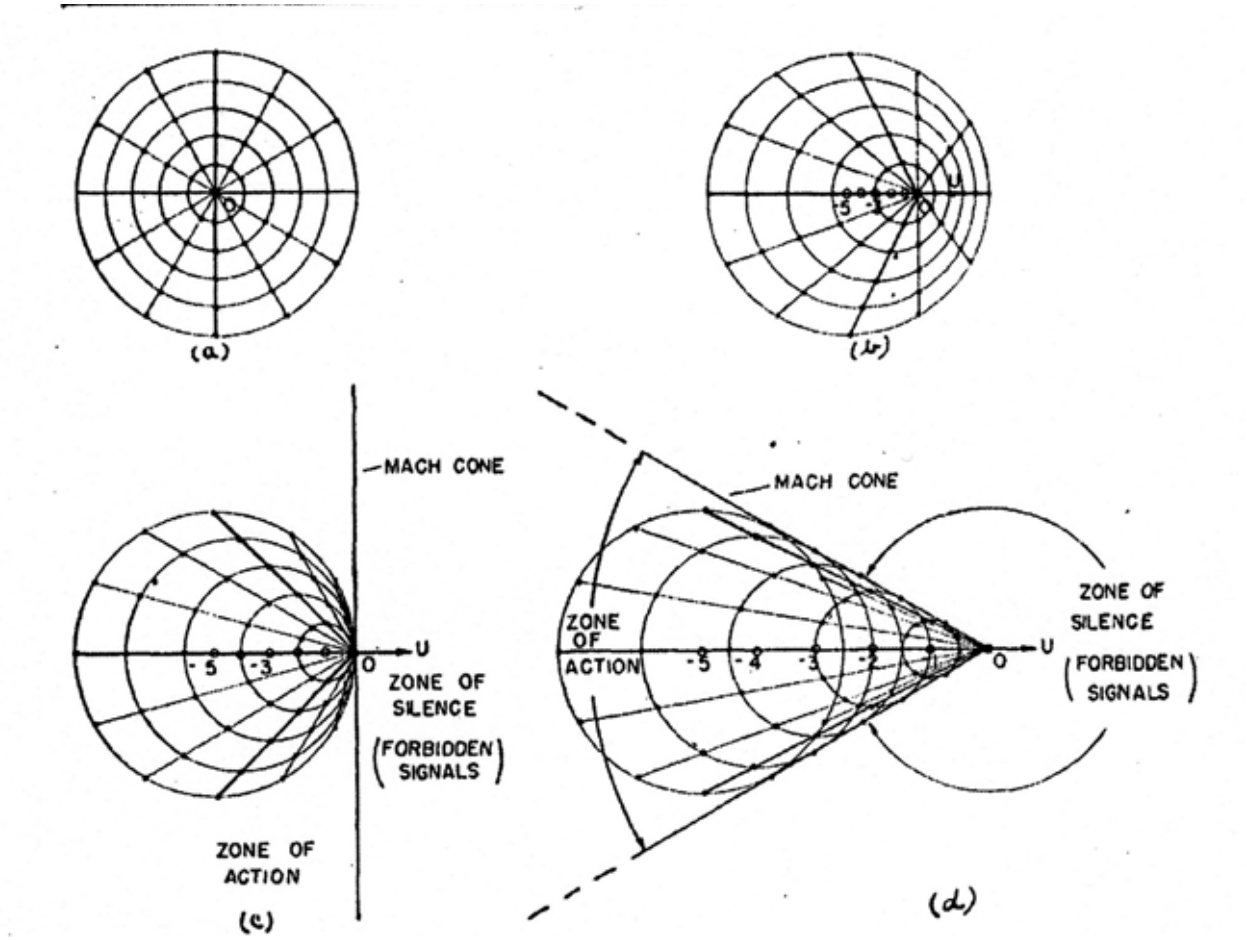

Figure 10-7. The change in flowfield physics from subsonic to supersonic speeds as explained by Kármán.[10] (a) stationary source, (b) source moving at half the speed of sound, (c) source moving at the speed of sound, (d) source moving at twice the speed of sounds.

Poisson-Quinton[5] has shown how the wave drag leads to a reduction in *L/D* at supersonic Mach numbers. This is illustrated in Figure 10-8. The chief culprit is the C_{D0} increase with Mach number due to the volumetric wave drag. Nicolai has collected the minimum drag values for a number of supersonic fighters. Figure 10-9 is from his book.[11] Clearly the wave drag is large. For modern supersonic designs the drag increase would be much less. However this figure provides insight into the challenge.

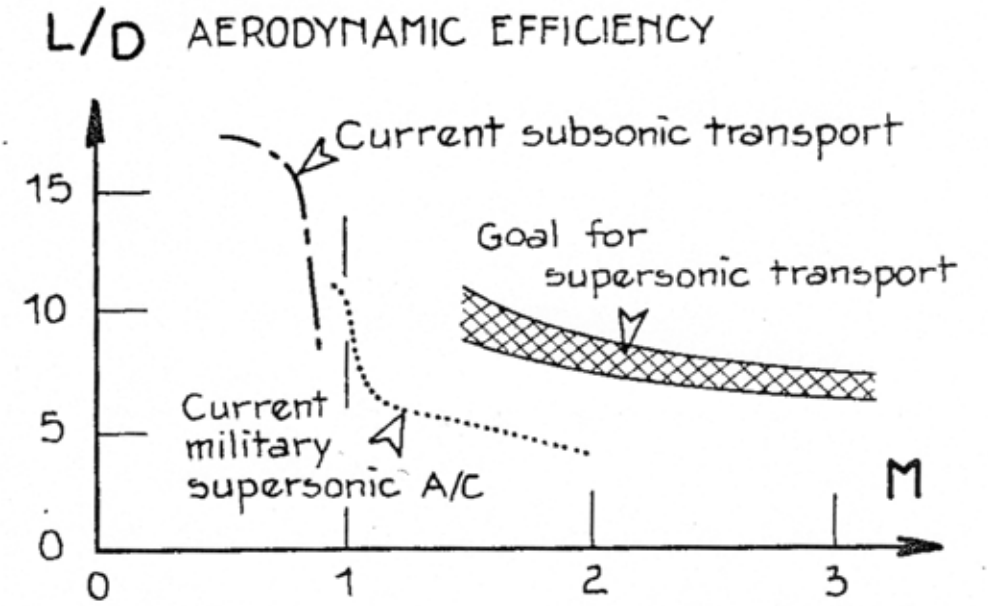

Figure 10-8. The *L/D* problem for supersonic flow.[5]

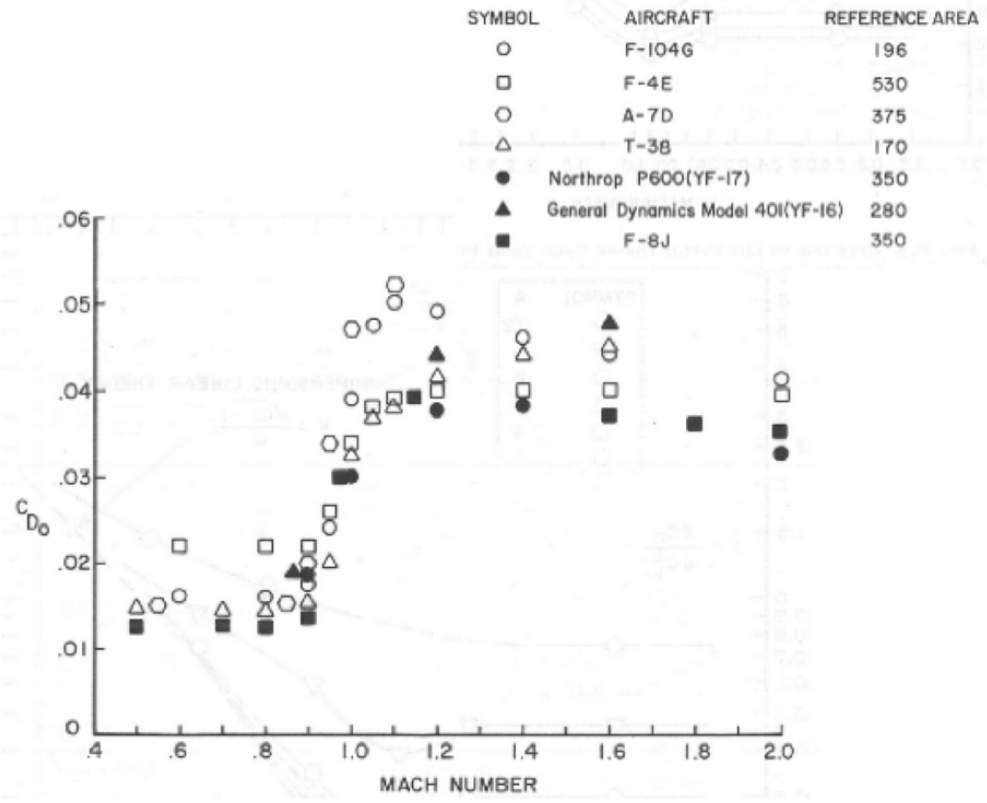

Figure 10-9. C_{D0} increase with Mach number (Nicolai[11])

A key overview of the supersonic aerodynamic design issues has been written by Baals, et al.[12] That paper provides a basis for thinking about supersonic airplane design and should be studied

for the details of the aerodynamic design thinking used in the US SST program to be described later.

In addition to the pure aerodynamic performance challenge, supersonic airplanes must address the noise problem, both around the airport (so-called community noise) and the sonic boom. This proved to be a significant issue during the studies of a possible new supersonic transport in the 1990s, the HSCT.[13] That airplane was intended to operate at Pacific-rim ranges with from 250-300 passengers. More recently, the possibility of designing small business-jet class supersonic airplanes with an acceptable level of boom noise is under study.[14,15] It is likely that these airplanes will be the next generation of supersonic airplanes, and we will discuss the boom issues below in Section 10.10.4.

Next, to understand some of the key aerodynamic ideas we will be break our discussion into two parts. First we will present an overview of zero lift drag in Section 10.4 (primarily looking at bodies of revolution), and then we will discuss drag due to lift in Section 10.5. By splitting the discussion into two parts we are implicitly using linear theory to help us understand the main contributors to supersonic aerodynamics.

Before proceeding, we note that the increase in zero lift drag means that the drag due to lift will also be higher at *L/Dmax* since to maximize *L/D* the drag due to lift should approach the zero lift drag. Thus, every effort must be made to reduce the volumetric wave drag. It is unlikely there will ever be enough thrust to cruise at L/D_{max}.

10.4 Wave Drag

The key idea to keep in mind for wave drag is the area rule. We already discussed this in Chapter 3, Drag. Basically we want a smooth area distribution. In addition, there are specific shapes that produce the minimum drag. They have been worked out analytically for axisymmetric bodies. The derivation of the wave drag integral is given in Ashley and Landahl,[16] Chapter 6, cited here because they also provide the derivation of minimum drag bodies of revolution. The integral given by Eqn. 10-2 requires that the ends be closed $S = 0$, or that $S'(l)$ is be zero. The resulting slender body wave drag formula is:

$$D_{wave} = -\frac{\rho_\infty U_\infty^2}{4\pi}\int_0^l\int_0^l S''(x_1)S''(x_2)\ln|x_1 - x_2|dx_1dx_2 \qquad (10\text{-}2)$$

where $S(x)$ is the cross-sectional area along the body. This equation is used to analyze different cross-sectional area distributions and also to find shapes with minimum drag. Since the equation is from slender body theory the Mach number does not appear (see the derivation in Ashley and Landahl, Sec. 9.3).

The integral shows that it is actually the second derivative of the area distribution that is required for the computation. Clearly we want to make $S''(x)$ small. Unless care is taken, the numerical method may result in values that are too high because of artificial noise in the interpolation procedures and the quality of the input data for the area distribution, *S*. This difficulty was substantially reduced with a rather ingenious scheme due to Evelyn Eminton in Great Britain,[17] and adopted for use in the now-standard wave drag program written by Boeing for Roy Harris at NASA Langley.[18] Eminton's approach to finding the value of the integral was to find the interpolating curve passing through the specified input points that minimized the value of the wave drag. Thus she solved an optimization problem to eliminate problems arising artificially

from the interpolation procedure. The code that makes this calculation is generally known as the Harris Wave Drag program and is available for free from Ralph Carmichael's PDAS web site.[19]

Minimum wave drag shapes subject to a variety of constraints have been found using the wave drag integral. For an open base (ignoring base pressure), the minimum wave drag is the von Kármán ogive. Given the base area and length, the minimum wave drag is:

$$D_{wave} = \frac{2\rho_\infty U_\infty^2}{\pi} \frac{[S(l)]^2}{l^2} \tag{10-3}$$

Or, if S_{ref} is the base area,

$$C_{D_{wave}} = \frac{4}{\pi} \frac{[S(l)]}{l^2} \tag{10-4}$$

See App. A, Geometry for Aerodynamicists for the equation of the shape. The radius and area distributions are shown in the Figs. 10-10 and 10-11.

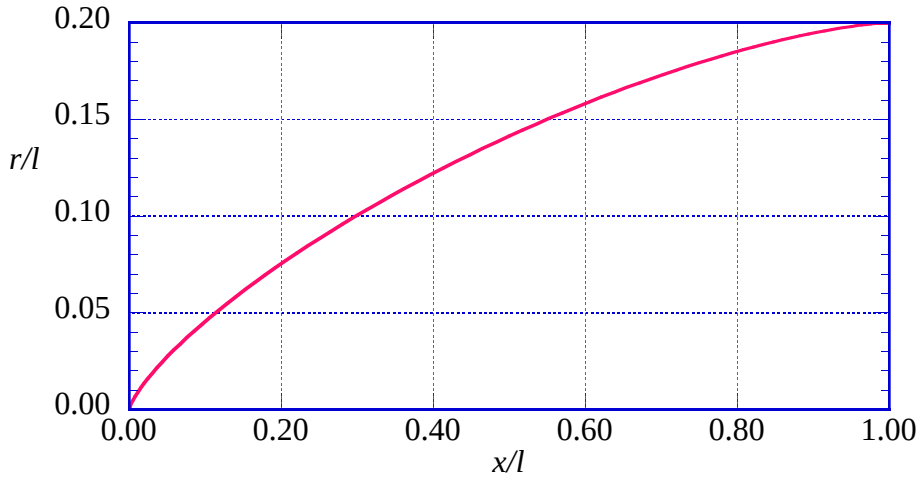

Figure 10-10. Radius distribution of a von Kármán Ogive.

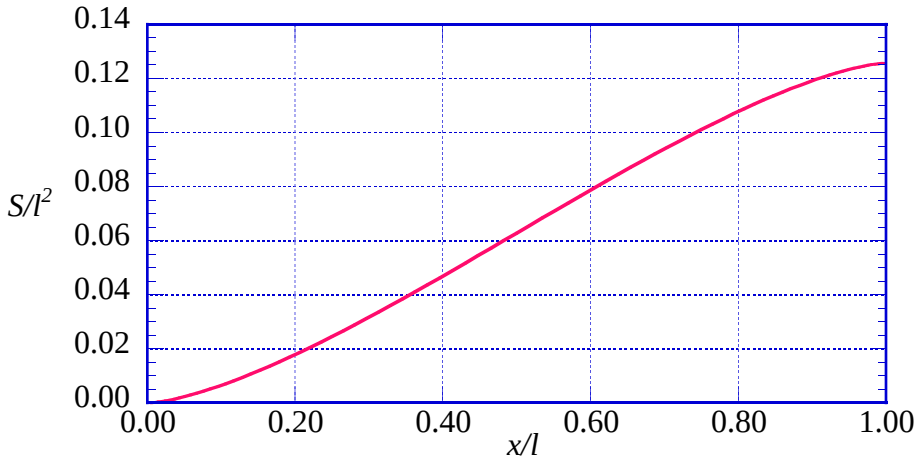

Figure 10-11. Cross-sectional area distribution of a von Kármán Ogive.

If the body is closed at both ends, then for a given length, l, and volume, V, the wave drag is:

$$D_{wave} = \frac{64V^2}{\pi l^4}\rho_\infty U_\infty^2 \tag{10-5}$$

or, based on the maximum cross-sectional area,

$$C_{D_{wave}} = \frac{24V}{l^3} \tag{10-6}$$

This is known as the Sears-Haack Body. See App. A, Geometry for Aerodynamicists for the equation of the shape. Figure 10-12 and 10-13 show the radius and cross sectional area distribution for this body.

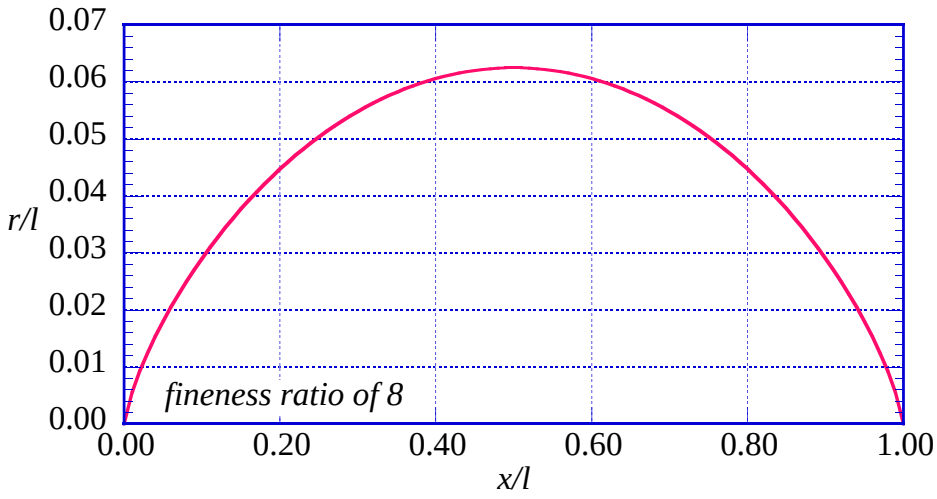

Figure 10-12 Radius distribution for the Sear-Haack body.

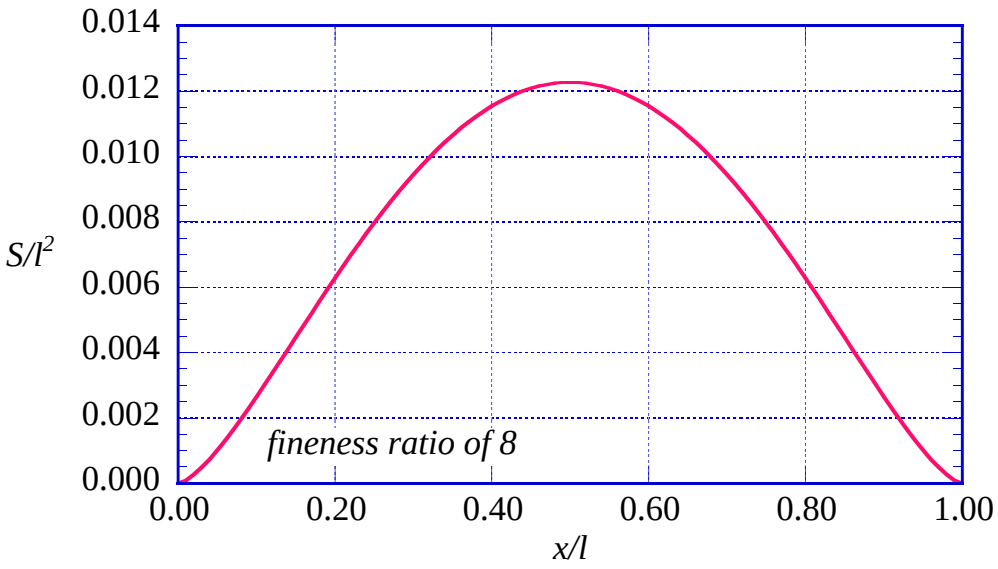

Figure 10-13 Cross-sectional area distribution for the Sear-Haack body.

Derivations of minimum wave drag axisymmetric body shapes for other constraints were given in NACA TN 2550 by M.C. Adams.[20]

Note: the Sears-Haack body is *not* the minimum wave drag body for a given max cross-sectional area, which may often be the more relevant constraint. However, using the connection between volume and maximum body radius:

$$V = \pi r_{\max}^2 \frac{3\pi l}{16}, \tag{10-7}$$

we get a form that shows the connection between the drag coefficient and fineness ratio, *l/d*:

$$C_{D_{wave}} = \frac{9\pi^2}{8} \frac{1}{(l/d_{\max})^2} \tag{10-8}$$

Figure 10-14 shows how important the use of a high fineness ratio is to reduce the wave drag. To make the drag non-dimensional we divide by the dynamic pressure and by the volume raised to the 2/3rds power. Care must always be taken when looking at drag values to make sure you understand the reference area. It is not unheard of for misleading values to be used!

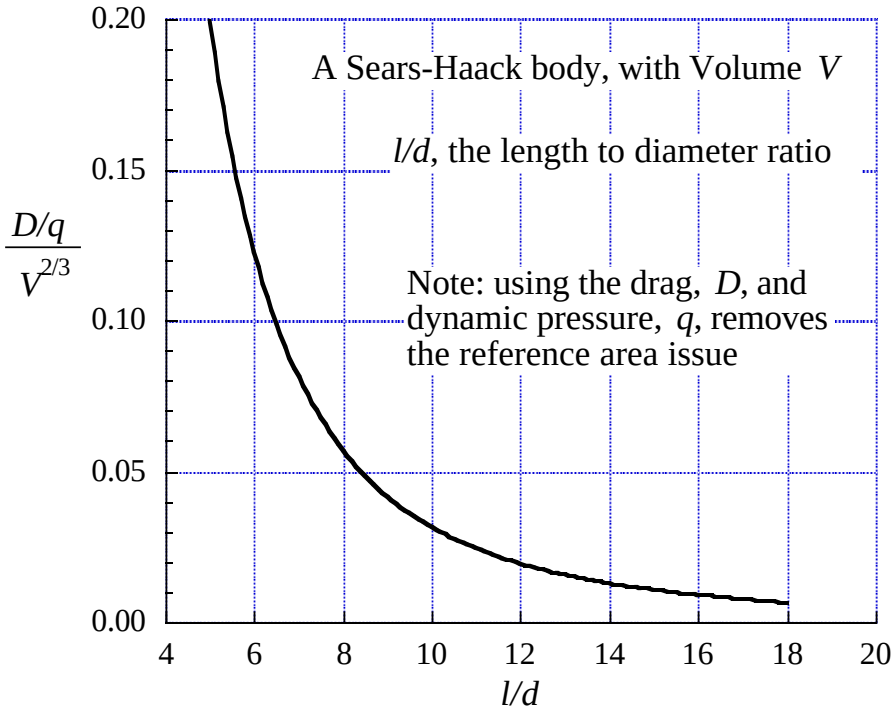

Figure 10-14. Wave drag reduction as fineness ratio increases.

It is worth investigating the minimum wave drag shapes in a little more detail. Since we've seen the key role that the fineness ratio plays in the drag, we can write the wave drag coefficient for three different cases, the Sears-Haack minimum wave drag for a given volume and length, the minimum wave drag for a specified maximum cross-sectional area, and the minimum wave drag for the Kármán ogive:

$$C_{D_{S-H}}\left(\frac{l}{d}\right)^2 = \frac{9\pi^2}{8} = 11.1 \tag{10-9}$$

$$C_{D_{S-H}}\left(\frac{l}{d}\right)^2 = \pi^2 = 9.87 \tag{10-10}$$

$$C_{D_{S-H}}\left(\frac{l}{d}\right)^2 = 1 \tag{10-11}$$

Thus the minimum wave drag body for a given max cross-sectional area is 11% less than the minimum wave drag body of a given volume with the same max cross-sectional area. This also shows that ignoring base drag (reasonable if the base is filled with a jet exhaust), the drag is much lower when the base is open. In fact, the wave drag is very nearly a linear function of the ratio of the base are to the max cross-sectional area (see Adam's Fig. 3):

$$C_{D_w}\left(\frac{l}{d}\right)^2 = \pi^2 - \left(\pi^2 - 1\right)\frac{S_B}{S_{max}} \tag{10-12}$$

The minimum drag for a body of revolution with a constant cross section placed between the front and back of a body with a "fairing" to close the shape in the front and back has been given by Heaslet and Lomax, see Section Part D section 16.[21] To be a little more complete, we note that Harder and Rennemann[22] found minimum drag shapes that have slightly less drag than Adams found. They present results for the case of given volume.

For comparison, Krasnov[23] points out that using a simple cone forebody has a drag of about twice the value of the optimum forebody value for a fineness ratio of 3. However, a tangent ogive only as a drag about 7% higher than the optimum value.

A general minimum wave drag axisymmetric shape can also be found using the analysis by Lord and Eminton.[24] This analysis has been implemented in the interactive program MinDrag.[25] It computes the minimum value of the supersonic wave drag for an axisymmetric body, and the area distribution required to attain this value for a given length, volume, nose area and base area, and with another area specified at a given location along the body. A screen shot of the program is shown in Fig. 10-15.

Often, wave drag of supersonic airplanes is given in terms of a multiple of the wave drag of a minimum drag body of revolution. Typically the Sear-Haack body is chosen because of its well-known drag expression. In the early stages of design it's worth collecting data from previous designs. One rule of thumb was to use $19/(l/d)^2$ as opposed to the Sears-Haack value of 11.1. Jobe has collected data in an AIAA book[26] based on his Air Force Report.[27] Also, example cross-sectional area distributions for the B-58 and XB-70 have been given by Tinetti, Maglieri and Bobbitt.[28]

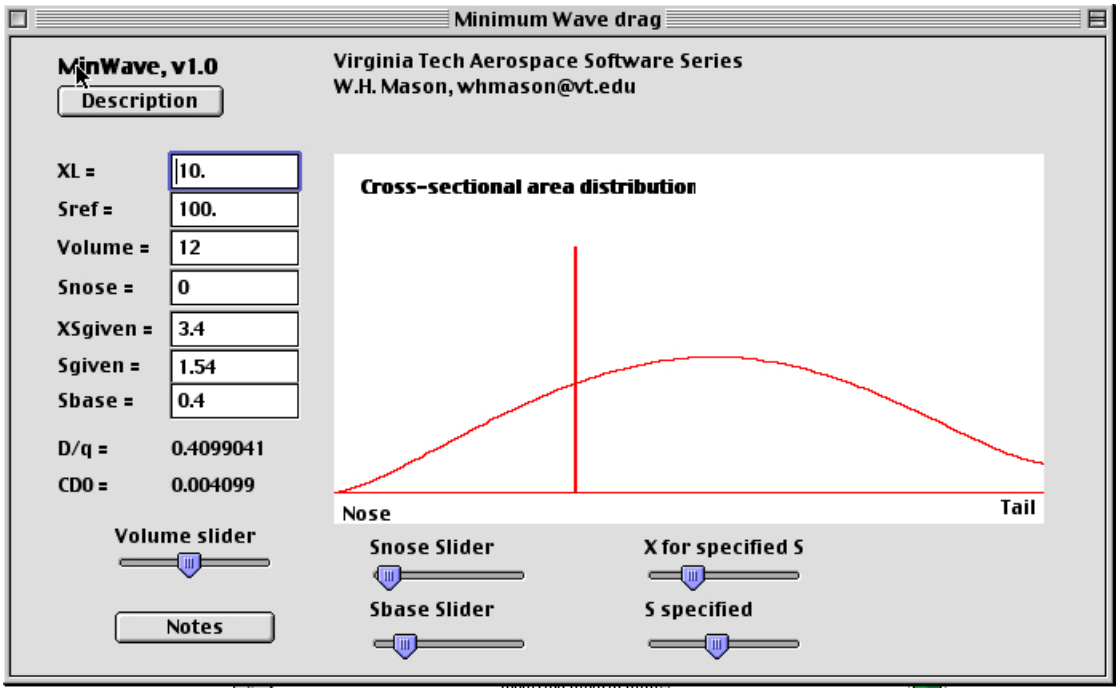

Figure 10-15. MinDrag, the minimum wave drag body shape interactive code subject to a variety of constraints available on Mason's software page.

Because the surface area can change as the fineness ratio changes it would be interesting to find the minimum of the sum of the friction and wave drag. Although I worked this out many years ago, I discovered that Bailey Oswald had already done it.[29] Figure 10-16 shows his result for two cases. The first is the minimum drag fineness ratio when the maximum cross sectional is specified, and the second case is the result when the volume is specified. For the first case the minimum fineness ratio occurs for a value slightly above 15 (this would be the usual case). When the volume is specified the minimum drag fineness ratio is a little less than 25 (this is much too high for a practical manned airplane). In both cases the minimum is fairly shallow, so you can select values significantly lower than the minimum without incurring a large penalty.

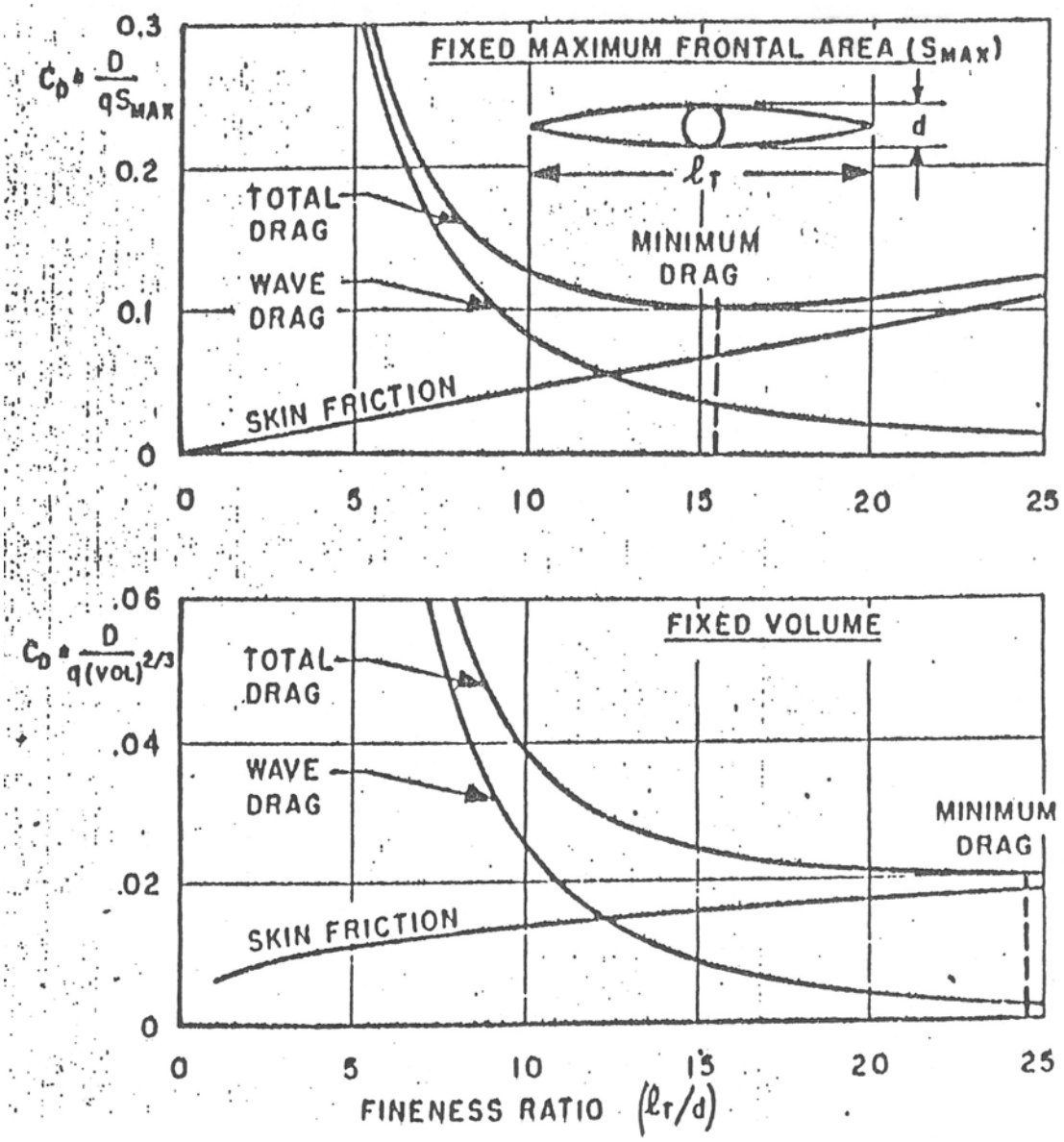

Figure 10-16. Minimum drag including both wave and friction drag.[29]

Once we get past saying "smooth area", the next step is to make the area distribution for the entire airplane close to the axisymmetric minimum wave drag shapes described above. We will see examples below.

10.4.1 A curious story

Both the Kármán Ogive and Sears-Haack Bodies have a curious feature. They are slightly blunted. Intuitively we expect them to have sharp noses. Yet, the slope at the nose is 90° and the leading edge radius is zero, which is hard to visualize. The explanation is that it's better to have a high slope, and thus high pressure, at the nose, where dS is small, rather than further aft, where r is larger, and dS is much larger ($dS = 2\pi r dr$). These shapes are geometrically blunt while being aerodynamically sharp. More details associated with this feature of the geometry are available.[30]

In addition, our analysis revealed that the nose shape of the Kármán Ogive and Sears-Haack bodies are essentially equivalent to a power law body with an exponent of 0.75. This means that the minimum drag supersonic and hypersonic bodies are related. Figure 10-17 shows an extreme "blow-up" of the power law body at the nose.

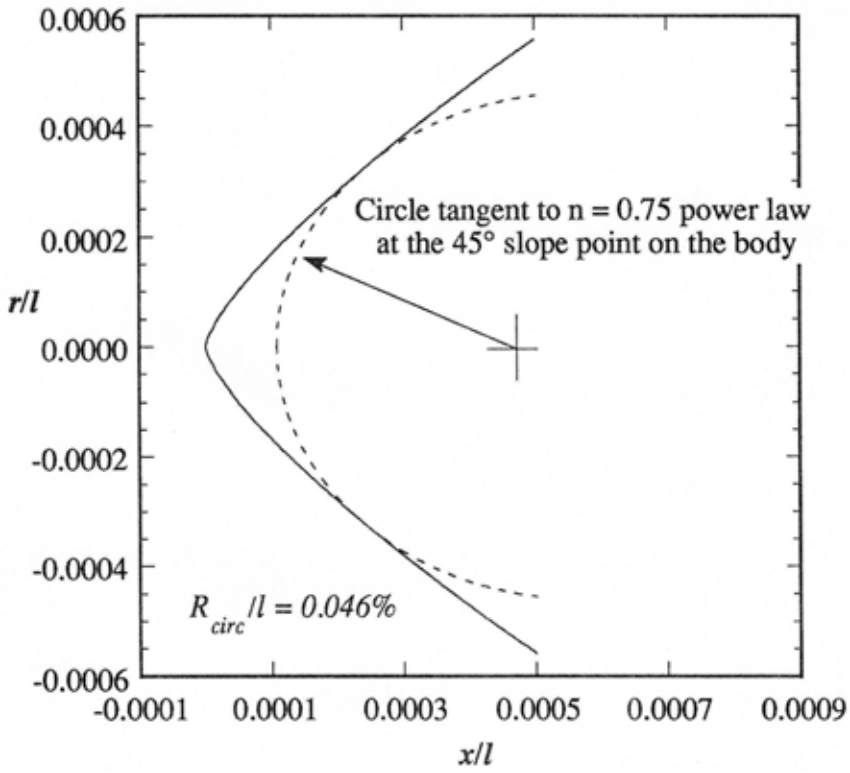

Figure 10-17. The nose region of a power law or Sear-Haack body[30]

10.4.2 Multiple Bodies to Reduce Wave Drag and Favorable Interference

Another possibility for reduction of wave drag occurs when multiple bodies of revolution are arranged to reduce wave drag. There can be both a favorable and an unfavorable interaction between bodies that are located in close proximity. The idea of favorable interaction is the reason for the concept presented at the start of this chapter. Unfortunately the interaction can be sensitive to the Mach number. One of the ideas has been to stagger stores with flight Mach number to reduce drag. This was the basis for the work of Jack Nielsen.[31] Previously Friedman had also done an analysis showing the possibility of favorable interaction.[32] Nielsen says that compared to the sum of the drag of the individual bodies; "The results show that the drag of a pair of bodies can be either double or nearly halved, depending upon the lateral and longitudinal spacing's of the bodies." Quoting from Friedman, "A three-body configuration is found for which the total wave drag is about 35 percent less than the sum of the individual wave drags of the three bodies," Figure 10-18 from Nielsen shows the sensitivity of the interference drag for one Mach number. The potential advantage is available, but it must be used very carefully.

Multiple axisymmetric bodies are just one possibility for favorable interference. A number of other possibilities exist. Kulfan has examined many of them for application to supersonic airplane.[33] See that paper for the ideas and an extensive reference list.

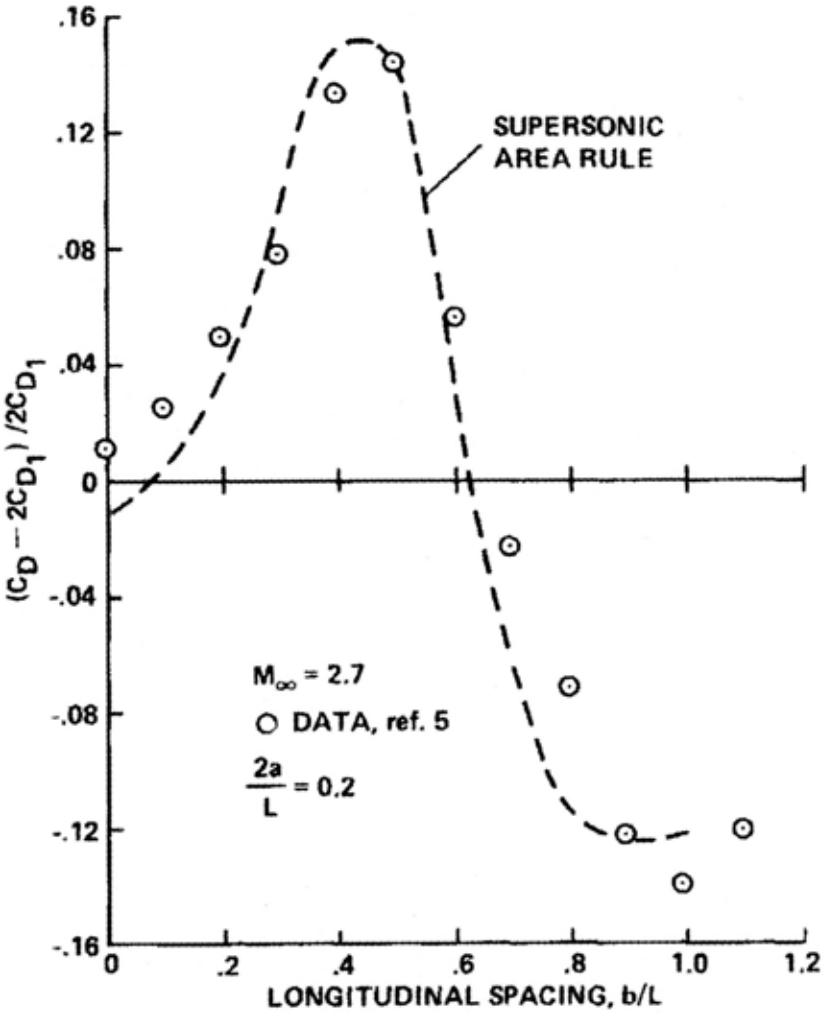

Figure 10-18. Effect of longitudinal spacing on the interference wave drag of a pair of Sears-Haack bodies at M = 2.7. Negative values denote favorable interference.[31]

10.4.3 Planar wing wave drag

We generally think of axisymmetric bodies as the shapes that minimize wave drag. However, this isn't the case. An example of a potential reduction has been shown in Kuchemann's book.[34] Planar wings with the same volume as a Sears-Haack body can actually have less drag than the axisymmetric body. The data is plotted as a fraction of the Sears-Haack drag values in Figure 10-19. A significant reduction in wave drag can be obtained with these "flattened out" volumes.

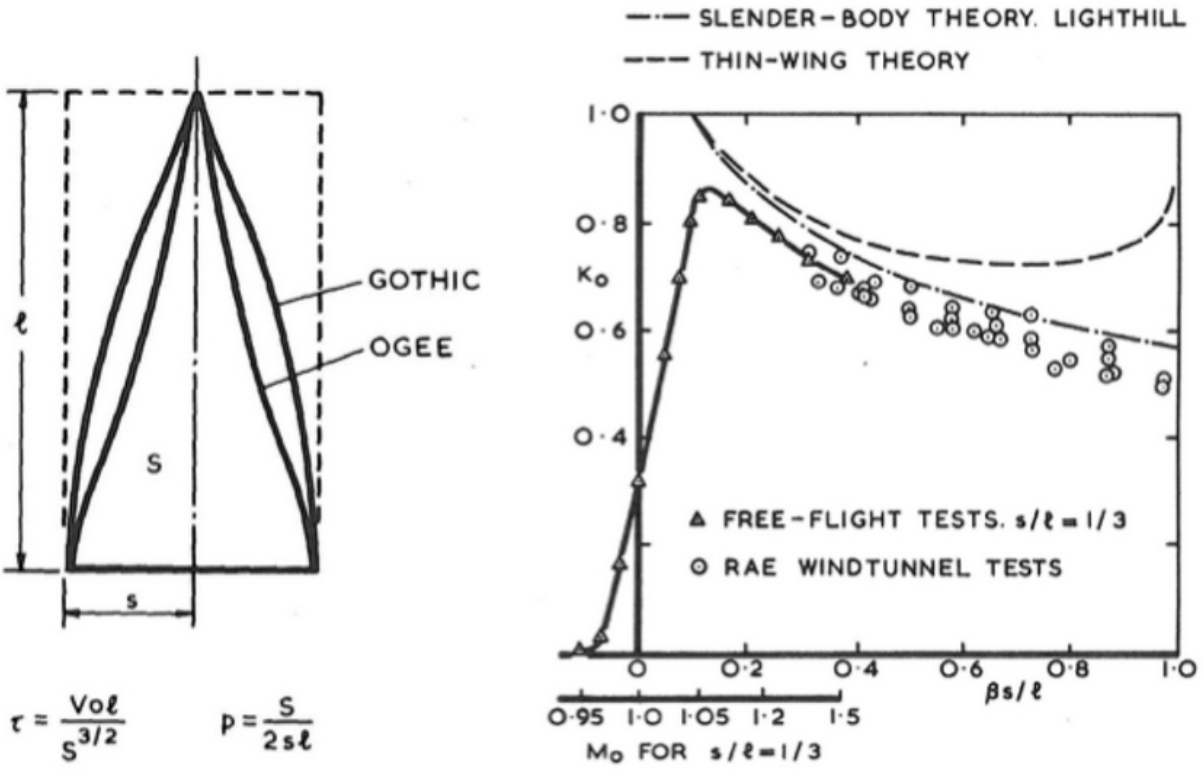

a) nomenclature b) drag results (relative to the Sears-Haack Body ($K_0 = 1$)

Figure 10-19. Wave drag reduction available for planar-type volumetric bodies.[34]

10.5 Wings: lift and drag due to lift

Now we consider the lift and drag for traditional supersonic wing planforms. One of the fundamental notions in supersonic aerodynamics is the distinction between a so-called sub- and super-sonic edge. The concept is illustrated in Fig. 10-20.

Most, in fact essentially all, trailing edges are supersonic. This disconnects the upper and lower surface pressure distributions at the trailing edge, there is no Kutta condition. The issue then becomes whether the leading edge is subsonic or supersonic. If the leading edge is subsonic, the flow about the leading edge is similar to the subsonic case in two dimensions. If the leading edge is supersonic, the flow at the leading edge behaves as if it were in a locally two-dimensional supersonic flow. This leads to a significant difference in the physics of the flow on the wing. We will use a delta wing planform as an example. Figure 10-21 shows the difference in the planform and shock wave locations. It also introduces the concept of conical flows as important in thinking about supersonic wing performance. In a conical flow both the geometry and the flow properties are constant along rays through the apex.

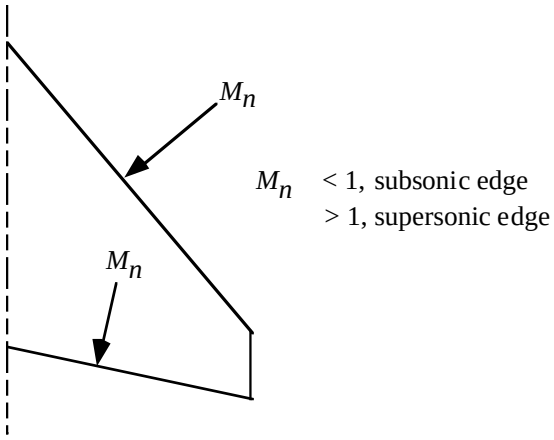

Figure 10-20. Definition of subsonic and supersonic edges in supersonic flow.

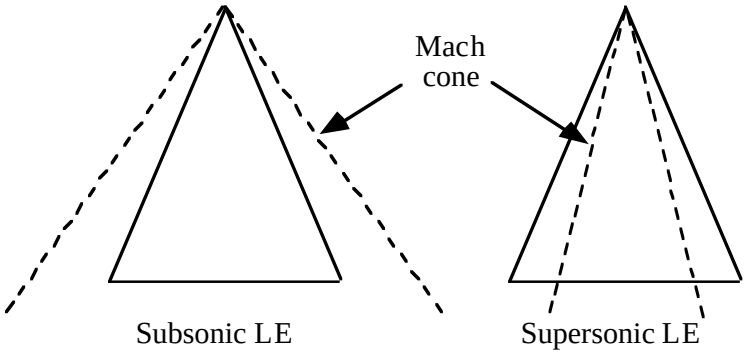

Figure 10-21. Examples of delta wings with subsonic and supersonic leading edges.

For the subsonic leading edge case the upper and lower surfaces can still communicate with each other as shown in the Fig. 10-22. Here, a point on the lower surface can create a disturbance that propagates in front of the wing, where a point on the upper surface aft of the lower surface disturbance point can be influenced.

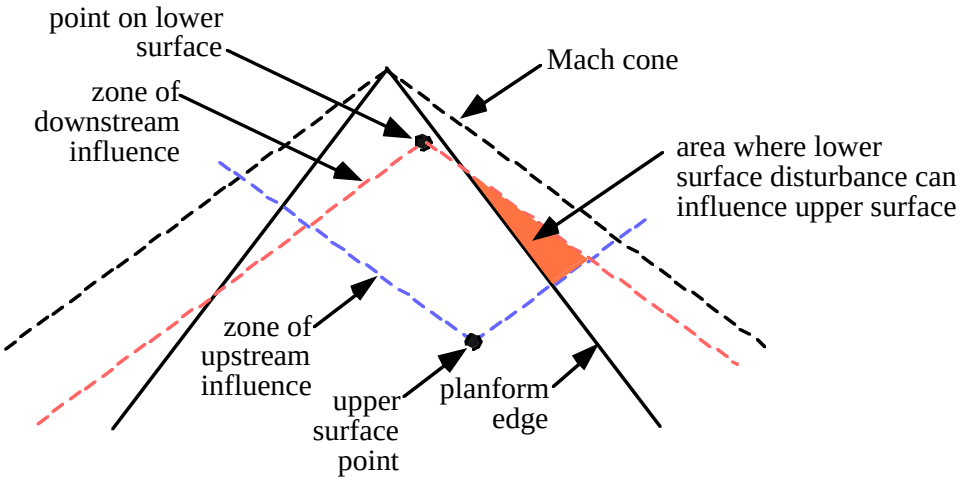

Figure 10-22. Example of how a disturbance on the lower surface of a wing in a supersonic flow with a subsonic leading edge can influence the flow on the upper surface.

Figures 10-23 and 10-24 show the linear theory spanwise pressure distributions for the two different cases. Figure 10-23 is for the case of a subsonic leading edge, and shows the singularity at the leading edge, just as we expect in subsonic flow. The equation for the loading is given by

$$\frac{\Delta C_p}{C_L} = \frac{2}{\pi} \frac{1}{\sqrt{1-\left(\frac{\tau}{m}\right)^2}} \tag{10-13}$$

where $m = \beta \cot \Lambda$, and $\tau = (\beta y / x)$. Recall $\beta = \sqrt{M^2 - 1}$.

Figure 10-24 is for a supersonic leading edge, and here we see that the pressures outside of the Mach cone are constant. Thus, outside the Mach cone, the constant value of the loading is given by:

$$\frac{\Delta C_p}{C_L} = \frac{1}{\sqrt{1-n^2}} \tag{10-14}$$

where $n = \tan \Lambda / \beta = 1/(\beta \cot \Lambda) = 1/m$, $m > 1$. Inside the Mach cone,

$$\frac{\Delta C_p}{C_L} = \frac{1}{\sqrt{1-n^2}} \left(1 - \frac{2}{\pi} \sin^{-1} \sqrt{\frac{n^2-\sigma^2}{1-\sigma^2}} \right) \tag{10-15}$$

where, $\sigma = y \tan \Lambda / x, \quad 0 < \sigma < 1$.

The solutions reflect the significant difference in the physics of the two cases.

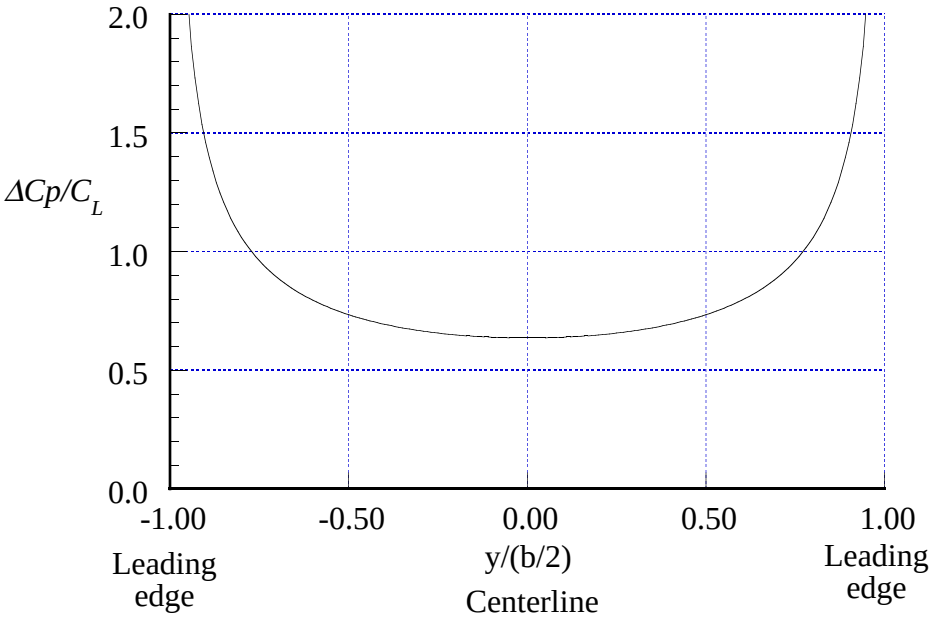

Figure 10-23. Spanwise pressure distribution (actually loading) for a subsonic edge case from linear theory.

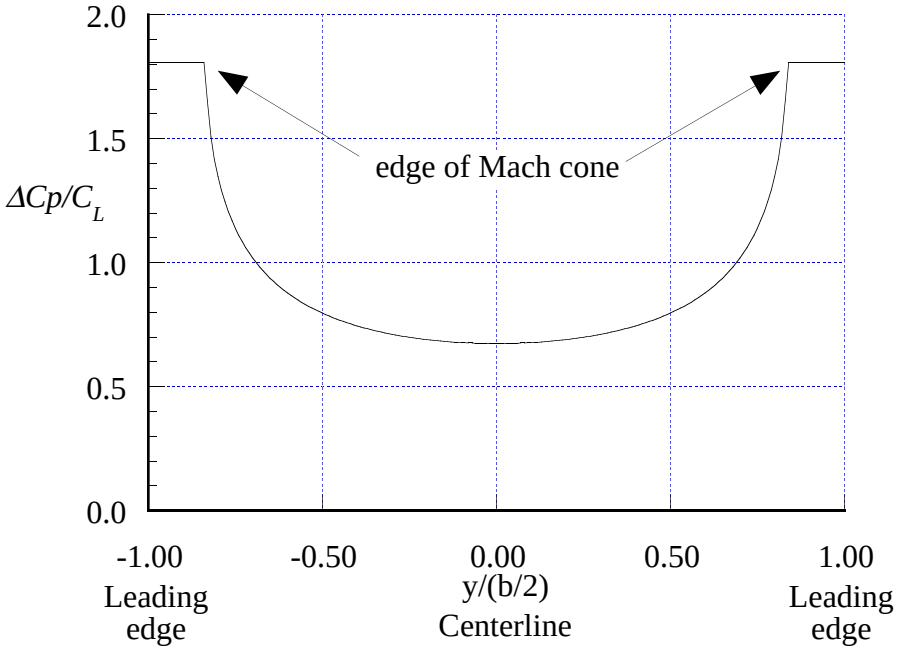

Figure 10-24. Spanwise pressure distribution (actually loading) for a supersonic edge case from linear theory (m = 1.2).

10.5.1 Arrow wings and conical camber

To think about the supersonic aerodynamics of wings it is useful to consider a class of planforms for which exact linear theory solutions are available, the arrow wing. The flow is still conical, and departs from a delta wing by adding a trailing edge cutout, usually described as the notch ratio. Figure 10-25 provides the nomenclature.

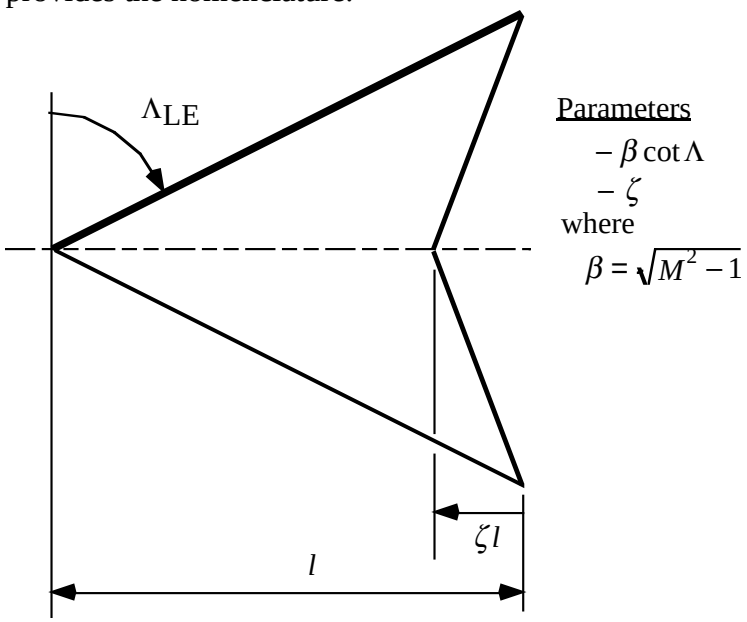

Figure 10-25. The classic arrow wing, and the describing terminology.

The linear theory lift is given in the Fig. 10-26 for two different notch ratios, ζ. The calculations were made using program *arrow.f*, which is available from our software web site. Note the change in character when passing from the subsonic edge case to the supersonic edge case. Also, note how the parameters are presented in the figure to "scale out" the Mach number, so the results are applicable for all Mach numbers. Using conical flow theory the analytic solution programmed in *arrow.f* for a subsonic leading edge is:[35]

$$\beta C_{L_\alpha} = \frac{4m}{E'(m)}\left[\frac{\zeta}{1+\zeta} + \frac{1-\zeta}{\left(1-\zeta^2\right)^{3/2}}\cos^{-1}(-\zeta)\right], \qquad m \le 1 \quad (10\text{-}16)$$

where $m = \beta\cot\Lambda_{LE}$ and $E'(m) = E(k)$, where $k = \sqrt{1-m^2}$, and $E(k)$ is the complete elliptic integral of the second kind. For the supersonic leading edge case,[35]

$$\beta C_{L_\alpha} = \frac{8m}{\pi(1+\zeta)}\left[\frac{1}{\sqrt{m^2-\zeta^2}}\cos^{-1}\left(-\frac{\zeta}{m}\right) + \frac{\zeta}{\sqrt{m^2-1}}\cos^{-1}\left(\frac{1}{m}\right)\right], \quad m \ge 1 \quad (10\text{-}17)$$

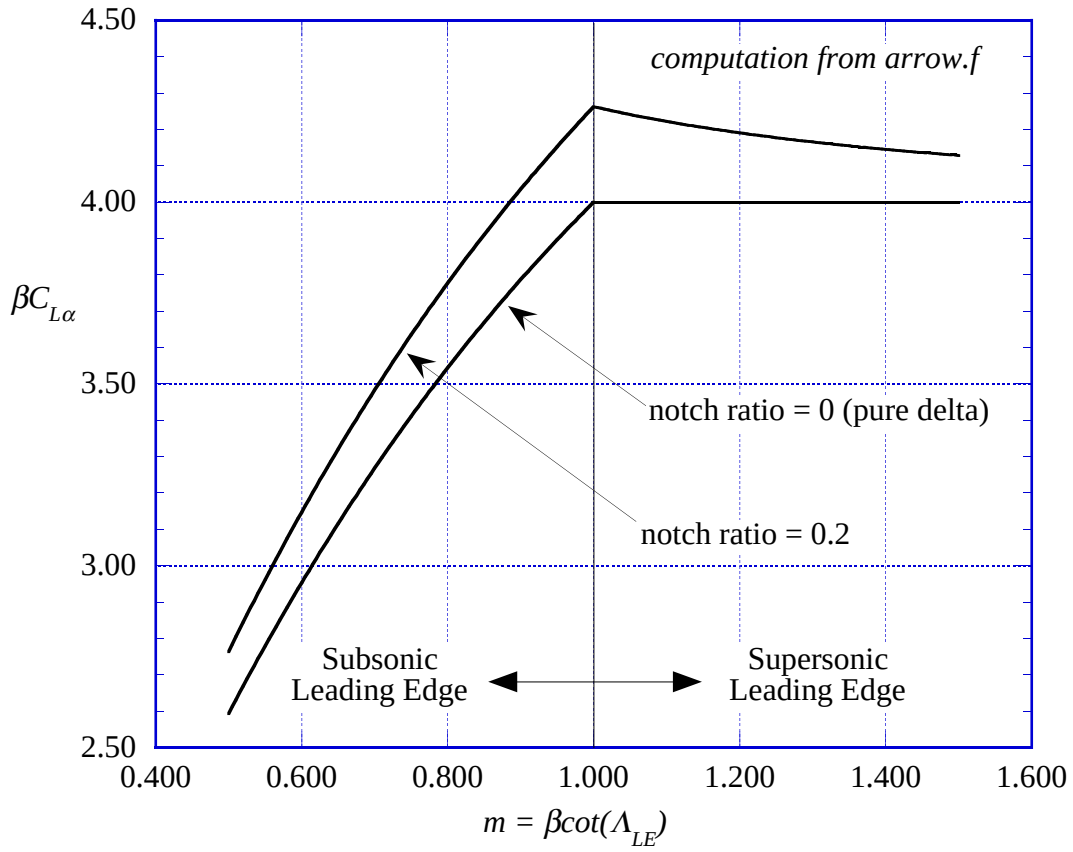

Figure 10-26. Arrow wing lift curve slope.

The drag due to lift is also available from the theory. It is computed based on the 0% leading suction drag, and then reduced if the leading edge is subsonic by the leading edge suction (the

component of the suction parallel to the velocity vector is called the leading edge thrust, *T*). Thus the drag due to lift is:

$$D = \alpha L - T \tag{10-18}$$

where *T* is zero if the leading edge is supersonic. This can be put in terms of the force coefficients and written in a form that eliminates both Mach number and C_L dependence using the equation given above. The second term inside the bracket is zero for the supersonic leading edge case:

$$\frac{\Delta C_D}{\beta C_L^2} = \frac{1}{\beta C_{L_\alpha}}\left[1 - \frac{\pi m}{\beta C_{L_\alpha}}\frac{1}{(1-\zeta)}\frac{\sqrt{1-m^2}}{E^2}\right] \tag{10-19}$$

The results are shown in Fig. 10-27. This time the figure is more complicated. For the subsonic edge cases two branches of the drag are shown. One assumes that the full leading edge suction can be realized, while the other assumes that no leading edge suction is achieved. If full leading edge suction can be obtained, subsonic edges are desirable to reduce the drag. However, if no suction can be obtained, then the drag is reduced when the edges are supersonic. Although we have presented results for planar wings, the effect of leading suction is attained in practice by cambering the wing. Essentially, the linear theory says that by cambering the wing a benefit equivalent to the full leading edge suction can be realized. Experience shows that only a portion of the leading edge suction predicted by linear theory can be achieved, possibly explaining why many of the supersonic airplanes listed above have had supersonic leading edges at the design Mach number. Many NASA designs were more aggressive, and selected an *m* of about 0.75. They were expected to attain the full value of leading edge suction. In general, the calculation of the leading edge suction is difficult. However, progress has been made recently.[36]

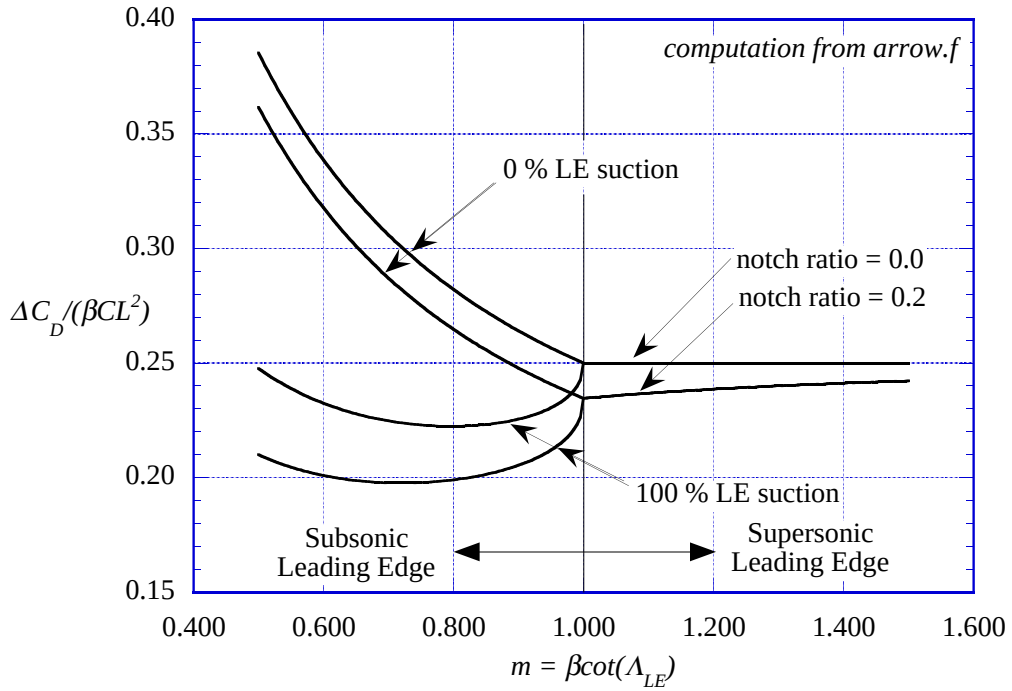

Figure 10-27. Arrow wing drag due to lift.

The conical flow theory used to obtain the solutions presented here was also the basis for a special type of camber that was widely applied to many delta wing supersonic aircraft to reduce the drag due to lift. Known as *conical camber*, the surface was cambered so that the geometry was straight along rays through the apex of the wing.[37] Conical camber was used on the F-102, F-106 and B-58. It was also used on the F-15.

Figure 10-28 shows the conical camber on an F-102. The photo was taken at the Pima Air & Space Museum outside of Tucson, Arizona. It is taken from the behind the airplane looking forward along the leading edge, showing the large amount of camber. The camber is pronounced on this plane because it was added after the plane was built and was limited to the wing outboard of the 85% spanwise cuts to maintain the basic structure. The F-15 has concical camber, but it is distributed across the span and difficult to see.

Figure 10-28. The F-102, showing the leading edge spanwise camber.

Figure 10-29 shows one of the inventors of conical camber, Charles Hall, looking at a model in a wind tunnel at NACA Ames Research Center.

Figure 10-29. Conically cambered model in the NACA Ames Wind Tunnel (NASA Photo)

Figure 10-30, from a survey paper by von Kármán, shows how the concept works.[38] With a small leading edge radius equired for supersonic flight, the effect of leading edge suction can be acieved by providing a forward facing surface with a low pressure. The resulting drag polar is shifted upward, approaching the value of a flat surface with 100% leading suction.

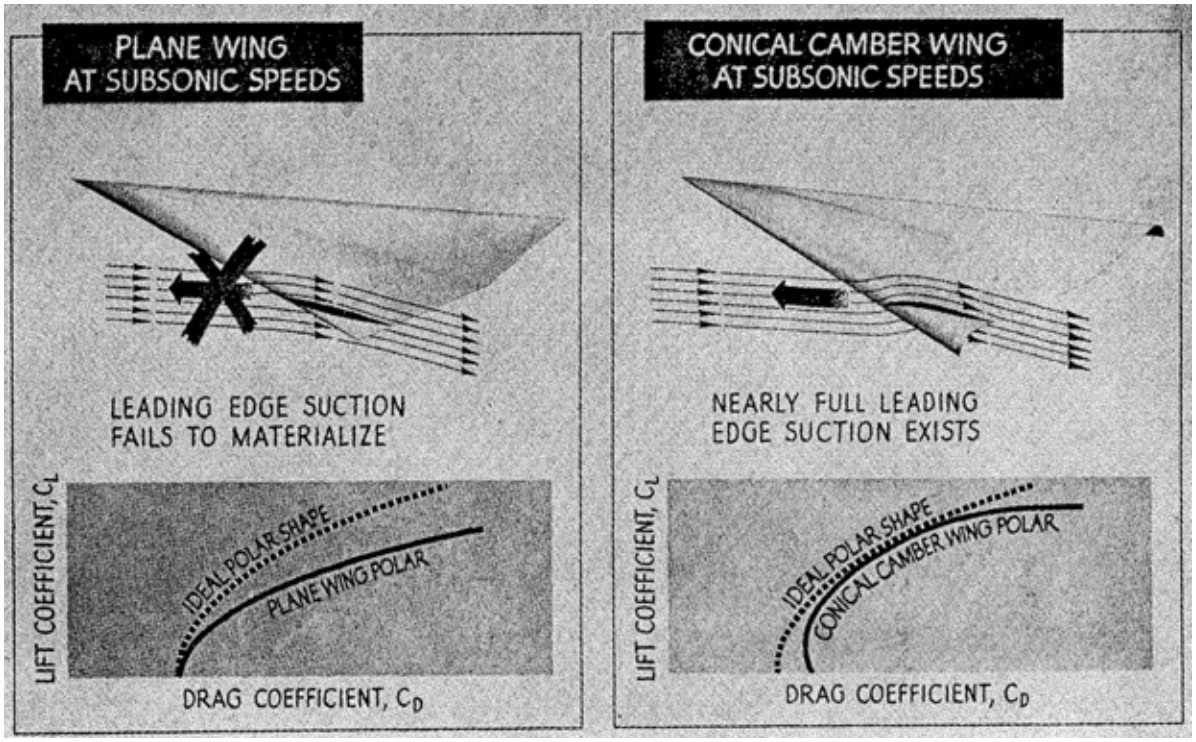

Figure 10-30. How conical camber works, shifting the drag polar.[38]

10.5.2 Modified arrow wings

Once the arrow wing is used to establish a basis for thinking about the aerodynamics of supersonic wings, one proceeds to think in terms of modifying it for practical application. One frequently reads in the literature of a "modified arrow wing" configuration that to me never appeared to be at all like the planform shown above.[39] Figure 10-31 traces the evolution of the arrow wing to a configuration applicable to actual aircraft design.

The sequence of modifications shown in Figure 10-31 can be described as follows.[12] For the Basic Arrow Planform the tip is "clipped." The structural span is decreased and a portion of the wing that doesn't actually contribute aerodynamically is eliminated. Next, for Planform A the outboard portion of the wing is unswept slightly. This improves the subsonic efficiency with little penalty supersonically. It also reduces the aerodynamic center (*ac*) shift. Finally, for planform B the trailing edge is "filled in." This helps the subsonic pitchup, makes trailing edge flaps more effective and also further reduces the *ac* shift. For a specified thickness the extra chord means that the root *t/c* is reduced. This explains why a planform that doesn't look anything like an arrow wing becomes a "modified arrow wing."

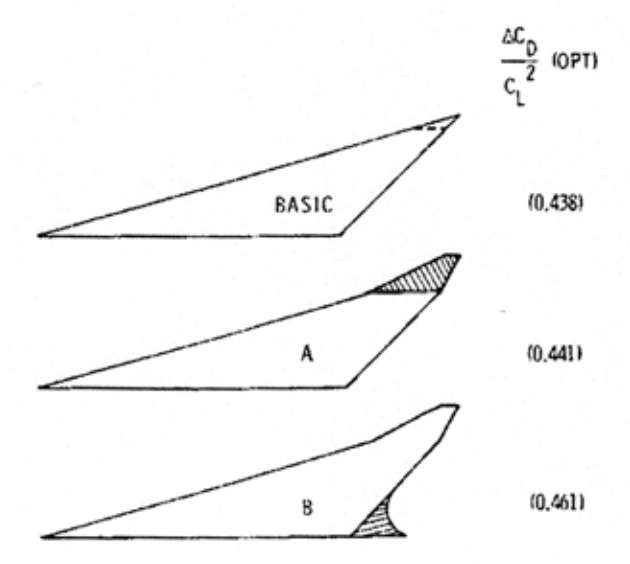

Figure 10-31. Classic modified arrow wing progression, from Baals, Robins and Harris.[12]

A related issue for modified arrow wings with the outboard portion unswept is the potential for pitchup at subsonic speeds and high angle of attack (described previously in Chapter 6). A review of this effect and an approximate method for estimating for pitchup for these types of planforms is available.[40]

10.6 The Aerodynamic Center Shift

Another important consideration in supersonic configuration design is the shift of the aerodynamic center (*ac*). In the classical 2D case illustrated in Figure 10-32, the aerodynamic center shifts from the 25% chord to 50% chord.

Program *arrow.f* also provides the aerodynamic center location as well as the lift and drag (but only at supersonic conditions). We need to see how modifications to the classic delta wing shape

can be used to reduce the *ac* shift. Figure 10-33 is taken from the Concorde case study,[6] and shows that the Concorde planform shaping is critical in reducing the shift. However, the shift is still significant and fuel transfer must be used to maintain an acceptable relation between the center of gravity and aerodynamic center. Note that the allowable *cg* range shown in Figure 10-34 for the Concorde shows how important the *cg* control was.[41] The Concorde used a root chord of 90.75 feet as the reference chord. At takeoff and landing, the *cg* was required to be between 52.5% and 53.5% of the root chord. At supersonic cruise the *ac* shifts about 5 1/2%, or 5 feet. The allowable *cg* limits are between 58% and 59% of the root chord. Thus for an airplane of slightly over 101 feet in length, the *cg* must be maintained within about 11 inches. This is why configuration designers consider airplane balance immediately upon examining any design drawing.

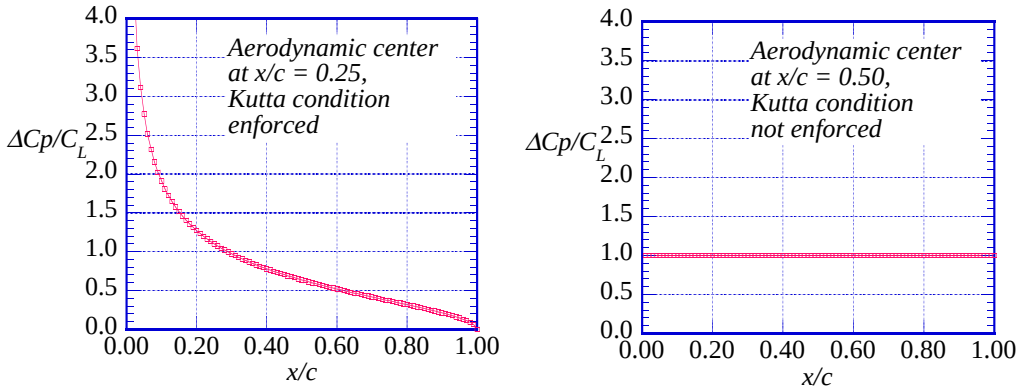

a) subsonic case b) supersonic case

Figure 10-32. Comparison of load distributions for 2D subsonic and supersonic flat plates

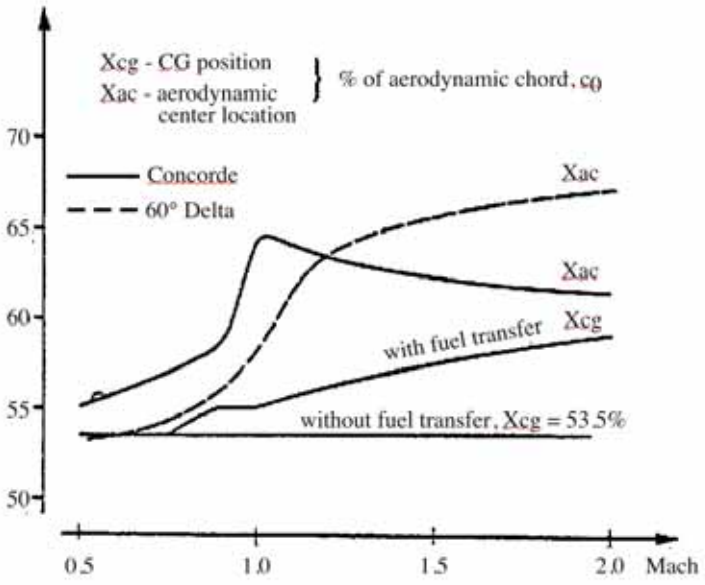

Figure 10-33. Concorde example, planform shaping to control the *ac* shift (from the AIAA Case Study[6])

All supersonic airplanes use fuel transfer to control the *cg* location and maintain a relation between the *cg* and *ac* that allows the airplane to be adequately controlled and also fly with minimum control surface deflections to minimize trim drag. The XB-70 was unusual in that the wing tips folded down in supersonic flight. Although usually described as providing extra aerodynamic efficiency and additional directional stability, perhaps the most important consequence of folding the tips was to control the *ac* shift.

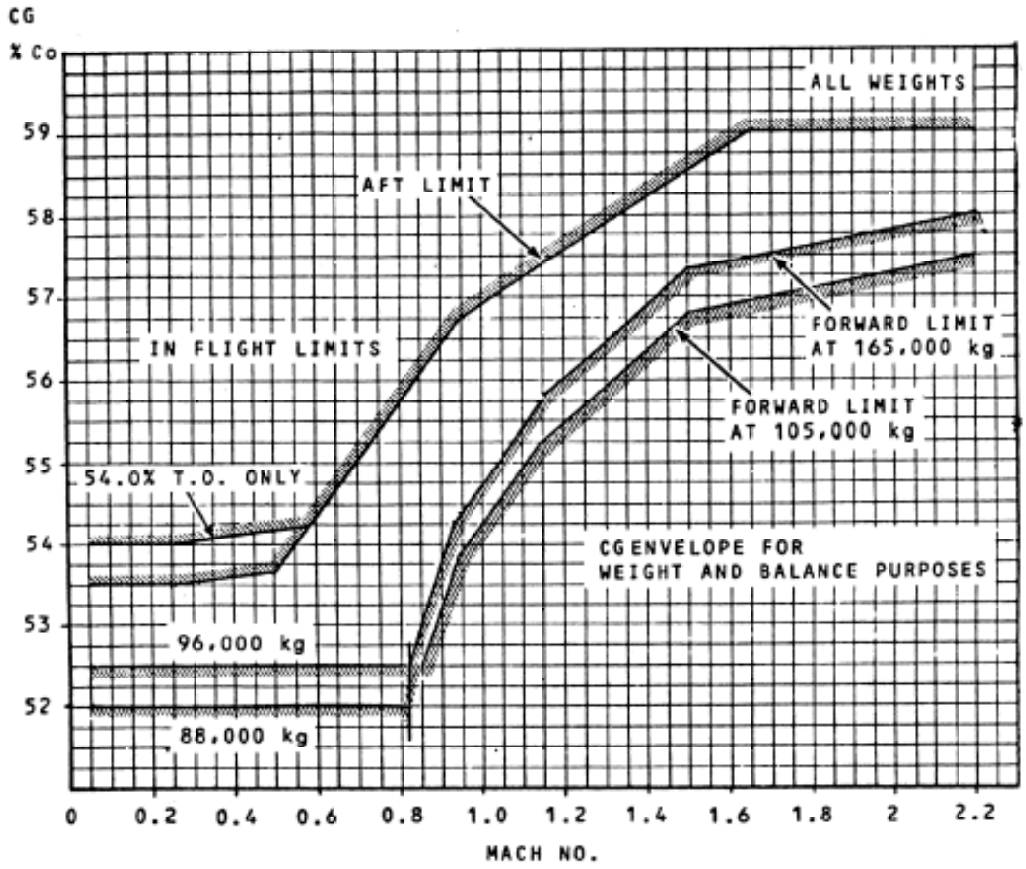

Figure 10-34. Concorde *cg* limit changes with Mach number, given as a fraction of the root chord.[41]

Additional examples of planform shaping to reduce the *ac* shift were presented by Lamar and Alford.[42] They used a slightly different parameter to correlate *ac* shift, and show the benefit of using a double delta planform, which would be a rough approximation of the Concorde planform. Figure 10-35 shows the result of their parametric study of the aerodynamic center shift. They show that a pure delta wing has a much larger *ac* shift then a double delta. They found that the inboard delta meeting the aft delta at about 45% of the semispan produces the smallest *ac* shift. The larger the extent of the more highly swept inboard delta the better.

Why does this work? The idea is that the inboard wing, being more highly swept, with a lower aspect ratio, has a lower $C_{L\alpha}$, that is insensitive to Mach number. The outboard section, with less sweep, has a higher aspect ratio and a $C_{L\alpha}$ that decreases with Mach number. Thus the composite planform has a smaller *ac* shift. How this was discovered is a little mysterious. The NASA paper has a date of 1966. Ben Rich provided a similar explanation is his paper on the SR-71.[2] The first

version of the SR-71, the A-12, was flown in 1962. The Lockheed proposed commercial supersonic transport (SST) design used a double delta and the configuration was apparently chosen in 1963. Dan Raymer[43] says that the aero types working in the Skunkworks gave their counterparts working on the SST a sketch and said "use it-it works-but don't ask how we know."

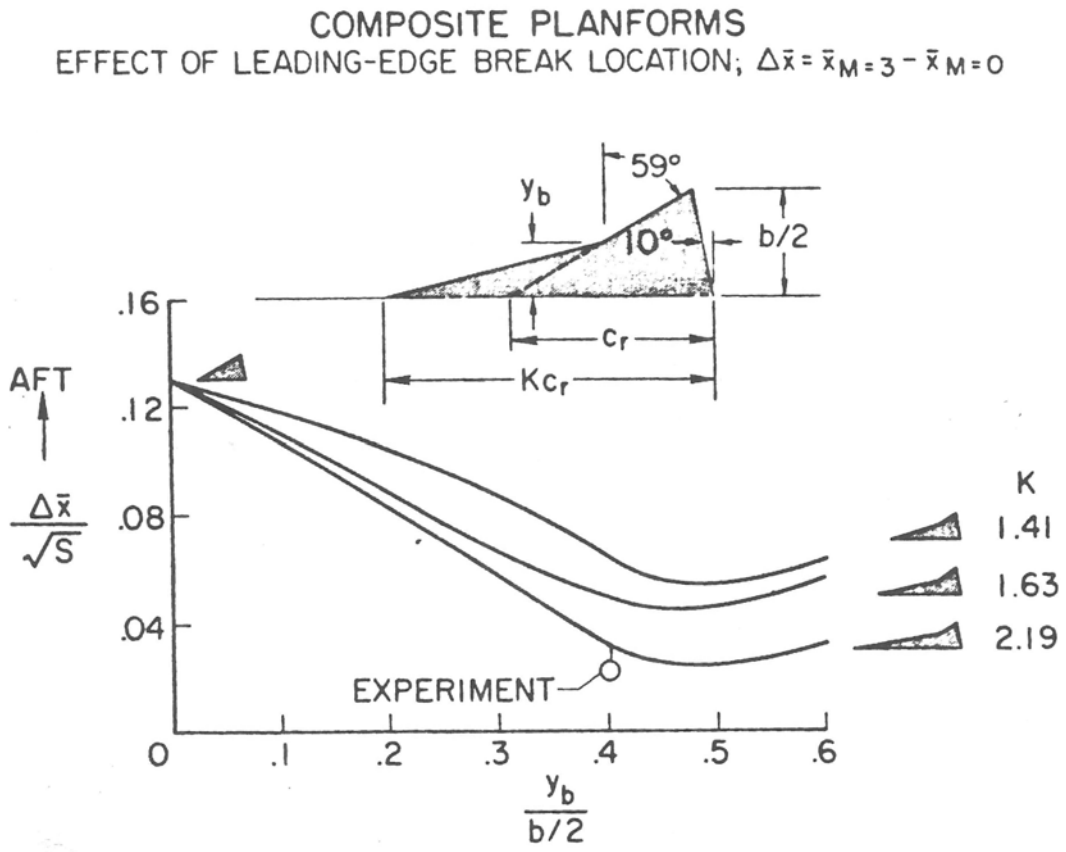

Figure 10-35 Effect of planform on the aerodynamic center shift, subsonic to supersonic.[42]

A final example requiring aerodynamic center shift attention arises for variable sweep wing airplanes. Although currently unfashionable, variable sweep wings have the attraction of performing well at both subsonic and supersonic speeds (the low aspect ratio when the wings are swept back also reduces the gust load response for high subsonic speed on-the-deck penetration missions). The problem of the airplane becoming too stable when the *ac* shifts aft is aggravated when the variable sweep wing is swept back at supersonic speeds. This adds more (stabilizing) planform area aft of the *cg*. Figure 10-36 illustrates the problem. It is from a paper by Bob Kress of Grumman[44] and focuses on the F-14 as compared to the F-111. Clearly the F-111 supersonic static margin is excessive. The F-14 has a lower static margin, and there is another feature that decreases the static margin even more. Kress invented the "glove-vane" that was used on the F-14 to reduce the static margin. When the wings were swept back the glove vane came out, adding planform area forward of the center of gravity. This resulted in reducing the *ac* shift.

The main reason that the F-14 had a reduced static margin shift was the use of a so-called "outboard pivot" location as compared to the F-111. The use of the outboard pivot reduced the

ac shift. The effect of pivot location had been the subject of numerous wing tunnel tests at NASA Langley. Good background information on variable sweep aircraft development can be found in the report by Polhamus and Toll.[45] Their paper also discusses the "skewed wing concept", that became know as an oblique wing and is discussed in the next section.

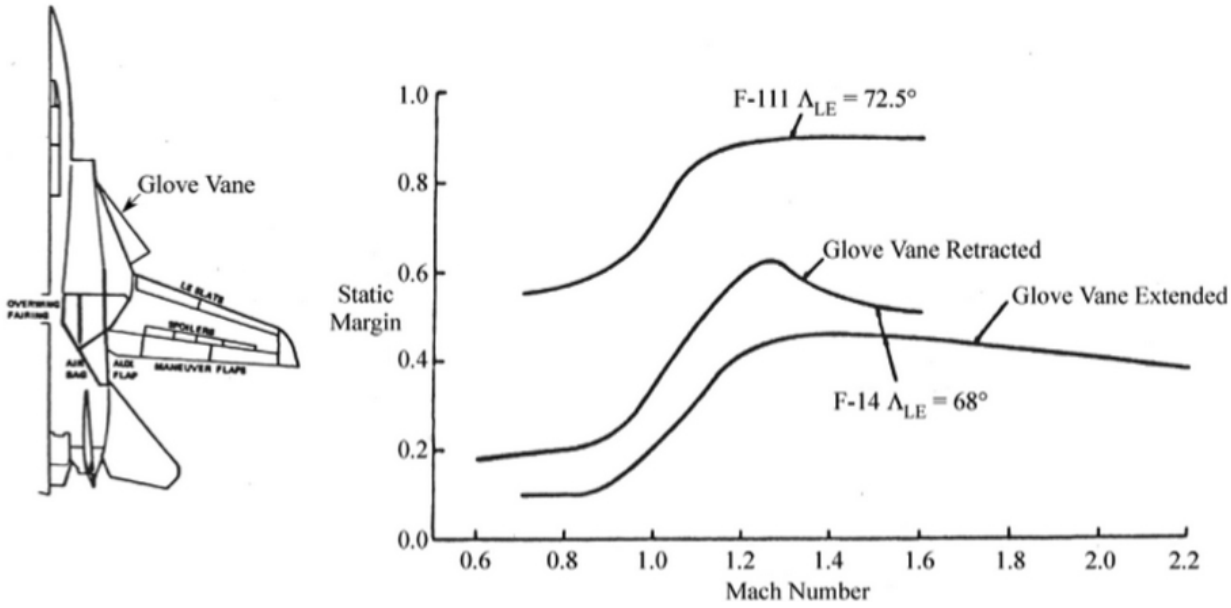

Figure 10-36. Static margin change with Mach number for variable sweep wings.[44]

10.7 The Oblique Wing Concept

We need to describe one more planform concept. When considering both lift and volumetric drag a somewhat radical wing concept with good potential for a supersonic transport application is the oblique wing idea advocated by R.T. Jones for many years.[46,47] The idea is that both the longitudinal as well as spanwise distribution of lift should be elliptical. The natural way to do this is with an oblique wing planform. Jones made the argument that that there is no reason that an airplane has to be symmetrical.

Originated for its good drag due to lift characteristics, this shape is also good for volumetric wave drag because the area diagram can be very good, especially for a flying wing configuration. Figure 10-37 from Jones's book[48] illustrates the advantage. It compares the wave drag for an oblique elliptic wing to a swept wing having the same aspect ratio and thickness to chord ratio. There is a clear advantage for the oblique wing. Note that the advantage occurs for Mach numbers around 1.4 to 1.5. Recall that we saw above how important length was in reducing the drag of axisymmetric bodies and that is important here too. Admittedly this is less than the usual notion of a Mach 2 airplane. Many of the wind tunnel tests were nominally "transonic" tests, but actually emphasized the upper transonic speed regime, which might actually be called lower supersonic. However, the large decrease in drag makes this concept compelling for a supersonic configuration. Because Jones worked at NACA/NASA and had made many contributions he was able to convince NASA to make numerous wind tunnel tests.

Many other aerodynamicists have examined the concept. It has always been found to be attractive. We only cite one among many, the paper by Li, Seebass ansd Sobieczky. They advocated the design of an oblique flying wing at a Mach number of 1.4.[49] Aeroelasticity was

also an issue, and numerous papers by Weisshaar and his colleagues have presented results of their work (we reference only one here[50]). Although aeroealsticity needs to be addressed, today's modern design and active control technology would be capable of handling any problems.

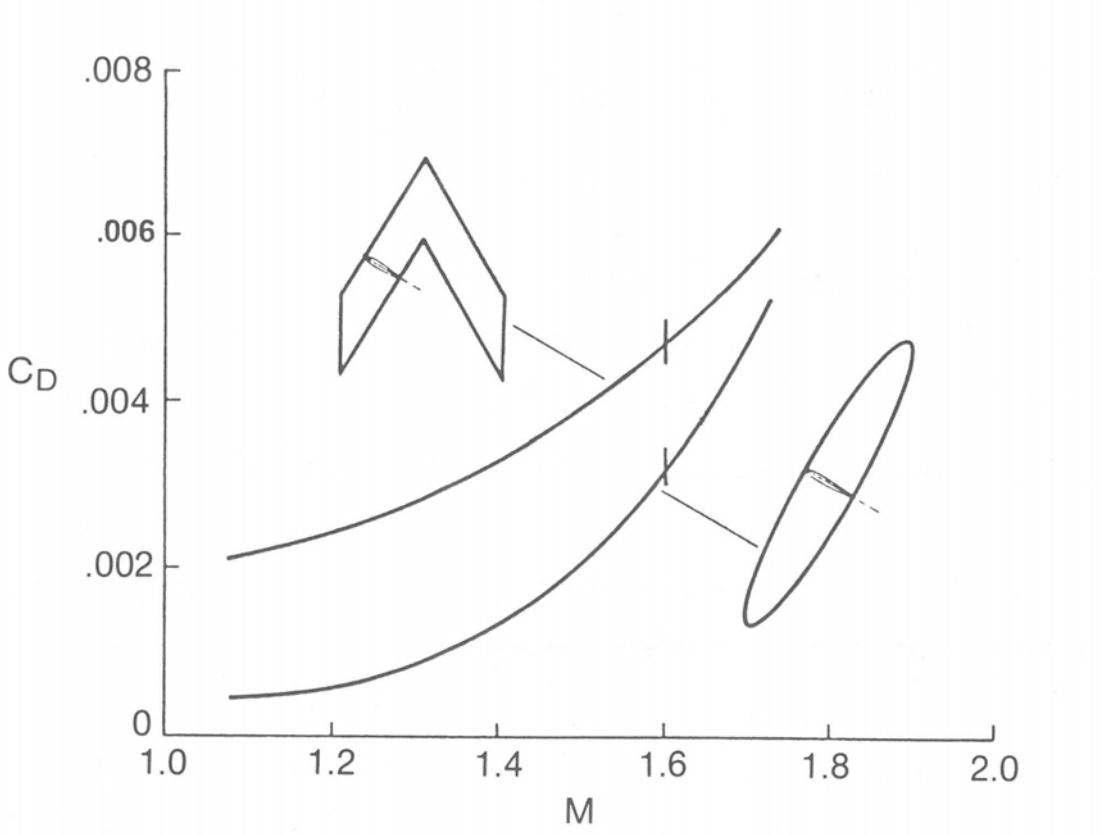

Figure 10-37. A comparison of an oblique and swept wing with the same aspect ratio and *t/c*.[48]

Because of its unconventional configuration, an oblique wing was built and flown by NASA. The AD-1 was successful and is shown here in flight in Figure 10-38. It was strictly a subsonic airplane, intended to investigate the flying qualities of an oblique wing. The wing could sweep from 0 to 60 degrees in flight. Its first flight was in December 1979 and it finished the flight test program in August of 1982. The demonstrator was very basic; there was no automatic flight control system. The plane did have some handling qualities issues, as well as adverse aeroelastic effects. However it seems that with the use of a modern flight control system the oblique wing would be a viable concept. A description of the program and outcomes are documented in two AIAA Papers.[51,52]

After it finished its demonstration it was displayed at the visitor's center at NASA Ames at Moffett Field, California as shown in Figure 10-39. It was so small that we have to include a photo with the pilot standing in front of it in Figure 10-40 to appreciate its size. Today it's on display indoors at Hiller Aviation Museum in San Carlos, California.

Numerous studies of the oblique wing as a new supersonic transport have been made.[53,54] although it was not considered in the recent HSCT studies conducted by NASA with industry in the 1990s.

Figure 10-38. Oblique wing flight demonstration by the AD-1.

Figure 10-39. The AD-1 outside the NASA Ames Visitor Center (many years ago)

Figure 10-40. The AD-1 shown with pilot Richard Gray to appreciate its small size.

A comprehensive survey of oblique wing work has been compiled by Hirschberg, Hart and Beutner.[55] Subsequent to that survey a major optimization study was carried out at NASA Ames showing that advanced computational methods could further improve oblique wing aerodynamic designs.[56] The case in favor of the oblique wing concept for modest supersonic speeds remains compelling.

10.8 Aero-Propulsion Integration

Efficiently integrating the propulsion system with the airframe requires much more effort for supersonic airplane design than for subsonic airplanes. We cannot cover the entire subject here, but point out a few of the issues and provide an example showing how to include the propulsion system efficiently. The design of the inlet and exhaust nozzle often requires as much computational and testing effort as the rest of the airframe. The inlet has to be carefully designed to handle the required mass flow at supersonic cruise, while also operating efficiently at low speed. A variable geometry inlet is often required if the cruise Mach number is more than 1.6. Many fighters that have inlets close to the side of the fuselage are offset and use boundary layer diverters to ensure a uniform flow into the inlet. The F-35 uses a diverterless inlet, where there is a “bump” on the fuselage side in front of the inlet to force most of the boundary layer to flow around the inlet. This became possible when CFD could be used to design the fuselage/inlet.

Figure 10-41 from Don Baals, et al[12] shows how integrating a podded engine installation under the wing can lead to favorable interference. The wing is reflexed around the nacelle. The drag of the aircraft is very sensitive to the location of the pod.[57]

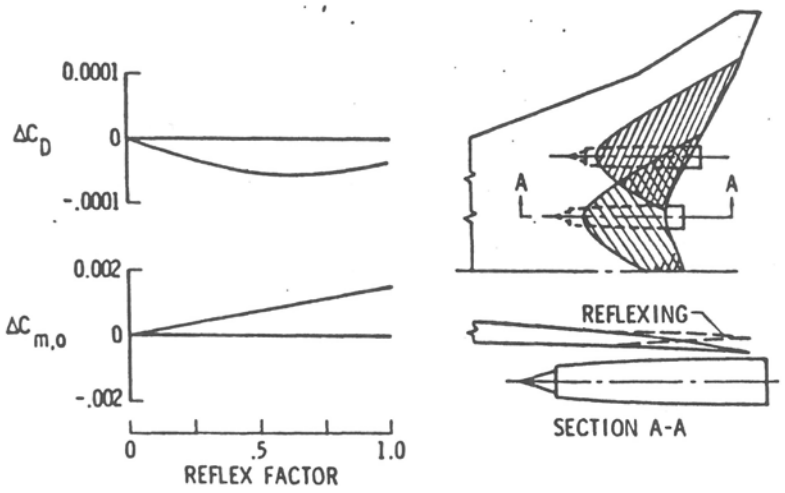

Figure 10-41. Possible favorable aero-propulsion interference when the engines are located in the right position.[12]

The exhaust nozzle also requires careful design. Because of the afterburner, the nozzle has to have a variable geometry. Thrust vectoring may also be used. Each of these features will require careful attention. The external contour typically has a so-called "boattail" shape. This has to be carefully shaped to avoid extra drag. Boattail analysis was one of the first intense CFD efforts.

The best place to learn about propulsion system installation in supersonic aircraft configuration work is in the book by Nicolai.[11] Chapter 16 describes inlet design, and nozzles are discussed in Chapter 17. Studies continue to be carried out for the aero-propulsion integration of proposed supersonic business jets.[58]

A stable the shock system providing the air to the engines is hard to maintain. The XB-70 and SR-71 had notorious problems with "unstarts." Eventually the SR-71 had an automated system to recover from an unstart.

10.9 Computational Methods and Supersonic Aerodynamic Design

Although powerful CFD methods are available today, we need to provide a context for their use. We've described the fundamental aerodynamic ideas that can be used to develop a supersonic configuration. These came from slender body and linear theory analysis. For most supersonic flight the flow is neccesarily attached to keep drag low, so that the inviscid flowfield combined with skin friction estimated from boundary layer theory can provide good estimates for drag. However, supersonic flight is demending and very sensitive to the accuracy of the estimates. We will describe methods to use as a starting point, but for accurate drag values complete CFD will have to be used.

The drawbacks to using CFD initially are threefold. First, CFD requires a detailed geometry to make the calculations and a high quality computational grid. These are still time consuming and a good "starting point" for the design helps to start the detailed work. The second issue is the need to represent the geometry with a flexible parametric representation that is capable of being readily changed to improve the design. The third issue is that to obtain the design shape using CFD some sort of optimization method is needed. Formulating the optimization problem to achieve a good design requires skill and experience. The optimizer is excelent at finding any

weaknesses in the problem formulation or the analysis. It's harder than it appears in typical student textbooks. Nevertheless numerical optimization methods very powerful and will be used to develop any future configuration. Finally, serious aerodynamic design is only of interest when the entire system is included. This means using the techniques known as multdisciplany design optimization (MDO) to do the design together with the other key disciplines.

With all this in mind we'll lay out a way to get to a good supersonic design. Details on CFD can be found in the companion volume to this work.[59]

10.9.1 The linear theory starting point

Linear theory was used to investigate many configurations at NASA and in industry during the 1960s, in conjunction with an active aerodynamic testing program. This was done in anticipation of the development of the US SST. The program produced many insights into supersonic aerodynamics for application to aircraft configurations. The basic tools are the Harris Wave Drag code,[18] a supersonic panel method and skin friction formulas. We will review how well these methods work. We look at the wave drag estimation first. Figure 10-42 is a review of the famous figure from Harris.

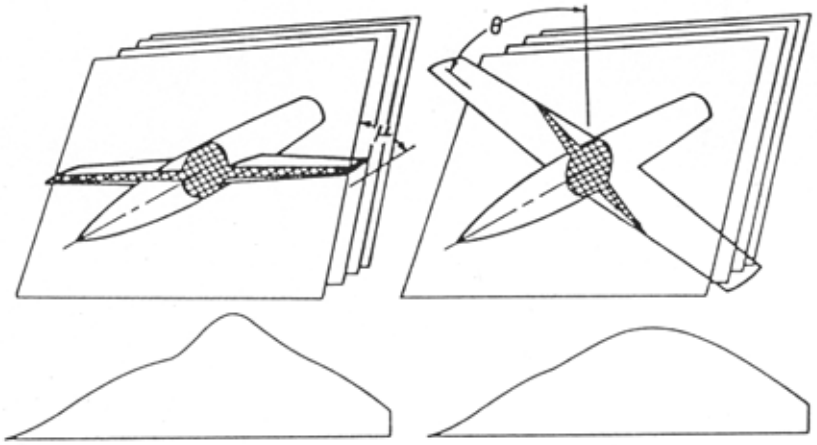

Figure 10-42. Illustration of cross-section area cuts used in the wave drag code.[18]

The code uses the input geometry to find the cross sectional areas to compute the wave drag integral. Like most NASA codes of that era, it used the so-called "Craidon input," as described in NASA TM X-2074.[60] It was much more effieicient to use essentially the same input geometry in numerous codes. Examples of the accuracy of the Harris code for a body of revolution are shown in Figure 10-43. This case has a fineness ratiuon, *l/d*, of 10. The geometry is shown in Figure 10-43a, the wave drag results are shown in Figure 10-43b. Wind tunnel data is from a NASA Langley Research Center Test.[61] The solution labeled GASP is an Euler solution from a CFD code.[62] At moderate Mach numbers the Harris code is reasonably good. These results are from work at Virginia Tech.[63]

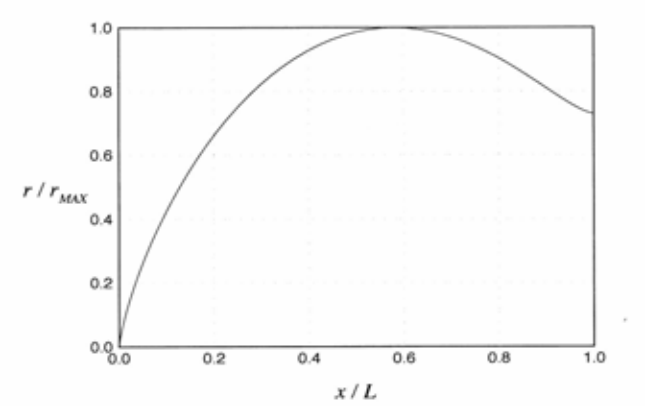

a) The Haack-Adams body of revolution, *l/d* = 10

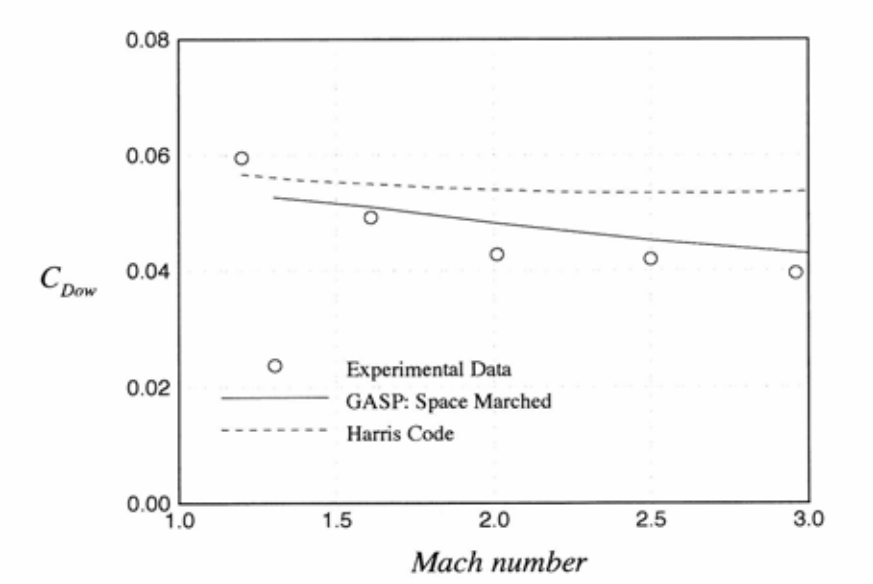

b) comparison of drag prediction for the Haack Adams Body.

Figure 10-43. Wave drag for a body of revolutiuon.[63]

The zero lift wave drag prediction for a wing shape is given in Figure 10-44 for the so-called Squire Wing.[64] The wing has a 9% thick biconvex airfoil section on the centerline and elliptic spanwise sections that ar picked to match the centerline airfoil. The wing may be a little thick for wave drag application but has wind tunnel data available for comparison. Below a Mach number of 2.2 the trend from the Harris code is correct. Harris overpredicts the drag as in the body of revolution case examined above.

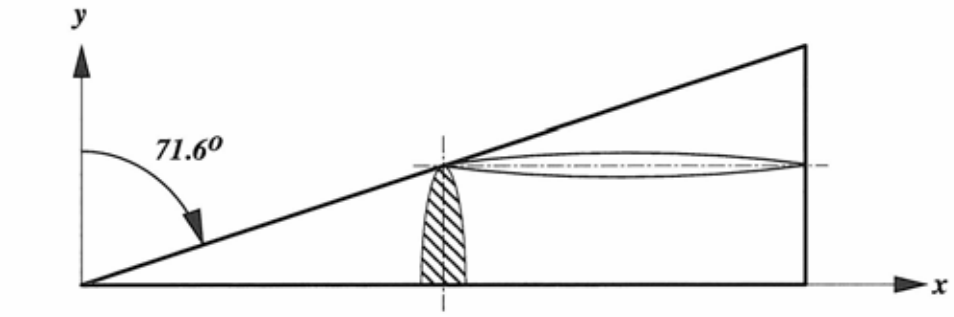

a) Squire Wing geometry

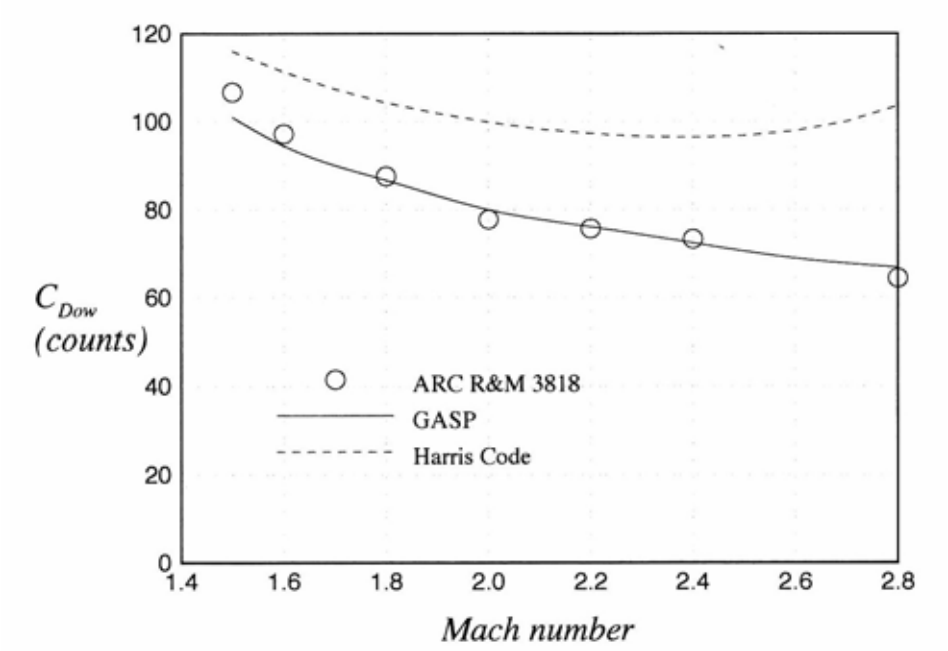

b) wave drag results

Figure 10-44. Wave drag for the Squire Wing[63]

We complete our examples of what to expect from the Harris code and a linear theory panel code by comparing results for a hypothetical high speed civel transport (HSCT) study from the same MAD Center Report that we used to compare wave drag above. Figure 10-45 shows the configuration and the grid. In much of our work we used the space marching option in GASP to reduce computer time. As long as the flow is supersonic we can replace iterations in time with iterations in space, starting at the nose and marching downstream. This scheme was key to our optimization work that required 1000s of analysis runs. We were fortunate to be able to use an automatic grid generation code written by Ray Barger at NASA Langley.[65,66]

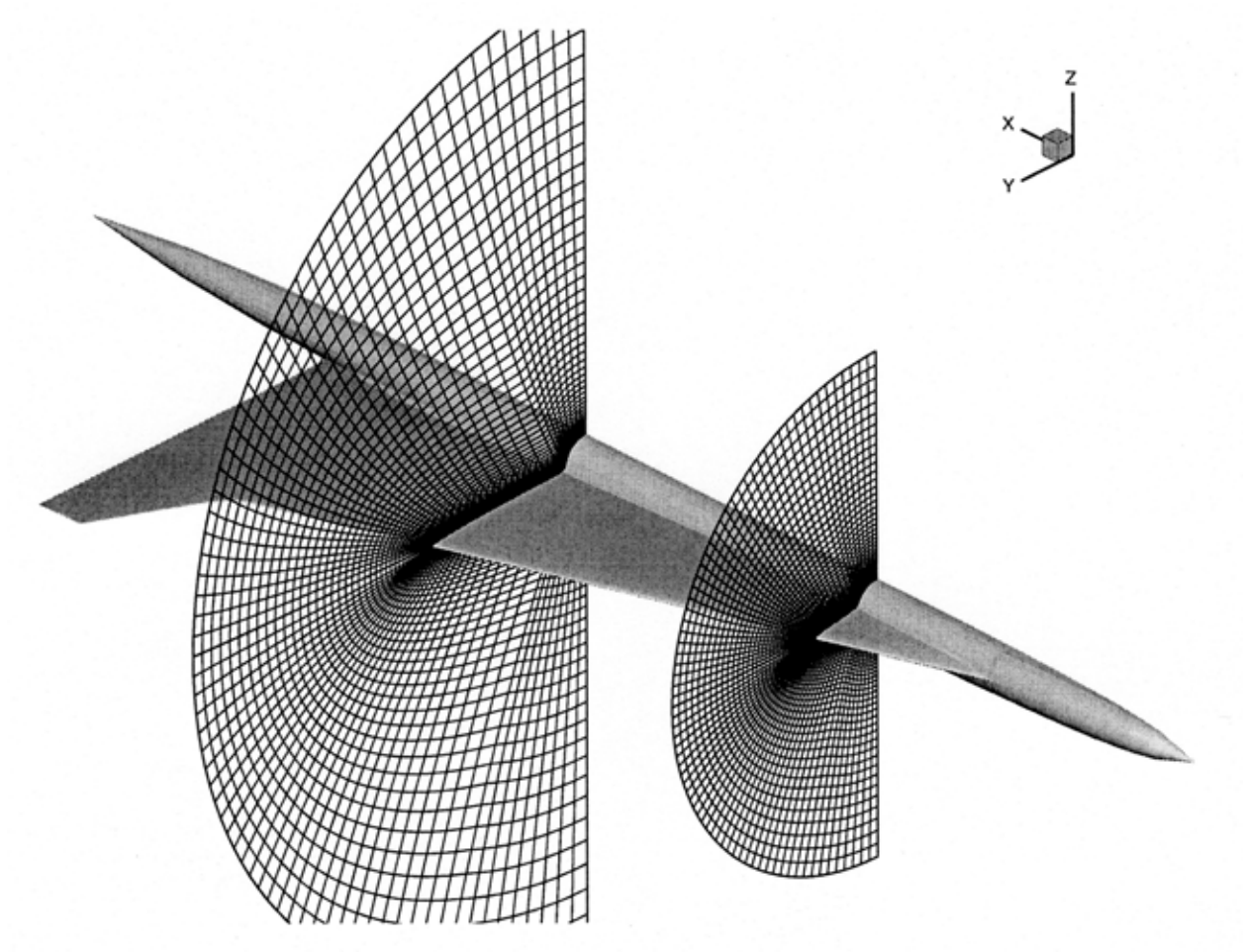

Figure 10-45. HSCT Configuration and the associated grid.[63]

Figure 10-46 compares the lift and pitching moment estimates from CFD and linear theory at $M = 2.4$. Both the linear theory and Euler results include skin friction, although they don't influence these estimates. The figure also contains the predictions from GASP using the Parabolized Navier-Stokes (PNS) option in GASP (and uses the Baldwin-Lomax Turbulence model, which can be expected to be accurate for attached flow). The linear theory overpredicts the lift slightly, as well as being slightly different for the pitching moment. However in general it appears that the simpler methods can provide valuable information.

The drag polar comparison is presented in Figure 10-47. This is the most important comparison for design. We will look at the values at the design C_L of 0.082, C_D(PNS) is 79.2 counts, the C_D for Euler plus c_f is 78.9 counts, and the C_D for linear theory and skin friction is 77.1 counts. We see that the linear theory predicts a drag that is consistently low. The Harris wave drag estimates are within 2 counts of the CFD value. The skin friction estimate is about 1 count higher than the PNS prediction. So at first glance it appears that the Harris plus linear theory plus skin friction provides an excellent estimate. The drawback is that for this case a 2 count drag underprediction results in a 120 nm overestimate of the range. This illustrates how sensitive the HSCT design was to drag. Eventually the HSCT program was cancelled, and presumably it was in part because of the extreme requirements, as reflected in the sensitivity to drag.

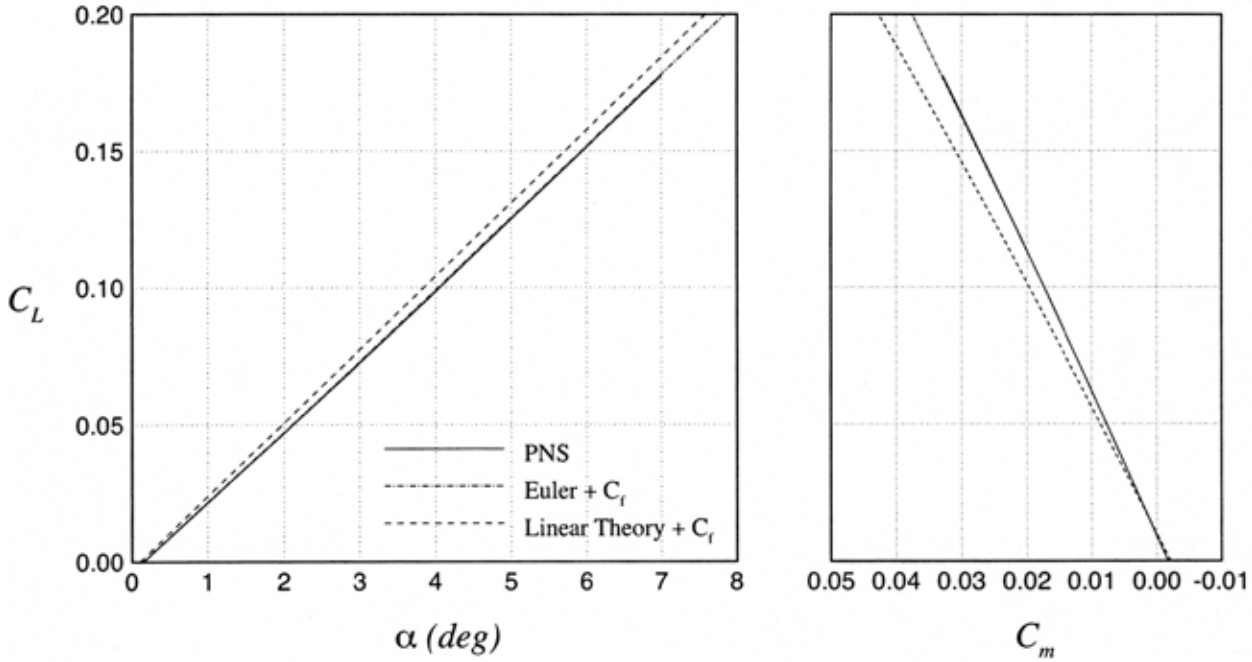

a) lift coefficient b) pitching moment coefficient

Figure 10-46. Comparison of lift and moment predictions[63]

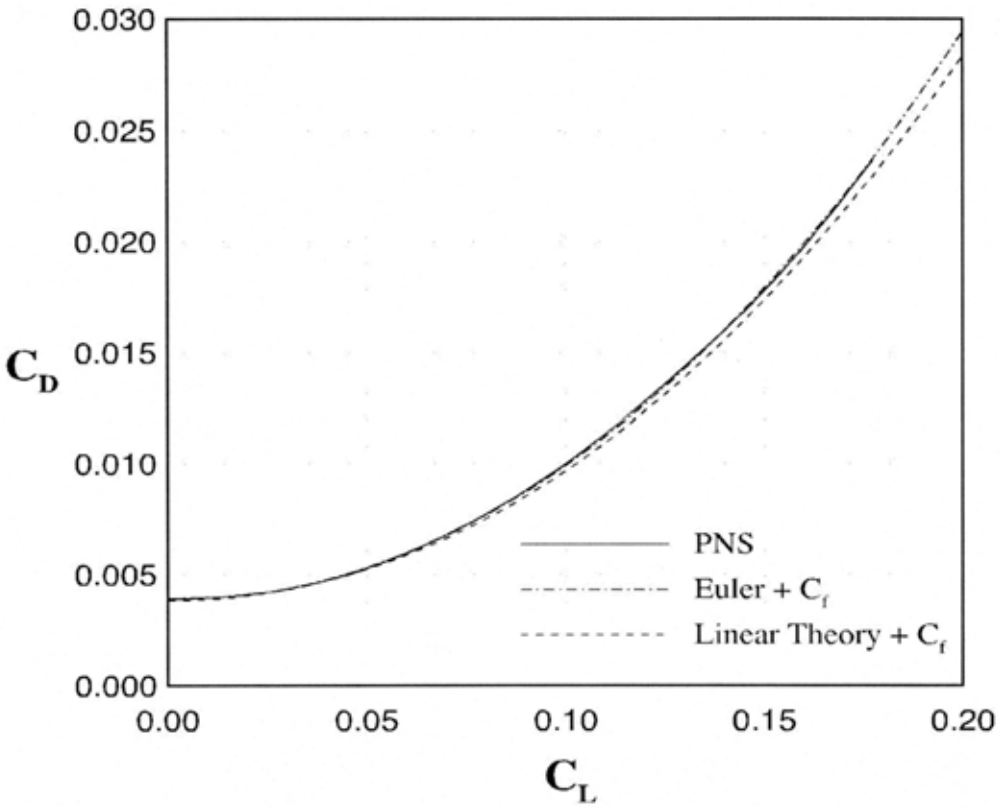

Figure 10-47. Comparison of drag predictions.[63]

Figure 10-48 is the final example of basic linear theory. The model is a mid-mounted wing swept 45° on an ogive sylinder body. It has an NACA 64A005 airfoil section. The correlation between wing pressures from a wind tunnel test[67] and predictions from the panel method code known as Woodward II[68] is pretty good. But the reason I'm including this figure is to make the point that for a supersonic trailing edge there is no Kutta condition and the upper and lower surface pressures don't come together. For highly swept wings we often look at spanwise pressure distributions and this feature of the trailing edge behavior isn't readily apparent. Students should be aware of this difference between subsonic and supersonic flow.

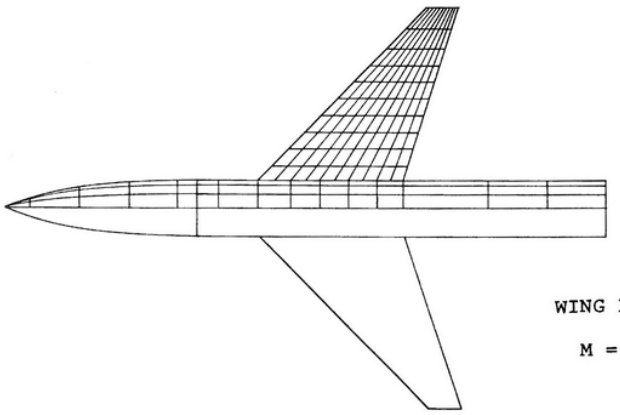

a) Ogive Cylinder Body with Mid-Mounted Swept Wing

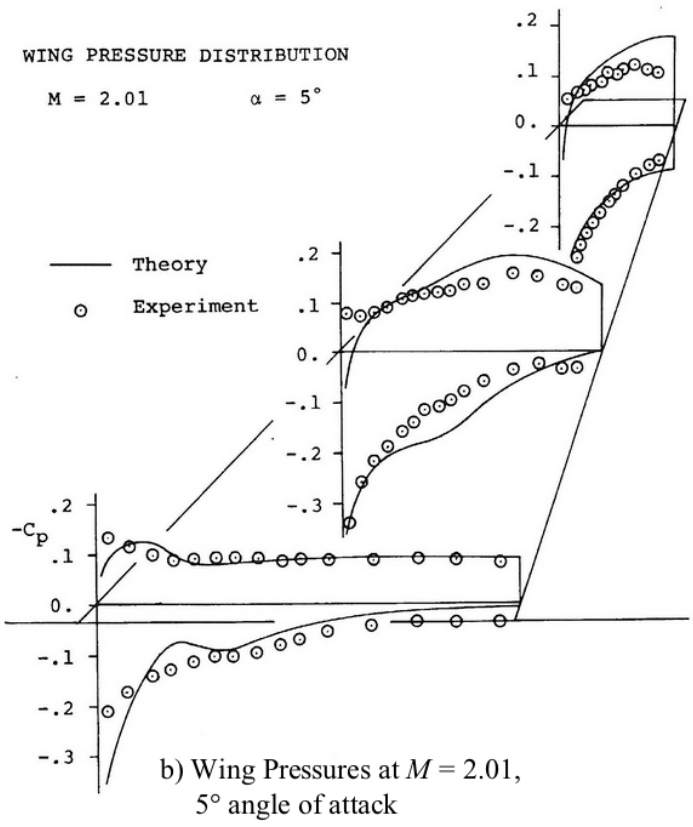

b) Wing Pressures at $M = 2.01$, 5° angle of attack

Figure 10-48. Comparison of Woodward II with pressures from a wind tunnel test.[67,68]

The linear theory tools available can be used very effectively to understand supersonic configurations. Before undertaking your own studies there are a few aspects of supersonic aerodynamics that are worth understanding.

Wave Drag: It is important to remember to subtract the capture area from the cross-sectional area values. Although the wave drag code does this automatically, students should be aware that this is how it's done. In addition, although we often talk about the Sears-Haack body as a minimum

wave drag value, opening up the base leads to an even lower value of drag. I suggest "playing" with the simple interactive MinDrag code on the software site. Of course base drag would have to be added to the wave drag. Often we assume that the base is the exhaust nozzle from the propulsion system and so there is no base drag. The Harris code is available from the PDAS site.[19]

Wing camber to reduce drag due to lift: At supersonic speeds the minimum drag design for a typical cruise lift coefficient (often 0.1 or less) has very little camber and twist compared to the camber and twist used in subsonic and transonic wings. The camber and twist tends to achieve a drag level essentially the same as a flat surface achieving 100% suction (of course this is zero for supersonic leading edges). This was surprising to me when I observed this. Linear theory methods nornally provide optimization options allowing the drag due to lift to be minimized subject to constraints on the specified lift coefficient and trim. This is an important advantage for these methods. For a supersonic planform we often think of the wing camber and twist as being combined and designated "warp." Three panel method codes are available at PDAS,[19] TEA201, the Boeing wing design methods originating from their US SST work,[69] the original Carmichael-Woodward Code,[70] and the combination of Woodward versions with other capabilities, W12SC3.[71] Several survey papers should be read or reread to review key aspects of supersonic configuration design before designing a new configuration.[72,12,73]

10.9.2 Modifications to linear theory: Attainable Thrust

"Normal" linear theory supersonic methods are weak with respect to the amount of leading edge suction predicted. Over many years Harry Carlson at NASA Langley developed a modified linear theory to address the problem. After studying massive amounts of experimental results he developed the concept of "Attainable Thrust", that supplements linear theory with an empirically-based expression for the degree of leading edge suction that should be expected in practice. Work was summarized together with a discussion of wing design in NASA TP 3202.[74] A final version of the attainable thrust formulation was published in NASA TP 3557.[75] This led to development of a design method to determine the wing camber and twist required to get the best possible wing.[76] The code is known as WNGDES, we will describe an application below.

10.9.3 Nonlinear aerodynamics of supersonic wings

To do wing design in conditions where linear theory may no longer be applicable we need to use higher fidelity methods. One way to include better physics was found using the full potential flow conical flow theory, not the linear theory approximation. It provides an excellent framework for thinking about wing design at supersonic speeds. For highly swept wings used at supersonic speeds, the equivalent of an airfoil on a moderately swept high aspect ratio transonic transport wing is the spanwise section. To analize spanwise sections on supersonic wings the first modern computational method used the full potential equation. The method solved the flow in the crossplane between the bow shock and the spanwise geometry on the wing (actually a spherical cut).[77] In this plane the crossflow can become "supercritical" and the result is that a crossflow shock wave may arise for high lift coefficients, just as the shock wave occurs in transonic flow over a two-dimensional airfoil. The full potential flow model is a good approximation under conditions where the shocks are not too stong. Extensive comparison with theory was done to validate the method for these applications.

The code developed to make this calculation is known as COREL for COnical RELaxation and several supersonic maneuver wings were designed and tested at supersonic speed. The idea was

to shape the spanwise section to control the crossflow such that the crossflow shock was weak. This concept was known as SC3, or SuperCritical Conical Camber. Wings tested in the NASA Langley Unitary Plan wind tunnel demonstrated that the full potential method could be used to design wings with superior performance.[78] SC3 will be discussed in more detail in Section 10.10.2. The conical flow code was extended to handle nonconical flows and was known as NCOREL.[79]

Today an Euler code would be used. The advantage of the approach used in COREL and NCOREL was that the grid generation was done as part of the calculation, removing that, often time consuming, step from the computational process.

10.10 Supersonic Airplane Configurations Design Examples

We conclude this chapter with examples of supersonic airplane and wing design experience.

10.10.1 The US SST Story

In the 1950s and 1960s the public assumed that rapid advances in aircraft performance would continue and the next step would be supersonic commercial passenger travel. The experts recognized that a supersonic transport would a difficult to achieve. Essentially no aircraft company could do this alone. By 1962 the British and French had merged their individual work into a single program and had agreed to build Concorde.

In response to the Anglo/French Program, and also because the Soviet Union was developing a supersonic transport, in 1963 President Kennedy made a US SST aircraft a national program. This was very much in the spirit of "the US has to be the leader." The following timeline recounts what turned out to be a poor decision. Since the program was too big for one company, a national program funded in large part by the government and administered mainly by the FAA (did they have experience with aircraft design?) was established. A very brief description of events is:

- Aug. 15, 1963: FAA Issues an RFP
- May 15, 1964: The FAA selects Boeing and Lockheed to propose the airframes, and General Electric & Pratt &Whitney to propose the engines
  - –Lockheed proposed a double delta
  - –Boeing proposed a variable sweep wing
- Dec. 31, 1966: Boeing and General Electric are selected to build the SST
- Oct. 21, 1968: Boeing abandoned the variable sweep concept
- Mar. 24, 1971: The program was cancelled by congress.[*]

A little more information may be helpful. The US SST was to be much bigger than the Concorde and fly faster. This necessitated using titanium instead of aluminum, a very difficult and expensive difference between the airplanes. During the time the design was being developed the government ruled that there would be no supersonic flight over the US (many other governments also made this restriction). Note that the much heavier US SST would have generated a stronger sonic boom than the Concorde. All the while, Boeing was discovering a multitude of problems with their variable sweep concept, as we'll see below. The US design was becoming much more

[*] As a student during this period I was very disappointed, although in hindsight the program cancellation was the right decision.

expensive. Congress was asking why the government should be expected to support this program. To add to the confusion, the noise, both around the airport and from the sonic boom, was not the only issue. Environmental concerns had emerged everywhere, and the SST was predicted to destroy the ozone layer. The result of all these issues was that the program was cancelled.

Despite controversy over noise and environmental pollution the Concorde entered service in 1976. Its last flights were in 2003.

Figure 10-49 compares the different planform for SSTs.[80] The Boeing 2707-300, that was the final proposed design, is clearly much larger than the others.

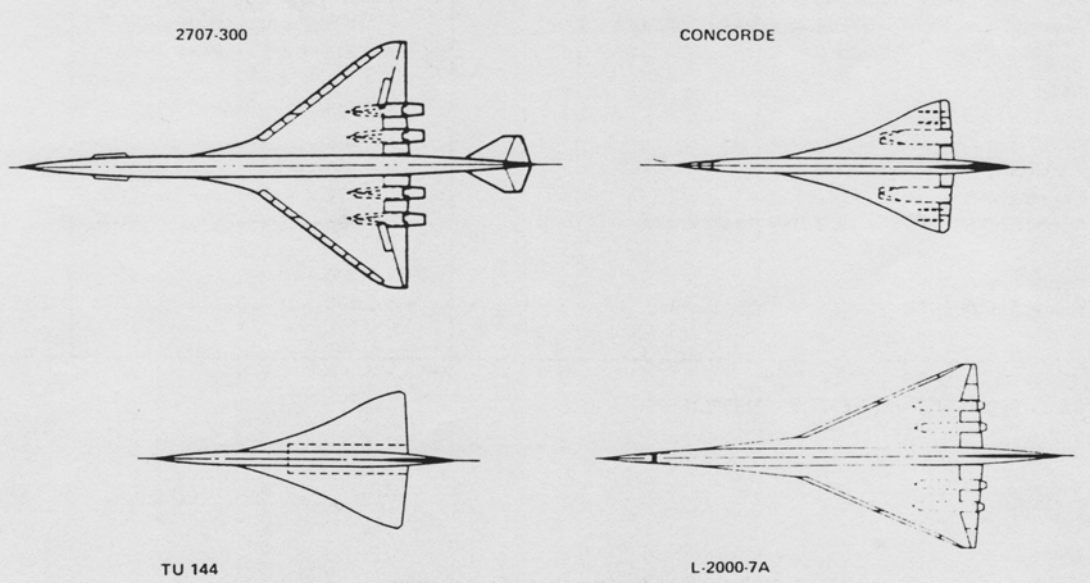

Figure 10-49. Comparison of Supersonic transport concepts.[80]

The paper by Swan is well worth reading. He describes the evolution of the configuration and includes a description of design criteria used in developing the final configuration. Any supersonic airplane designer should read Swan's paper. The issues he discribes are just as valid today as they were back then. Also of note is that the Boeing 2707-300 had a horizontal tail, while the other designs were tailless. Swan explains this also. Essentially although the horizontal tail contributed little to the stability at low alpha (Remember the term $(1 - d\varepsilon/d\alpha)$? It can be very small or negative for a tail behind a huge wing), at high alpha it helped prevent the configuration from pitching up.

It is worth taking a look at the initial design. The original variable sweep wing had become what can only be described as a monstrosity. Figure 10-50 shows the design, Boeing 2707-200. The figure is from a review by Leroy Spearman.[81] Since Spearman worked at NASA Langley his review also covers the Langley work. The Boeing 2707-200 had engines that were mounted on the horizontal tail. The inboard engines were mounted behind the landing gear (not shown in Spearman's figure). To avoid ingesting the landing gear wake and any spray from a wet runway, a ramp was used to provide air for the inboard engines from the wing upper surface. Clearly the design was out of control! Figure 10-50 doesn't do the problems justice. Figure 10-51 is of a plastic model that was sold at the time.

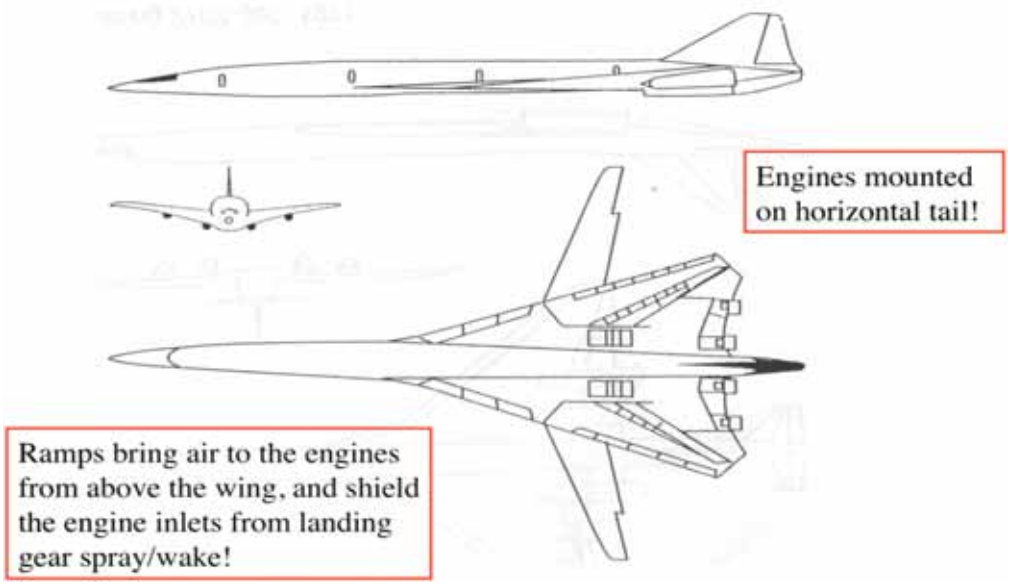

Figure 10-50. Boeing design 2707-200[81]

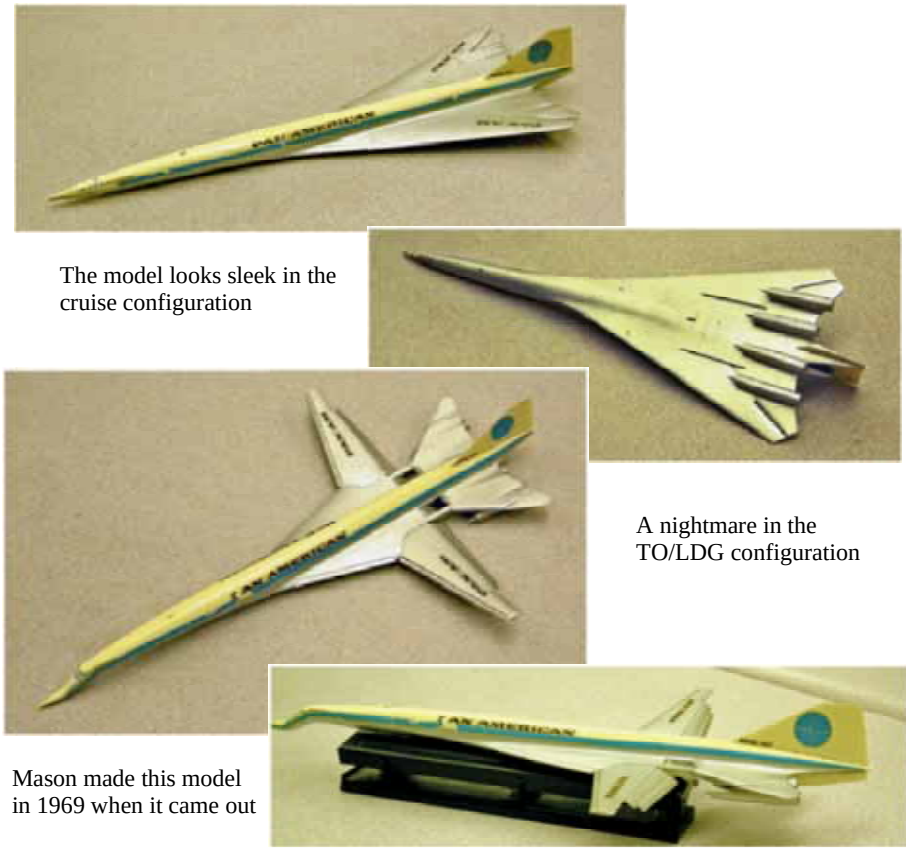

Figure 10-51. Photo of the plastic models of the Boeing 2707-200 (Mason photo)

Figure 10-51 shows the upper and lower surface for both the cruise and low speed configurations (the landing gear have been broken off for many years). The cruise configuration does indeed look terrific. However, look at the landing configuration. First see that instead of the single drooped nose on the Concorde, the plane has a double droop design. Then note that high lift

system and airflow ramps are much more complicated than the impression given in Figure 10-50. Taken all together it's easy to see why the design was abandoned. I can't imagine the chaos that was going on inside the project. There's another key issue. We have neglected aeroelasticity in most of our discussions, but this was also a major problem. Figure 10-52 is from a paper Kumar Bhatia wrote when the government resurrected SST design, this time calling it the High Speed Civil Transport (HSCT).[82] Clearly aeroelasticity needs to be included immediately in the design process.

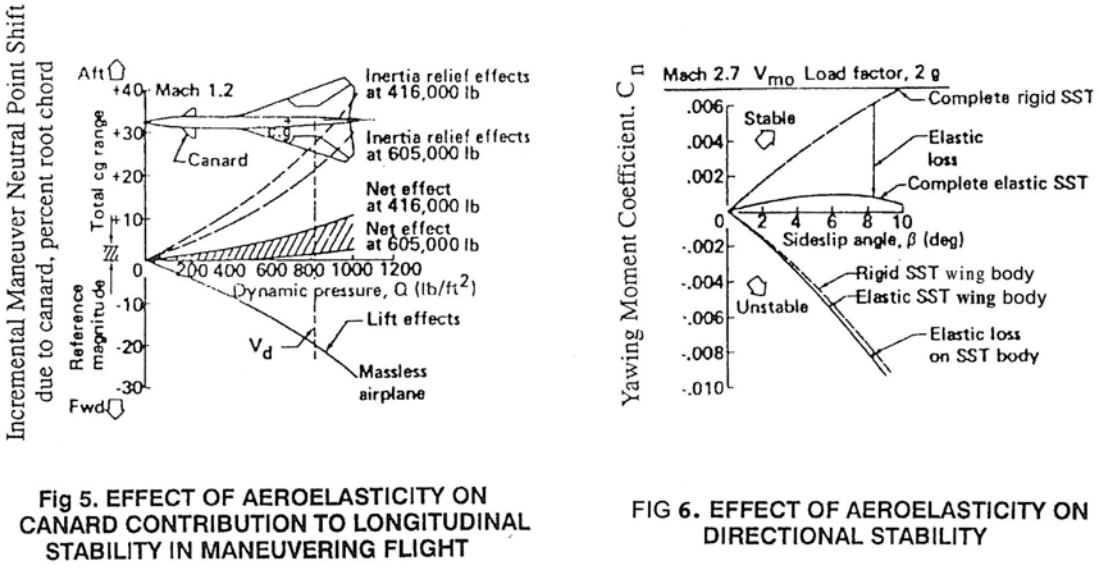

Figure 10-52. Aeroelastic effects were important.[82]

Once the Boeing engineers realized that the variable sweep wing concept had to be abandoned they selected a fixed delta wing with a horizontal tail and a slight inboard glove. Many of the Lockheed engineers are of the opinion that Boeing decided to build the Lockheed design. Looking at the designs that position seems to be a little bit of a stretch. At the time there was a discussion of re-competing, but it was decided to continue with Boeing as the airframer. The resulting redesign was known as the Boeing 2707-300 and is shown in Figure 10-53 from Swan's paper. It was obviously much simpler. Although the plane was still supposed to fly at Mach 2.7, most of the wing was swept at 50° and thus had a supersonic leading edge. This must have been hard for the NASA Langley engineers to accept. It points to the importance of making the design with all the considerations, not just aerodynamics. We'll see this below when we discuss the HSCT and MDO.

Erik Conway has written a book that I perceive to be an accurate description of the US SST program.[83] I got interested in the book because it also describes the HSCT program of the 1990s. Often and naturally, authors frequently describe programs from a personal viewpoint that may not be entirely objective. Conway's book strikes me as being a candid description of all the complicating events. He is an historian and combines both the technical issues and the political environment that is ever present in large government programs. This is another book well worth reading.

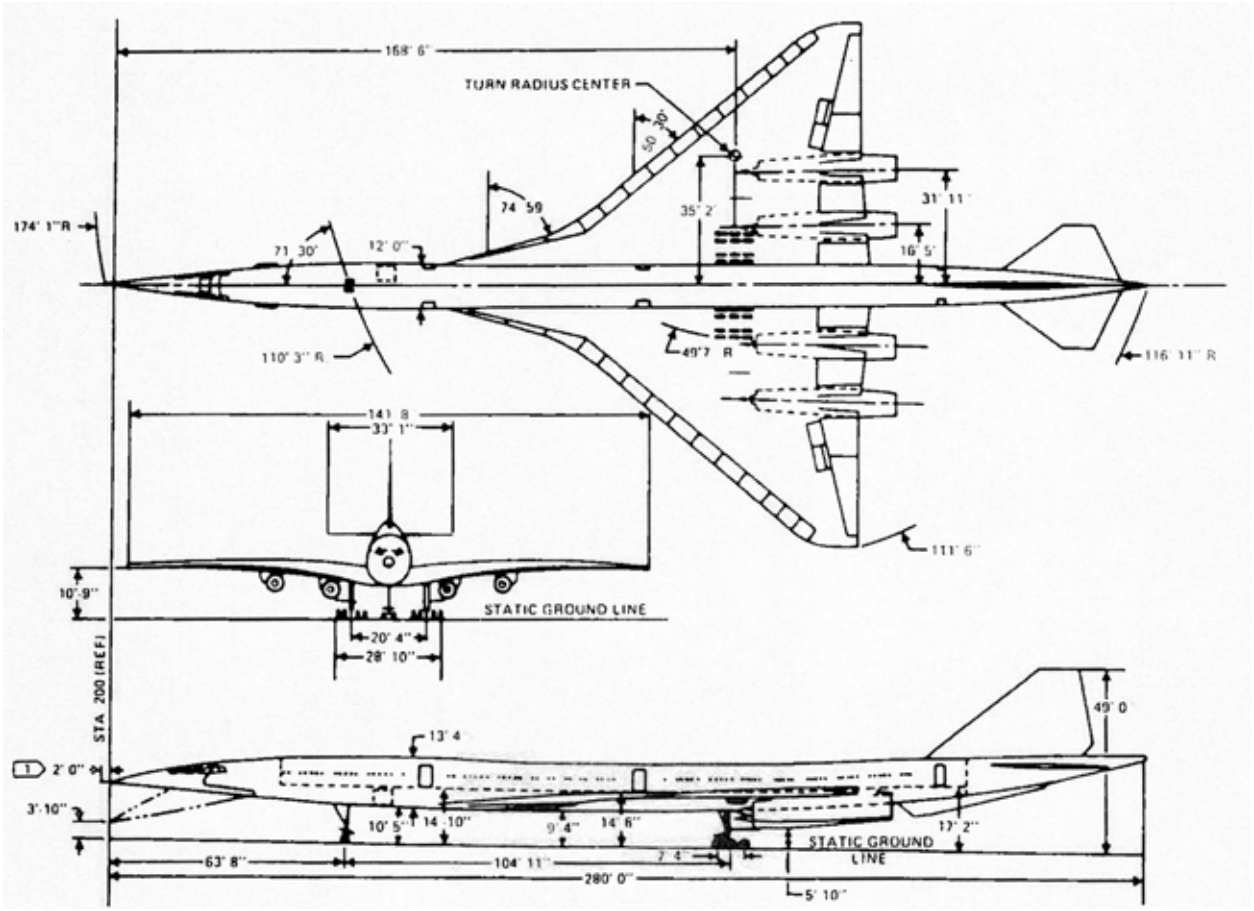

Figure 10-53. Final proposed design, Boeing 2707-300[80]

10.10.2 Supersonic Maneuver Wing – Transonic Aerodynamics at Supersonic Speed

In the late 1970s, in the early stages of the ATF program, there was interest in the design of a wing capable of maneuvering efficiently at supersonic speeds. As the supercruise requirement emerged it was clear that efficient supersonic maneuvering could be a requirement also. As previously discussed, linear theory was adequate for cruise design. However, it was not adequate for maneuvering C_L's. This shortfall was shown in work from NASA Langley, as illustrated in Figure 10-54.[84] Although linear theory predicted good performance, wings designed and tested at higher C_L's fell short of the predictions. The requirement for supersonic maneuvering meant that C_L's well above the linear theory limit would be required. The figure also shows the expected maneuver C_L's.

We have included this discussion on supersonic maneuver wing design because it shows how an understanding of flow physics can be used to develop an aerodynamic concept. Rudy Meyer at Grumman realized that there was a close correspondence between the 2D full potential equation that was then being solved numerically at transonic speeds and the full potential conical flow equations for supersonic flow[85].* He knew that the same techniques could be used for supersonic

* Recall that the classic version of the full potential flow model used for early two dimensions transonic flow calculations has coefficients that cause the type of the equation to change between elliptic and hyperbolic. Rudy recalled that at supersonic speeds the potential flow model for conical flow had a very similar structure, so that the numerical methods used for 2D transonic flow would be directly applicable for supersonic conical flow.

conical flow. He had also read a paper by Clint Brown that attributed the performance shortfall of wings designed by linear theory to the presence of cross-flow shocks on the wing.[86] Rudy was sure that a numerical method that included cross flow shocks could be used to shape the spanwise wing section to reduce the strength of the cross flow shock. The resulting concept was called SuperCritical Conical Camber, SC3.

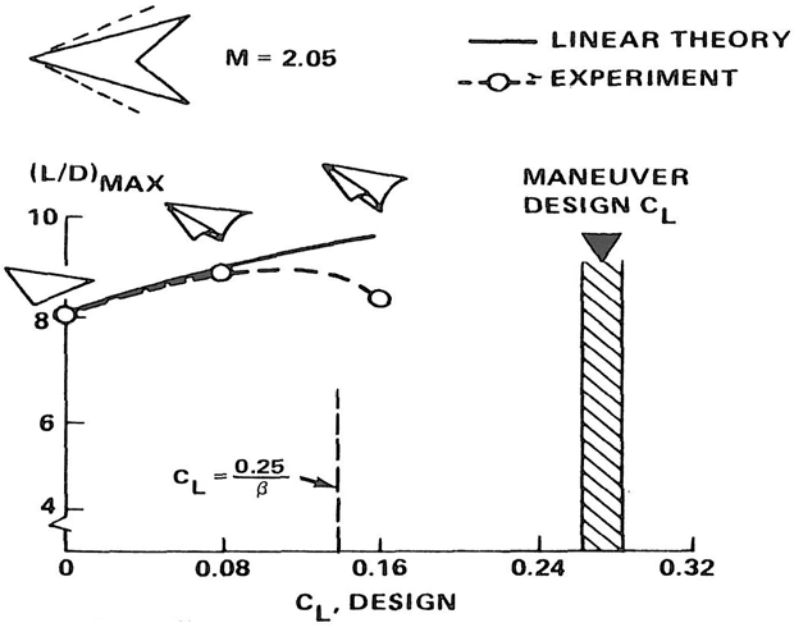

Figure 10-54. Experience with linear theory wing design and maneuver requirements.[84]

Figure 10-55 from the final report on this work[78] shows an illustration of the flowfield physics and the associated spanwise pressure distribution. Part A is a schematic that shows a conical geometry and the spanwise section pressure distribution that will be used to do the design. Part B shows the predicted spanwise pressure distribution for an uncambered conical wing computed using the full potential flow model that can include the supercritical crossflow shock and the prediction from linear theory that clearly can't include the key physics of the flowfield. Clearly the nonlinear effect has to be included on the calculation.

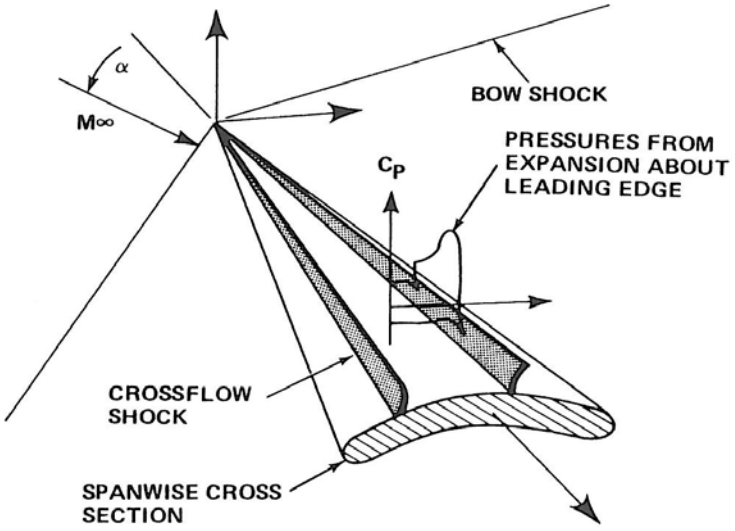

A. TYPICAL FLOW IN CROSSFLOW PLANE

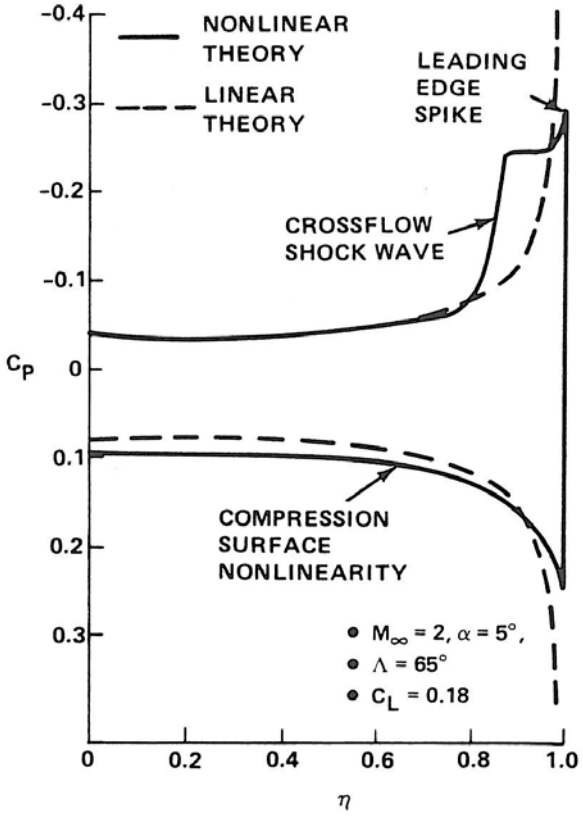

B. UNCAMBERED DELTA WING WITH ELLIPTIC THICKNESS DISTRIBUTION

Figure 10-55. Conical flow and related spanwise pressure distribution (concluded).[78]

The program to design a wing demonstrating controlled supercritical cross flow was carried out in a series of steps. The following history illustrates a physics based approach to aerodynamic development:

- SC3 was conceived by Rudy Meyer in 1977.
- The program concept was developed by Gianky DaForno in 1977and funded by NASA.
- The computational method COREL was developed by Bernie Grossman in 1978.
- Aerodynamic design was done by W. H. Mason from 1978 to1982 in cooperation with NASA Langley, primarily Dave Miller.

The SC3 program included three wind tunnel entries in the NASA Langley Unitary Wind Tunnel. To start, two purely conical wings were designed, built and tested. One was flat, the other cambered based on the computational design work. This wing was termed the "conceptual wing" and was designed using iterative analysis with COREL. Initially the wing used a simple cambered spanwise shape. The thickness distribution used a so-called superellipse, with the leading edge slightly "rounder" than a typical parabolic nose shape. The crossflow shock was considerably weaker than the flat wing. Next, local shaping was used in the vicinity of the cross flow shock to completely eliminate the cross flow shock. This was done by reducing the spanwise curvature around the crossflow shock in the same way that Whitcomb had reduced the shock strength for transonic supercritical airfoils. Figure 10-56 shows both the initial spanwise camber design and the final shockless supercritical crossflow design.[84] The model using this shape and a photo of model in the wind tunnel are shown in Figure 10-57.[84] Figure 10-58 shows the resulting pressure distribution at several angles of attack. The results were considered highly successful.[84]

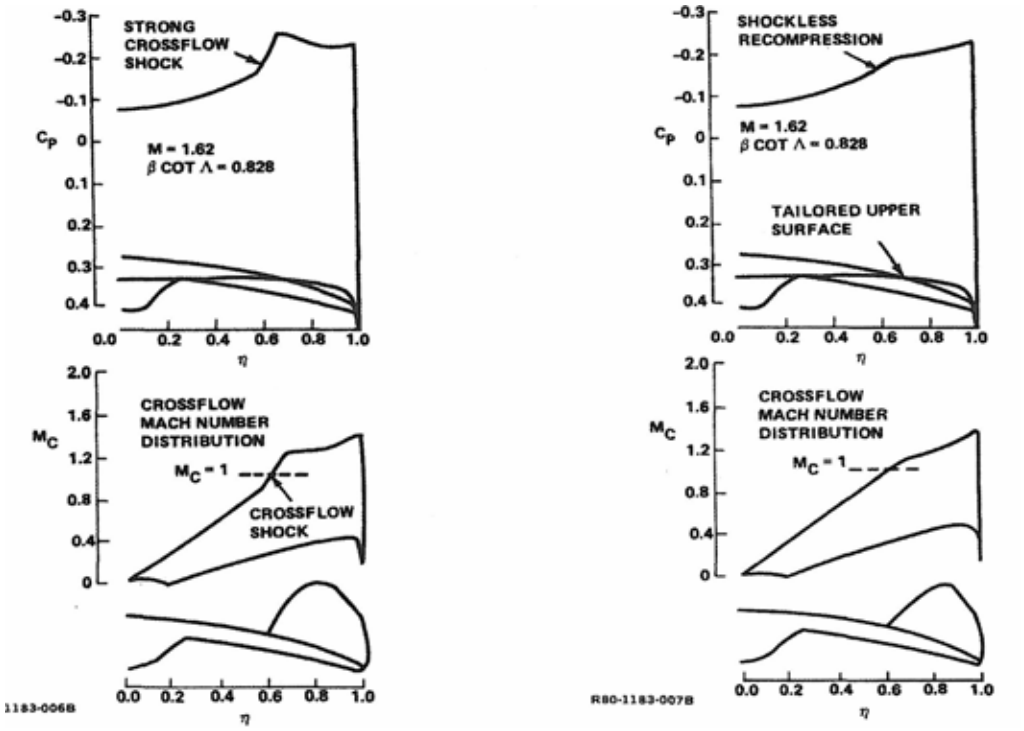

Figure 10-56. Example of conical flow design, showing the crossflow Mach number distribution.[84]

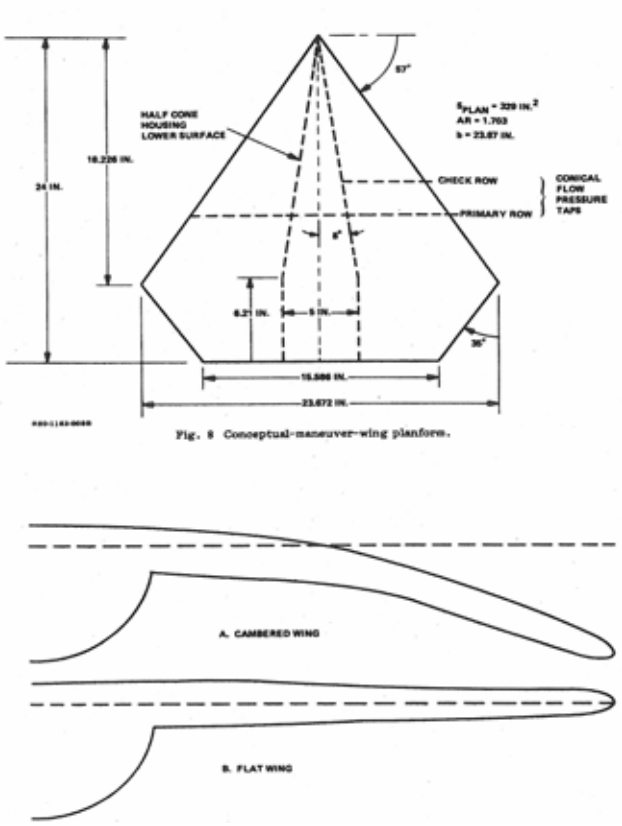

Fig. 8 Conceptual-maneuver-wing planform.

a) the conical Conceptual Wing

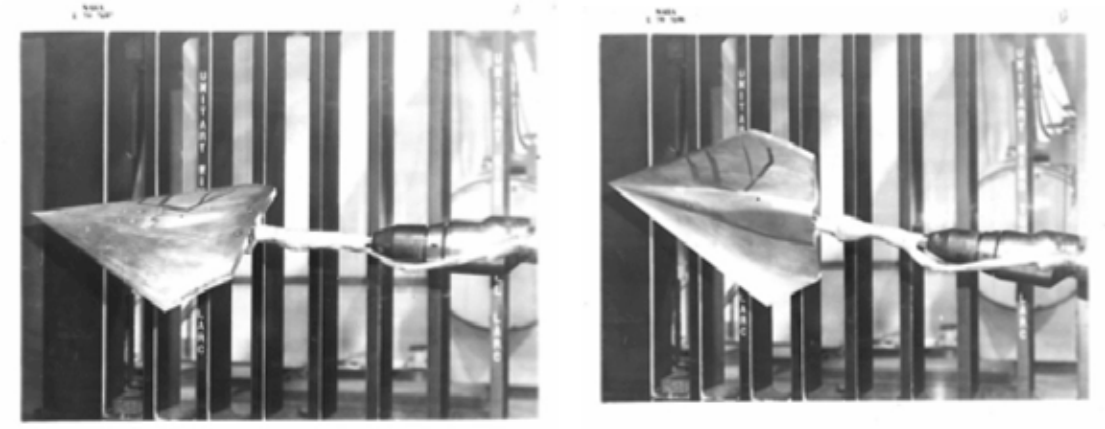

b) top and bottom views of the conceptual wing in the tunnel

Figure 10-57. The Conceptual Wing design and the model in the wind tunnel (concluded).[84]

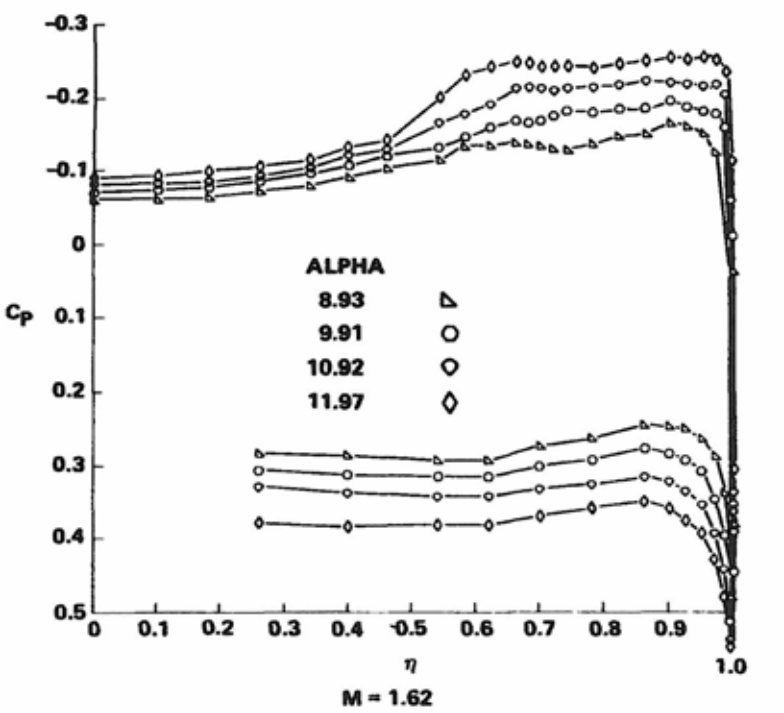

Figure 10-58. Spanwise Pressure distributions at $M = 1.62$ at several angles of attack from the wind tunnel test, showing the shockfree recompression of the supercritical crossflow.[84]

The next step was to design and test a three-dimensional wing using the SC3 concept. This was called the "Demonstration Wing." Figure 10-59 shows the demonstration wing. The drag polar from the wind tunnel test is shown in Figure 10-60. At a lift coefficient of 0.4 a 21% drag due to lift reduction was achieved compared to the 0% and 100% leading edge suction envelopes. The work is described in the paper by Mason, et al.[87]

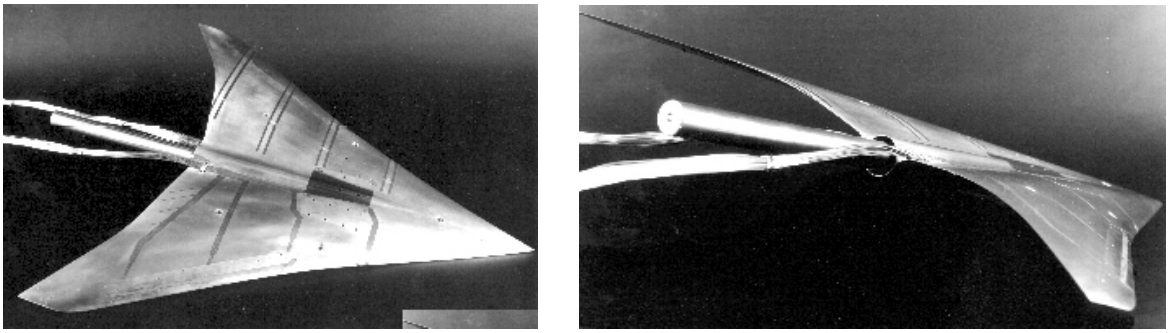

a) upper surface view b) aft quarter showing spanwise camber

Figure 10-59. SC3 Demonstration Wing. The rows of spanwise pressure taps are shown coved by tape.[78]

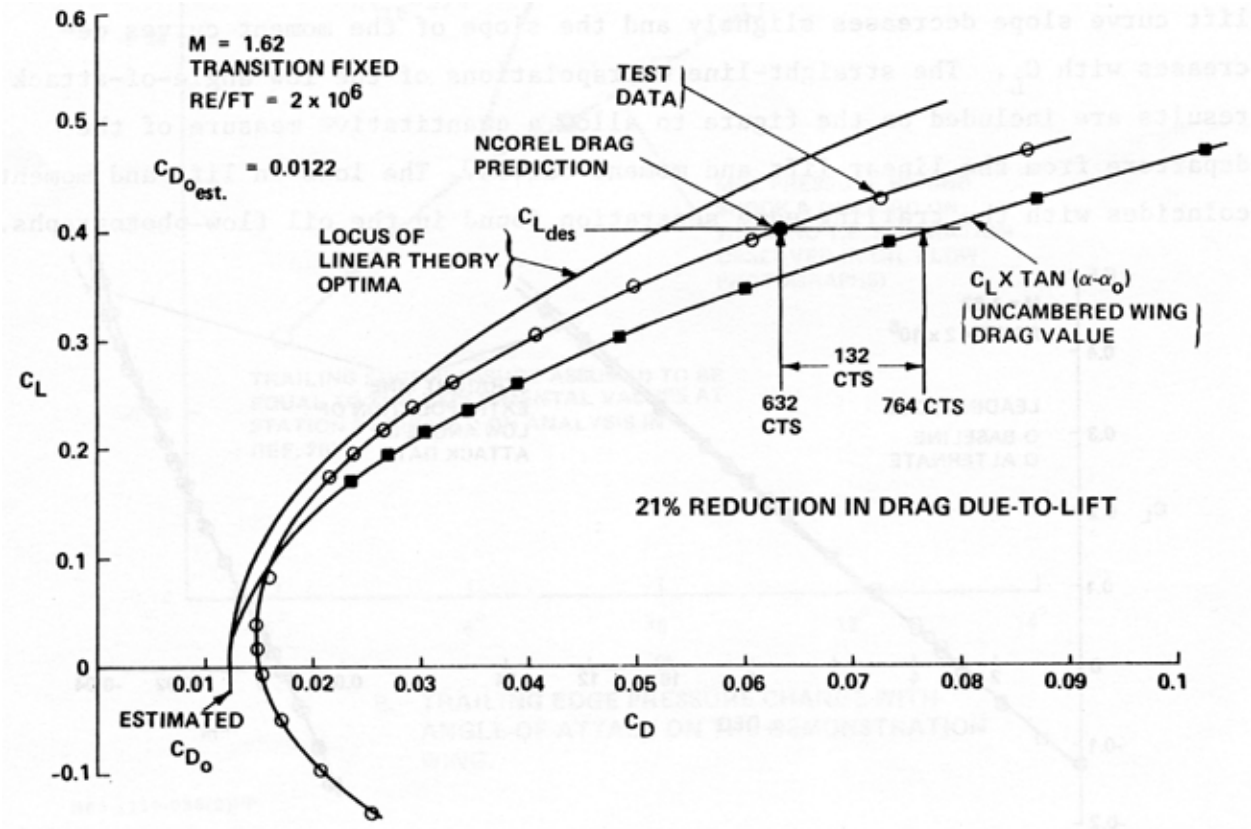

Figure 10-60. The demo wing drag polar78

The work produced a number of papers, both AIAA papers and NASA reports (The NASA reports are available for free online and contain details of the work and wind tunnel results with tab data. See NASA TP 1759, April 1981, NASA TP 2249, February 1984, NASA TP 2336, August 1984).

10.10.3 HSCT and MDO

In the 1980s NASA began to revisit the possibility of a supersonic commercial transport (supersonic research had continued as a low-level effort ever since the US SST was cancelled). The initial NASA study was for a tailless Mach 3 design exploiting the ideas of attainable leading edge thrust.[88] This design was wind tunnel tested.[89] Both McDonnell Douglas and Boeing were involved in the program (Boeing had not bought McDonnell Douglas yet).[90,91] After these studies a Mach number of 2.4 was chosen as the HSCT design Mach number. The companies also investigated control issues for an HSCT.[92,93] Although the program was not classified as such, access was restricted. Eventually the results of the work were made available and many papers were given at AIAA Meetings. See the book by Conway for details of the evolution of the program.[83] The public planform was known as Reference H, and is shown in Figure 10-61.[94] The design Mach number was 2.4, and it was required to have a range of 5,000-6000 nm. It was intended to carry from 250-300 passengers. The notional TOGW was 700,000 lbs.

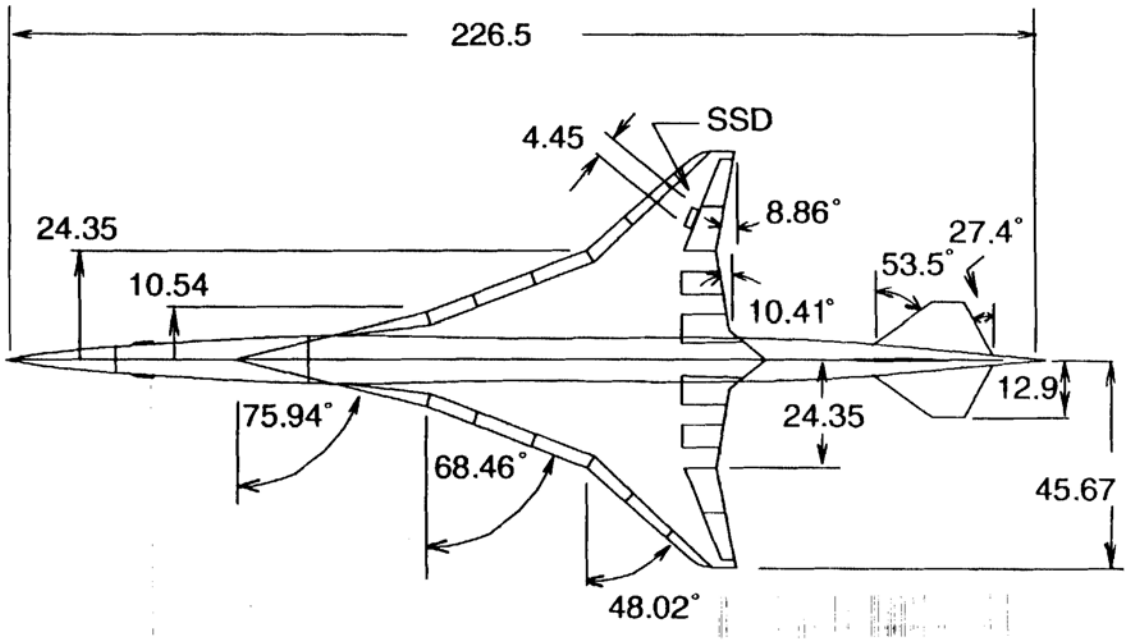

Figure 10-61. The public Reference H HSCT Configuration, NASA/TM-1999-209702, Kemmerly, et al.94

At the Reference H configuration cruise Mach number the major portion of the leading edge is subsonic. The planform is much closer to the ideas we described above for the so-called modified arrow wing. This design was pushing technology to the limit, and the sensitivity of the takeoff gross weight to drag was quoted as 10,400 lb per count. From work we will describe below we found a value of 14,000 lbs per count. From a commercial point of view this was too sensitive to be practical. Some of my peers at NASA turned this around to say that if the drag could only be reduced by a few more counts the design would be a success. Nevertheless, concerns over the environment, both noise (community and sonic boom) and emissions concerns about high-altitude atmospheric chemistry, remained formidable challenges. These concerns, together with the uncertainty about economic viability resulted in the program being cancelled. The story is well-told by Conway.[83]

10.10.3.1 Multidisciplinary Design Optimization, MDO

As part of the HSCT program a near ten-year program developing MDO methods for the HSCT design was conducted at Virginia Tech, as well as other universities. The work explored a number of approaches to MDO. The key objective was to find ways to include high fidelity disciplinary analysis methods in conceptual design, where the high fidelity methods could have the most impact. The primary disciplines included consisted of aerodynamics and structures. Numerous constraints were specified. Some of these were practical geometric constraints, but many also addressed trim and static stability and control requirements. Figure 10-62 is a nominal statement of the optimization problem. One of the key issues was the development of a general parametric geometry model, where the parameters could be used as design variable in the optimization, as described in the figure. Numerous variations of this problem were investigated.

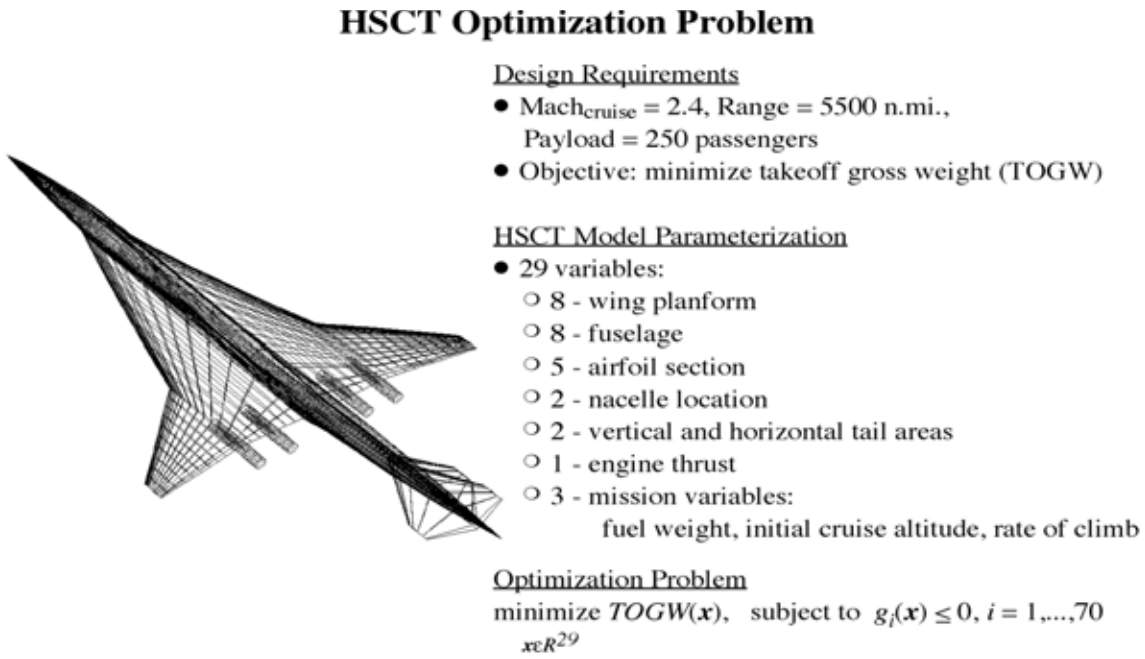

Figure 10-62. The Virginia Tech HSCT optimization problem.

There were a variety of outcomes from this work. Perhaps the key understanding was that it was impractical to include high-fidelity analysis methods into a "giant" program. The term we used was disaggregation.[95] Instead, it was necessary to represent the disciplines by models that could be used during the optimization. These models are termed *response surface models* by the statisticians. There were several reasons for this. First, we were interested primarily in using gradient based optimization. Just about any analysis method will produce slightly "noisy" results as geometry changes are made (shocks bounce between grid lines, etc.). Gradient-based optimizers are extremely sensitive to this artificial noise. In addition, the experts can use the latest versions of their software to provide data for the models to be used in the optimization. Finally, in this approach the many analysis runs needed from an analysis code can be done simultaneously rather than sequentially. This allows the use of coarse-grained parallel computing to reduce the time required to do a design. The models representing the disciplines can be used with a variety of optimization schemes. Because we found local minima in the design space the models could be employed with global optimization schemes. The models also allowed parameter studies to be made very easily. We've repeated some of the discussion given previously in Chap. 5, because this was the work that led to our preferred aerodynamic design and optimization process.

An example result from the HSCT optimization work described above is shown in Figure 10-63. That figure contains the results from two different approaches.[96] The first is termed a "variable complexity model", VCM, where low fidelity models for the aerodynamics are used together with a few high fidelity aerodynamic models. The other approach uses response surface models, termed Drag RS Optimum. Similar results are obtained. Note that in the process we used numerous different starting designs or "starting points." With the high dimensional design space used here there are many local minima in which a gradient-based optimization can get "stuck." Figure 10-64 show the convergence history of the optimization. An example of design space visualization illustrating the local minima issue is discussed in the paper by Knill et al.[97]

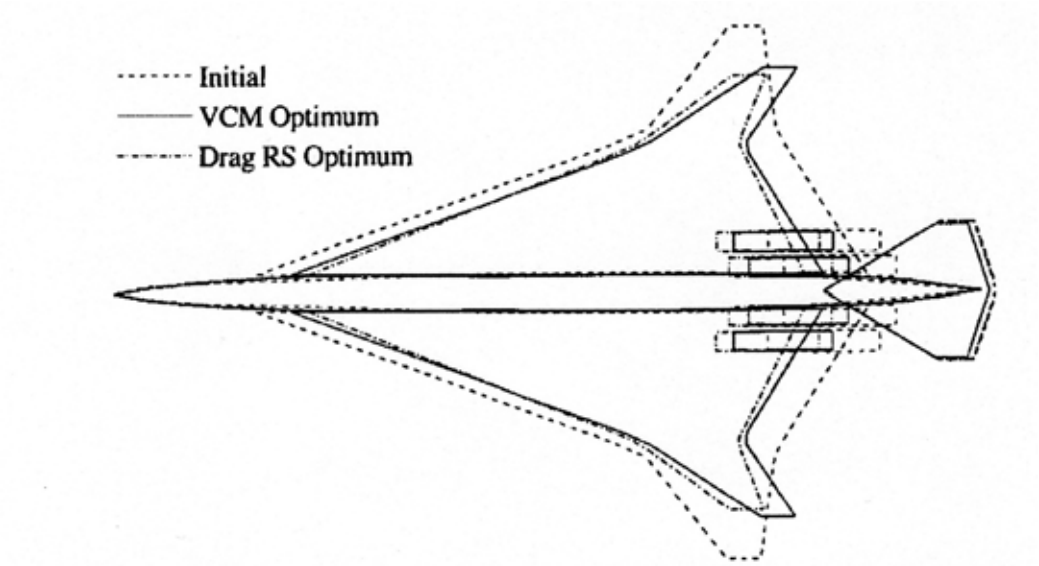

Figure 10-63. HSCT Planform from two different optimization approaches[96]

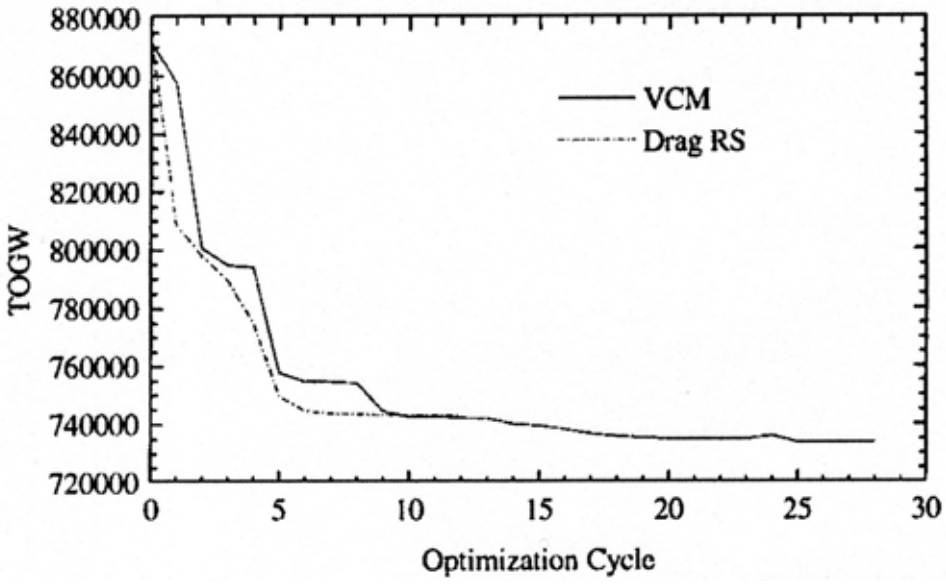

Figure 10-64. Weight reduction convergence history from different optimization approaches[96]

A great deal of work on this problem has been carried out by other researchers, and we cite two that are in interest.[98,99]

10.10.4 Design to reduce the strength of the sonic boom

As stated above, supersonic flight is not allowed over the United States as well as most other countries. This is a major limiting factor preventing the development of a commercial supersonic airplane. Thus attention in the research community turned to an effort to reduce the strength of the sonic boom. The goal is to reduce the boom strength enough that a new noise criteria can be established allowing low/no-boom strength supersonic flight over land. On August 27, 2003, a modified F-5 was flown at Edwards AFB demonstrating sonic boom shaping, proving that the strength of the sonic boom hitting the ground could be reduced.[100] The modified F-5 used for the demonstration is shown in Figure 10-65.

Examples of the theory that can be used to design low-boom concepts have been published by Li and Rallabhandi[101] and Rallabhandi, Nielsen and Diskin.[102] This is an area of active research.

The idea of the shaped boom research is to change the shape of the classic N-Wave associated with the sonic boom. Figure 10-66 shows the N-wave and a design from a paper by Aronstein and Schueler that reduces the sudden pressure jump.[103] Another idea is to use an extensible nose spike to make the length of an airplane longer. Figure 10-67 shows an F-15 modified to extend a nose boom in flight, termed a "Quiet Spike." This was a program conducted by Gulfstream and NASA from 2004-2007.[104]

Figure 10-65 Demonstrator for the shaped boom test. (NASA Photo)

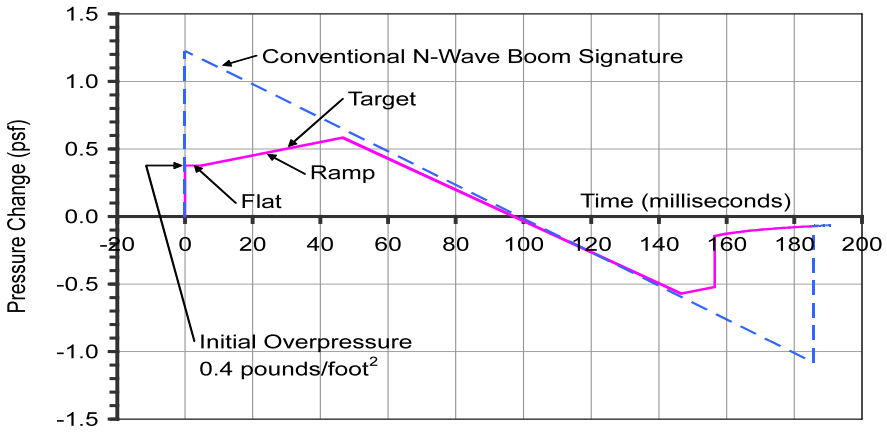

Figure 10-66. Example of the sonic boom N-wave and design to reduce the overpressure.[103]

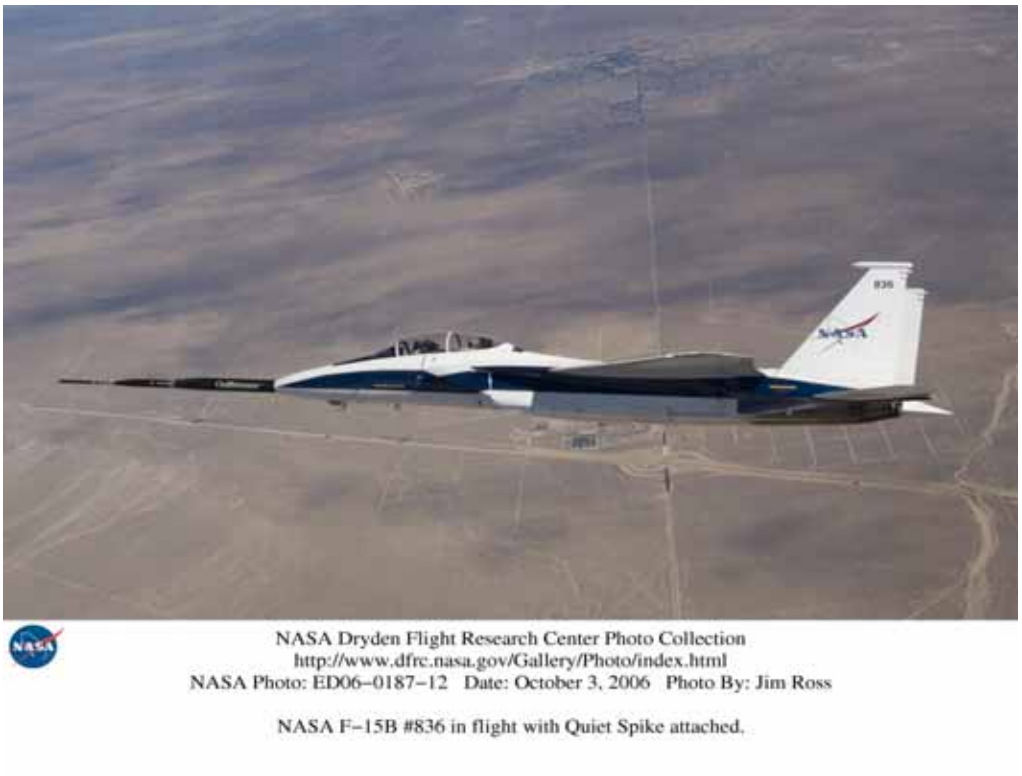

Figure 10-67. The "Quiet-Spike" concept to reduce the strength of the sonic boom. (NASA Photo)

10.10.5 Modern Efforts

In this section we describe two current projects that may lead to new supersonic airplanes. After having tried to pursue a large commercial transport without success, the future appears to be in more modest designs to be used as executive jets. One has been underway for a number of years, and the other is a new NASA effort. Both are much smaller than the HSCT discussed above. The NASA design has the purpose of demonstrating a supersonic airplane with a low sonic boom strength. Hopefully the NASA work will establish the basis for relaxing the restriction on supersonic flight over land in the US.

10.10.5.1 Aerion

The Aerion Corporation has been working on a small supersonic airplane design for a number of years. During that time the design has evolved. Figure 10-68 shows the current concept. It is now a three-engine design. Nominally they expect to be able to have a boomless cruise at Mach 1.1 – 1.2, with a long range cruise Mach number of 1.4. They have an eight-place cabin design and expect to operate at runways from 6,000 to 7,500 feet depending on the weight. The range is expected to be 7,500 nm.

The Aerion concept depends on a fundamental property of fluid mechanics. Note the essentially unswept wing. The concept arose from the idea that for an unswept wing at supersonic speed the the pressure distribution on the wing falls continuously from the leading edge to the trailing edge. This means that the pressure gradient is favorable over the entire wing and for a modest Reynolds number the flow should be laminar. The resulting low skin friction drag is an enabling technology. Here we have an example where two-dimensional supersonic airfoil theory is useful.[105]

Figure 10-68 The Aerion AS2 (from the Aerion website)

10.10.5.1.1 2D: The Supersonic Airfoil Story

Supersonic airfoil theory has not been particularly useful in the swept wing concepts discussed above. Now we have a case where supersonic airfoil characteristics can be exploited. We provide an example. Generally the textbooks have students work the diamond airfoil problem. In this section we'll look at a biconvex airfoil. Let's examine the pressure distribution on the 5% thick biconvex airfoil given in Figure 10-69.

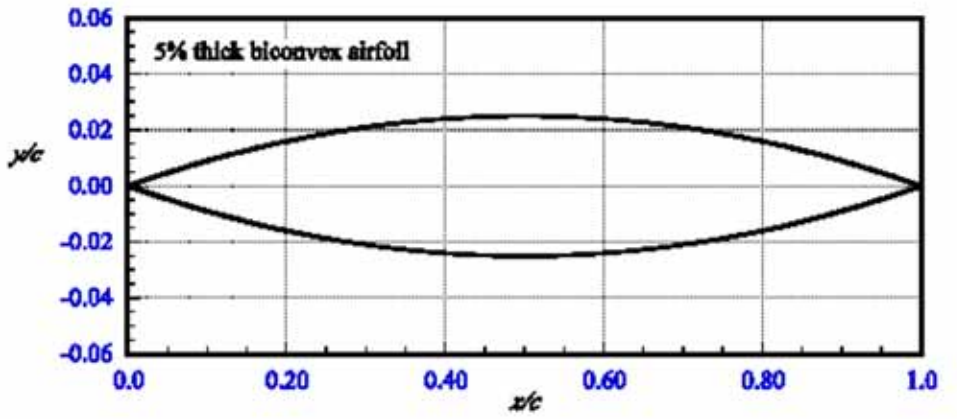

Figure 10-69. A 5% thick biconvex airfoil

The related linear theory pressure distribution is given in Figure 10-70 for a Mach 2 case at 5 degrees angle of attack. Note that the pressures vary linearly so that there is a constant favorable pressure gradient all the way from the leading edge to the trailing edge. And of course since the trailing edge is supersonic the pressures don't need to come together at the trailing edge as they would for a subsonic case.

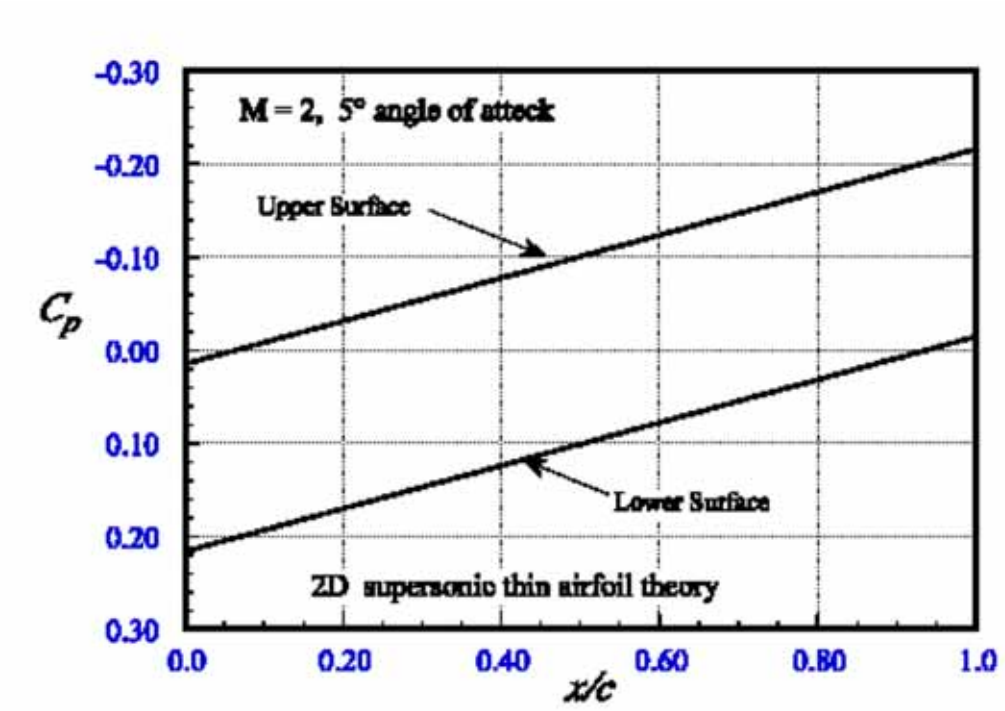

Figure 10-70 Linear theory pressure distributions for the biconvex airfoil shown in Fig. 10-69.

This is the idea behind using the unswept wing on the Aerion. The hope is that without an adverse pressure gradient the wing will achieve a significant amount of natural laminar flow. Once we've started this discussion we use the opportunity to make a few other points.

Although Figure 10-70 shows the idea for the Aerion concept, we are left to wonder how well linear theory agrees with data. Looking at the literature, almost all data used for comparison with airfoils comes from the wind tunnel tests conducted by Antonio Ferri at Guidonia in Italy.[106] Figure 10-71 shows a comparison of the predictions from linear theory, Ferri's wind tunnel data and predictions from second order supersonic airfoil theory. The model was a 10% thick biconvex airfoil at 10 degrees angle of attack and Mach 2.13. This is a fairly thick airfoil at a fairly high angle of attack, so we may be asking too much from linear theory. The second order airfoil theory formulas are available in NACA TN 1428.[107] The figure shows that the second order theory is in generally good agreement with the wind tunnel data, and the idea of a favorable pressure gradient is still essentially valid.

Because first and second order supersonic airfoil theory is relatively simple analytically, numerous studies finding optimum aerodynamic characteristics have been made. We will not repeat them here, but rather refer to an entire book that covers the subject.[108]

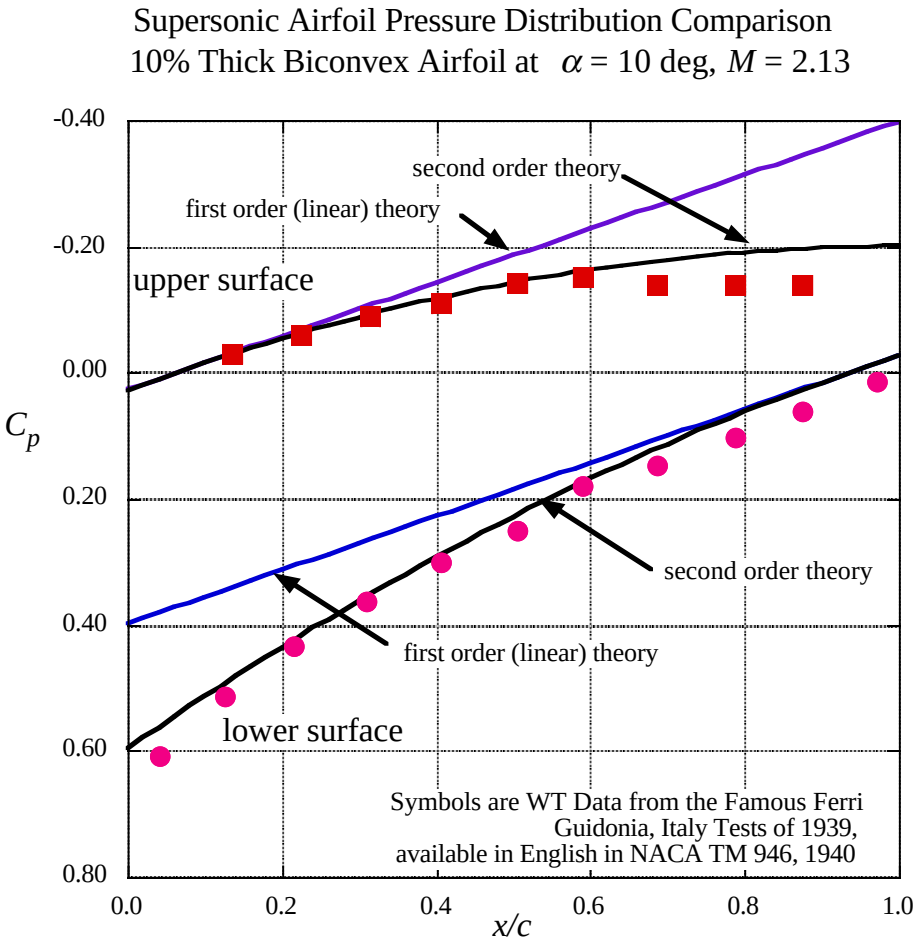

Figure 10-71. Comparison of theoretical airfoil pressure predictions and wind tunnel data.

The other interesting feature of supersonic airfoil theory is the effect of camber. Linear theory only considers the leading and trailing edge values, camber and thickness don't affect lift. This is not true for second order supersonic airfoil theory. For a flat lower surface and a curved upper surface, generally considered positive camber, the lift at zero angle of attack is negative. Figure 10-72 shows this effect for one of the airfoils tested by Ferri. This case is for a one-sided wedge 6.3% thick. Although not a huge effect, it is noticeable. This is particularly interesting in that it explains the F-16 device deflection schedule. At supersonic speed the F-16 automatic device schedule includes leading and trailing edges with a negative deflection, as shown in Figure 10-73. The F-16 has a NACA 64A204 airfoil, and the leading and trailing edges use an automatic -2 degree deflection at supersonic speeds.[109]

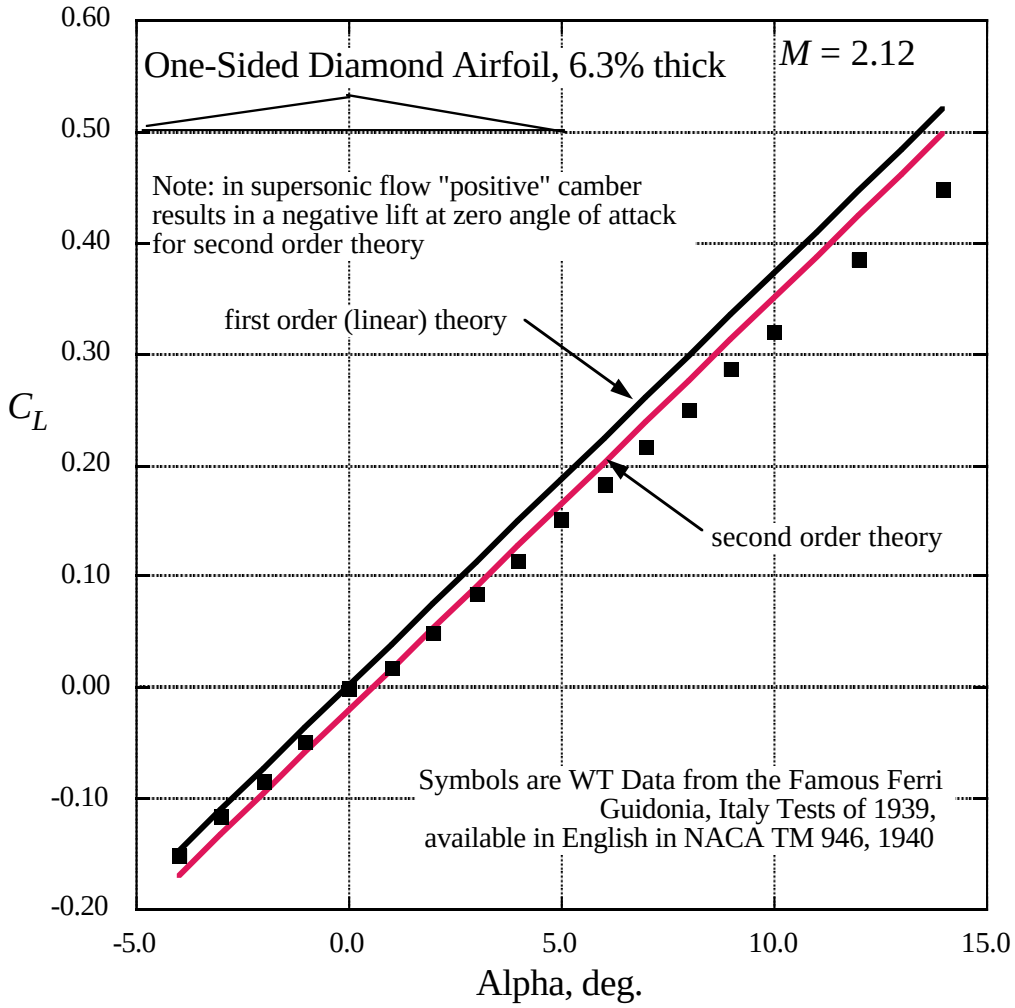

Figure 10-72. Although not large, the effect of camber is clear when considering second order supersonic airfoil theory.

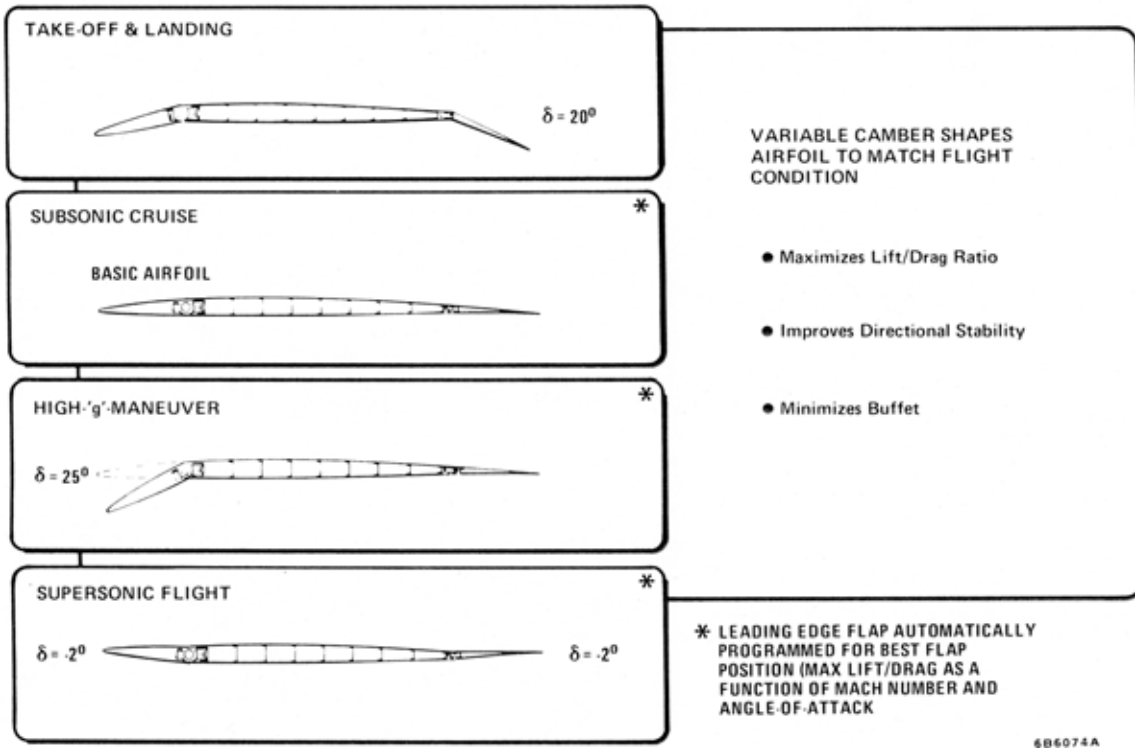

Figure 10-73. The F-16 device schedule.

10.10.5.2 Sonic QueSST

In 2016 NASA started work on a low-boom demonstrator. The Lockheed Martin Skunk Works is doing the design. The project is known as the QueSST. We can expect this design to get an X-plane designation. Figure 10-74 shows the concept.[110] It is a very long lightweight design with a low wing loading (46 psf). The design Mach number is 1.42.

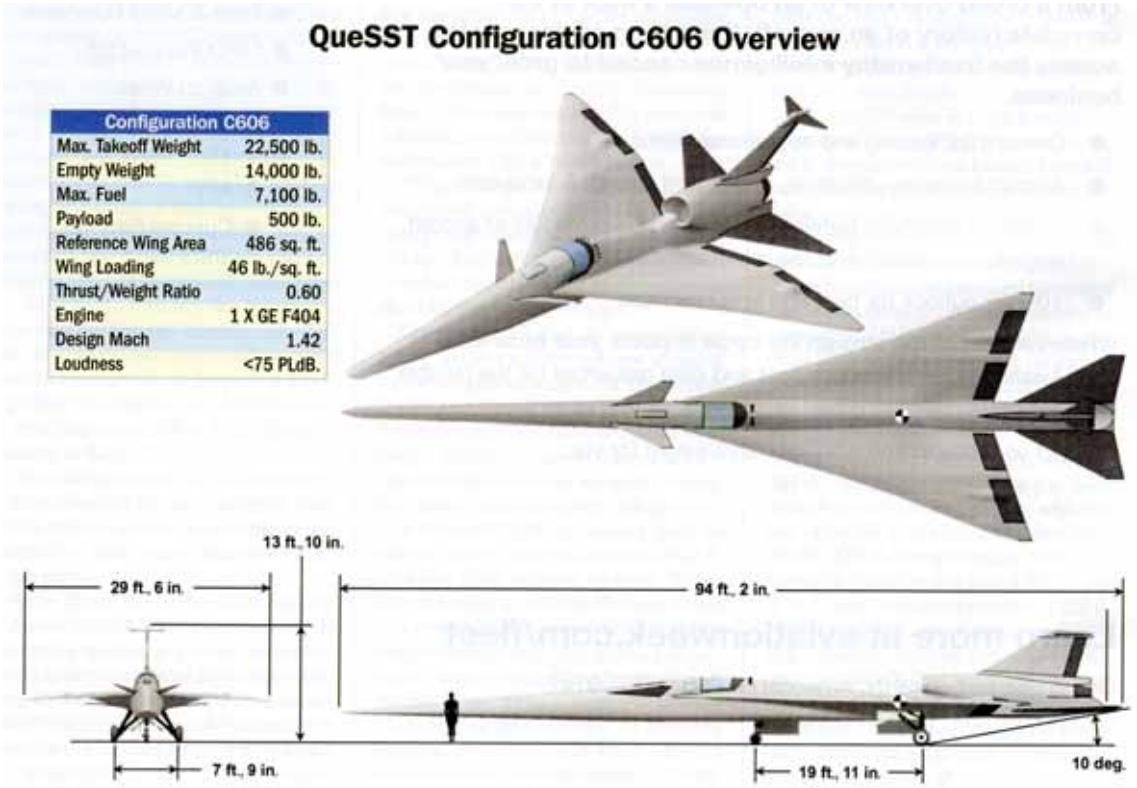

Figure 10-74. QueSST Configuration C606[110]

10.11 Exercises

1. Consider the following airplanes,

    i. the F-22

    ii. the B-58

    iii. the XB-70

    For each airplane at its supersonic cruise Mach number, determine if the leading edge is subsonic or supersonic. Is the trailing edge subsonic or supersonic? Comment on your findings.

2. Build and fly an oblique wing glider.

    Use the plans on the next page as a start. Submit a photo and hopefully a video of your glider in flight.

from *Popular Science*, May 1991, pg 9.

THE OBLIQUE-WING GLIDER: BUILD YOUR OWN

Many readers requested information on building a model oblique flying-wing glider like the one shown in February's "From the Editor" about that month's cover story, "The Next SST." Dr. Robert T. Jones, inventor of the wing concept, drafted these plans.

To make an oblique-wing glider, start with a strip of balsa wood that's one inch wide, 1/16 inch thick, and 8 1/2 inches long. You'll also need some small pieces of 1/32-inch-thick balsa for the end fins. The rear fin should be somewhat larger than that of the forward tip. A tab of 1/16-inch balsa glued to the underside's center serves as a handhold for launching the model. Cyanoacrylate adhesive works best for assembling the parts.

Mark a line on the inch-wide balsa strip 1/4 inch from its leading edge; this is the line of neutral pitch stability. For stability, the glider's center of gravity must be positioned slightly ahead of this line; to do this, you need a nose weight. A short wood stick with a blob of modeling clay at its tip works well. Glue the weight to the center of the wing's underside at an angle of 45 degrees to the leading edge.

To determine the center of gravity, mount a pencil in a vise with its point upward. Carefully move the glider around on the pencil tip until you find the balance point. A gentle downward push marks this point. If necessary, add or subtract clay from the nose weight until the center of gravity is correctly positioned.

Next, trim the glider to counteract its tendency to dive. With sanding block and fine sandpaper, bevel the airfoil section's underside upward, starting about 3/8 inch ahead of the trailing edge. Then use the sanding block to smooth and round the wing's leading edge.

To add curvature to the trailing edge, moisten the balsa wood and bend it upward. Too much curvature will cause stalling or poor gliding performance; too little, and the model will dive. Determine the exact upward curvature by flight tests. A hint for smooth gliding: The oblique wing behaves best when launched with its right-hand, or rearward, wing tip slightly lower than the left one.

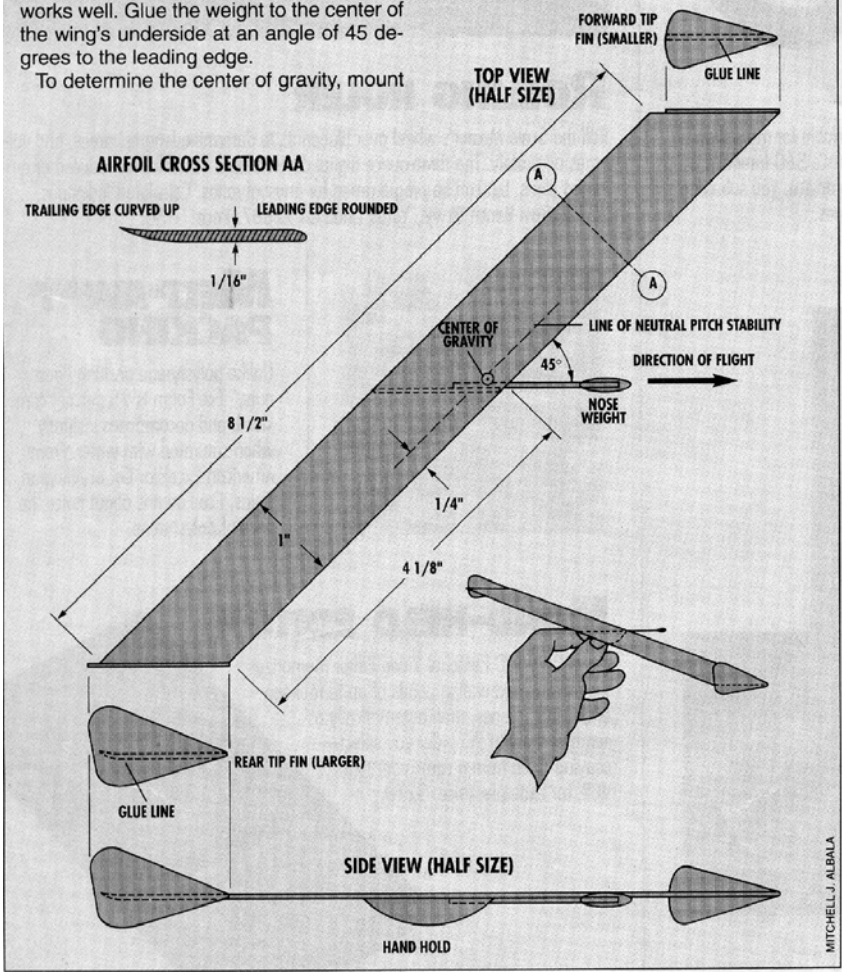

10.12 References

[1] Beryl A. Erickson, "Flight Characteristics of the B58 Mach 2 Bomber," *J. of the Royal Aero. Soc.*, Nov. 1962, Vol. 66, No. 623, pp 665-671.

[2] Ben R. Rich, "F-12 Series Aircraft Aerodynamic and Thermodynamic Design in Retrospect," *Journal of Aircraft*, Vol. 11, No. 7, July 1974, pp. 401-406.

[3] Peter W. Merlin, *From Archangel to Senior Crown: Design and Development of the Blackbird*, AIAA Legacy of Flight Series, 2008.

[4] I. Pike, "B-70: The State of the Art Improver," Part I, 25 June 1964, Part II, 2 July 1964, *Flight International*

[5] Philippe Poisson-Quinton, "First Generation Supersonic Transport," Princeton University Conference Mtg. On the Future of Aeronautical Transportation, Nov. 10-11, 1975.

[6] Jean Rech and Clive S. Leyman, *A Case Study by Aerospatiale and British Aerospace on the Concorde*, AIAA Professional study series.

[7] M. G. Wilde and G. Cormery, "The Aerodynamic Derivation of the Concorde Wing," *Canadian Aeronautics and Space Journal*, May 1970, pp. 175-184.

[8] David C. Aronstein, Michael J. Hirschberg and Albert C. Piccirillo, *Advanced Tactical Fighter to F-22 Raptor: Origins of the 21st Century Air Dominance Fighter*, AIAA, Reston, 1998.

[9] Sherman N. Mullin, "The Evolution of the F-22 Advanced Tactical Fighter," AIAA Paper 1992-4138, Aug. 1992.

[10] Theodore von Karman, "Supersonic Aerodynamics - Principles and Applications," *Journal of the Aeronautical Sciences*, Vol. 14, No 7, July 1947, pp. 373-402.

[11] Leland M. Nicolai, *Fundamentals of Aircraft Design*, METS, 1975. Pg. E-6 (A new edition has been published by the AIAA).

[12] Donald D. Baals, A. Warner Robins and Roy V. Haris, Jr., "Aerodynamic Design Integration of Supersonic Aircraft," *Journal of Aircraft*, Vol. 7, No. 5, Nov-Dec. 1970. pp. 385-394.

[13] Peter G. Coen, Jaroslaw Sobieszczanski-Sobieski, and Samuel M. Dollyhigh, "Preliminary Results from the High-Speed Airframe Integration Research Project," AIAA Paper 1992-1004, Feb. 1992.

[14] J.R. Wilson, "The New Shape of Supersonics," *Aerospace America*, June 2002, pp. 26-33.

[15] David C. Aronstein and Kurt L. Schuler, "Conceptual Design of a Sonic Boom Constrained Supersonic Business Jet," AIAA Paper 2004-0697, Reno, NV, Jan. 2004.

[16] Holt Ashley and Marten Landahl, *Aerodynamics of Wings and Bodies*, Addison-Wesley, Reading, 1965. (now published by Dover)

[17] Eminton, E., and Lord, W.T., "Note on the Numerical Evaluation of the Wave Drag of Smooth Bodies Using Optimum Area Distributions for Minimum Wave Drag," *J. of the Royal Aeronautical Society*, Jan. 1956, pp. 61-63.

[18] Roy V. Haris, Jr., "An Analysis and Correlation of Aircraft Wave Drag," NASA TM X-947, 1964.

[19] Public Domain Aeronautical Software, http://www.pdas.com

[20] M.C. Adams, "Determination of Shapes of Boattail Bodies of Revolution for Minimum Wave Drag," NACA TN 2550, Nov. 1951

[21] Max A. Heaslet and Harvard Lomax, "Supersonic and Transonic Small Perturbation Theory," in *General Theory of High Speed Aerodynamics*, W.R. Sear, Ed., Princeton University Press, Princeton, 1954, pg 240-249.

[22] Keith C. Harder and Conrad Rennemann, Jr., "On Boattail Bodies of Revolution Having Minimum Wave Drag," NACA R 1271, 1956.

[23] N. F. Krasnov, *Aerodynamics of Bodies of Revolution*, American Elsevier Publishing, New York, 1970, pp. pp. 376-378.

[24] W.T. Lord and E. Eminton in "Slender Bodies of Minimum Wave Drag," *Journal of the Aeronautical Sciences*, August, 1954, pages 569-570.

[25] W.H. Mason, Software web Site. http://www.dept.aoe.vt.edu/%7Emason/Mason_f/MRsoft.html

[26] Charles E. Jobe, "Prediction and Verification of Aerodynamic Drag, Part 1: Prediction" in *Thrust and Drag: Its Prediction and Verification*, Eugene E. Covert, Ed., AIAA Progress in Astronaautics and Aeronautics, Vol. 98, AIAA, New York, 1985, pg. 152.

[27] Charles E. Jobe, "Prediction of Aerodynamic Drag," AFWAL-TM-84-203, July 1984, Fig. 23. (available on the web via Google search).

[28] Ana F. Tinetti, Domenic J. Maglieri and Percy J. Bobbitt, "Equivalent Longitudinal Area Distributions of the B-58 and XB-70-1 Airplanes for Use in Wave Drag and Sonic Boom Calculations," NASA/CR-2011-217078, March 2011.

[29] W. Bailey Oswald, "Applied Aerodynamics and Flight Mechanics," *Journal of the Aeronautical Sciences*, Vol. 23, No. 5, May 1956. pp 469-484.

[30] W.H. Mason and J. Lee, "Aerodynamically Blunt and Sharp Bodies," *Journal of Spacecraft and Rockets*, Vol. 31, No. 3, May-June 1994, pp. 406-413.

[31] Jack N. Nielsen, "Arrays of Bodies of Revolution for Minimum Wave Drag," *Journal of Aircraft*, Vol. 22, No. 10, October 1985, pp. 901-909.

[32] Morris D. Friedman, "Arrangement of Bodies of Revolution in Supersonic Flow to Reduce Wave Drag," NACA RM A51I20, 1961.

[33] R. M. Kulfan, "Application of Hypersonic Favorable Interference Concepts to Supersonic Aircraft," AIAA Paper 1978-1458, August 1978.

[34] Dietrich Kuchemann, *The Aerodynamic Design of Aircraft*, Pergamon Press, Oxford, 1978 (now reissued from the AIAA) pages 352 and 420.

[35] Robert T. Jones and Doris Cohen, *High Speed Wing Theory*, Princeton Aeronautical Paperbacks, Princeton, 1960.

[36] Wei-Lin Li and Eli Livne, "Design-Oriented Leading-Edge Thrust Force Prediction for Supersonic Lifting Surfaces," *Journal of Aircraft*, Vol. 34, No. 4, July-Aug. 1997, pp. 457-464.

[37] John W. Boyd, Eugene Migotsky, and Benton E. Wetzel, "A Study of Conical Camber for Triangular and Sweptback Wings," NACA A55G19, Nov. 1955.

[38] Theodore von Kármán, "Some Significant Developments in Aerodynamics Since 1946," *Journal of the Aero/Space Sciences*, Vol. 26, No. 3, March, 1959 pp. 129-144,154.

[39] B.R. Wright, F. Bruckman and N.A. Radovcich, "Arrow Wings for Supersonic Cruise Aircraft," *Journal of Aircraft*, Vol. 15, No12, Dec. 1978. pp. 829-836

[40] Alex Benoliel and W.H. Mason, "Pitch-Up Characteristics for HSCT Class Planforms: Survey and Estimation," AIAA Paper 94-1819, June 20-23, 1994.

[41] Courtesy of British Aerospace Corporation.

[42] John E. Lamar and William J. Alford, Jr., "Aerodynamic-Center Considerations of Wings and Wing-Body Combinations," Conference on Aircraft Aerodynamics, NASA SP-124, May 1966.

[43] Daniel P. Raymer, *Aircraft Design: A Conceptual Approach*, 4th Ed., AIAA, Reston, 2006. pg. 667.

[44] Robert W. Kress, "Variable Sweep Wing Design," AIAA Paper 80-3043.

[45] Edward C. Polhamus and Thomas A. Toll, "Rsearch Related to Variable Sweep Aircraft Development," NASA TM 83121, 1981.

[46] Robert T. Jones, "New Design Goals and a New Shape for the SST," *Astronautics & Aeronautics*, Vol. 10, Dec. 1972, pp. 66-70.

[47] Robert T. Jones and James W. Nisbet, "Transonic Transport Wings-Oblique or Swept?" *Astronautics and Aeronautics*, Jan. 1974, pp. 40-47.

[48] Robert T. Jones, *Wing Theory*, Princeton University Press, Princeton, 1990.

[49] Pei Li, Richard Seebass and Helmut Sobieczky, "Oblique flying wing aerodynamics," AIAA Paper 1996-2120, June 1996. (includes a good reference list to other work)

[50] J. B. Crittenden, T.A. Weisshaar, E.H. Johnson and M.J. Rutkowski, "Aeroelastic Stability Characteristics of an Oblique-Wing Aircraft," *Journal of Aircraft*, Vo. 15, No. 7, July 1978, pp. 429-434.

[51] T. C. McMurtry, A.G. Sim and W.H. Andrews, "AD-1 oblique wing research program," AIAA Paper 1981-2354, Nov. 1981.

[52] Robert E. Curry and Alex G. Sim, "Unique flight characteristics of the AD-1 oblique-wing research airplane," *Journal of Aircraft*, Vol. 20. No. 6, June 1983, pp. 564-568.

[53] Alexander J. M. Van der Velden, "The Conceptual Design of a Mach 2 Oblique Flying Wing Supersonic Transport," NASA CR 177529, May 1989.

[54] Tom Galloway, Paul Gelhausen and Mark Moore, "Oblique Wing Supersonic Transport," AIAA Paper 92-4230, Aug. 1992.

[55] Michael J. Herschberg, David M. Hart and Thomas J. Beutner, "A Survey of a Half-Century of Oblique Wing Research," AIAA Paper 2007-0150, Jan. 2007.

[56] Susan E. Cliff, Scott D. Thomas and Veronica M. Hawke, "Swing-Wing Inline-Fuselage Transport Design Studies at Supersonic Flight Conditions," AIAA Paper 2009-7073, Sept. 2009.

[57] Armand Sigalla and Thomas H. Hallstaff, "Aerodynamics of Powerplant Installation on Supersonic Aircraft," *Journal of Aircraft*, Vol. 4, No. 4, July-August 1967, pp. 273-277.

[58] David L. Rodriguez, "Propulsion/Airframe Integration and Optimization on a Supersonic Business Jet," AIAA Paper 2007-1048, Jan. 2007.

[59] Russell M. Cummings, William H. Mason, Scott A. Morton and David R. McDaniel, *Applied Computational Aerodynamics: A Modern Engineering Approach*, Cambridge University Press, 2015.

[60] Charlotte B. Craidon, "Description of a Digital Computer Program for Airplane Configuration Plots," NASA TM X-2074, Sept. 1970.

[61] Roy V. Harris and Emma Jean Landrum, "Drag Characteristics of a Series of Low-Drag Bodies of Revolution at Mach Numbers from 0.6 to 4.0," NASA TN D-3163, December 1965,

[62] William D. McGrory, David C. Slack, Michael P. Applebaum and Robert W. Walters, *GASP Version 2.2 Users Manual*, Aerosoft, Inc., 1993.

[63] Duane L. Knill, Vladimir Balabanov, Oleg Golovidov, Bernard Grossman, William H. Mason, Raphael T. Haftka and Layne T. Watson, "Accuracy of Aerodynamic Predictions and Its Effects on Supersonic Transport Design," MAD Center Report 96-12-01, December 1996. Available on http://www.dept.aoe.vt.edu/%7Emason/Mason_f/MRNR96.html

[64] J. Weber and C. King, "Analysis of the Zero-Lift Wave Drag Measured on Delta Wings," Aeronautical Research Council Reports and Memoranda No. 3818, 1978.

[65] Raymond L. Barger, M. S. Adams and R. R. Krishnan, "Automatic Computation of Euler-Marching and Subsonic Grids for a Wing-Fuselage Configuration," NASA TM 4573, July 1994.

[66] Raymond L. Barger and Mary S. Adams, "Automatic Computation of Wing-Fuselage Intersection Lines and Fillet Inserts with Fixed-Area Constraints," NASA TM 4406, March 1993.

[67] J. P. Gapcynski and Emma Jean Landrum, "Tabulated Data from a Pressure Distribution Investigation at Mach Number 2.01 of a 45 Deg Sweptback Wing Airplane Model at Combined Angles of Attack and Sideslip," NASA-MEMO-10-15-58L, Nov. 1958.

[68] Frank A. Woodward, "An Improved Method for the Aerodynamic Analysis of Wing-Body-Tail Configurations in Subsonic and Supersonic Flow," Part I – Theory and Application, NASA CR-2228 Part 1, May 1973.

[69] Wilbur D. Middleton and Jerry L. Lundry, "A System for Aerodynamic Design and Analysis of Supersonic Aircraft," Part 1 – General Description and Theoretical Development, NASA CR-3351, Part 2 – User's Manual, NASA CR 3352, Part 3 – Computer Program Description, NASA CR-3353, Part 4 – Test Cases, NASA CR-3354, December 1980.

[70] Ralph L. Carmichael and Frank A. Woodward, "An Integrated Approach to the Analysis and Design of Wings and Wing-Body Combinations in Supersonic Flow," NASA TN D-3685, Oct. 1966.

[71] W.H. Mason and B.S. Rosen, "The COREL and W12SC3 Computer Programs for Supersonic Wing Design and Analysis," NASA CR-3676, December 1983.

[72] Warner Robins, Odell A. Morris, and Roy Harris, Jr., "Recent Research Results in the Aerodynamics of Supersonic Vehicles," *Journal of Aircraft*, Vol. 3, No. 6, Nov-Dec. 1966. pp. 573-577.

[73] Robert M. Kulfan and Armand Sigalla, "Real Flow Limitations in Supersonic Wing Design," *Journal of Aircraft*, Vol. 16, No. 10, October 1979, pp. 645-658.

[74] Harry W. Carlson and Michael J. Mann, "Survey and Analysis of Research on Supersonic Drag-Due-to-Lift Minimization With Recommendations for Wing Design," NASA TP 3202, September 1992.

[75] Harry W. Carlson, Marcus O. McElroy, Wendy B. Lessard and L. Arnold McCullers, "Improved Method for Prediction of Attainable Wing Leading-Edge Thrust," NASA TP 3557, April 1996.

[76] Harry W. Carlson, Julio Chu, Lori Ozoroski, and L. Arnold McCullers, "Guide to AERO2S and WINGDES Computer Codes for Prediction and Minimization of Drag," NASA TP 3637, Nov. 1997.

[77] B. Grossman, "Numerical Procedure for the Computation of Irrotational Conical Flows," *AIAA J*., Vol. 17, No. 9, Aug. 1979. pp. 828-837.

[78] W.H. Mason, "SC3 — A Wing Concept for Supersonic Maneuvering," AIAA Paper 83-1858, July 1983, see also NASA CR 3763, Dec. 1983.

[79] M.J. Siclari, "The NCOREL Computer Program for 3D Nonlinear Supersonic Potential Flow Computations," NASA CR 3694, Aug. 1983.

[80] Walter C. Swan, "A Review of the Configuration Development of the U.S. Supersonic Transport," 11th Anglo-American Aeronautical Conference, London, Sept., 1969. (included in the AIAA Selected Reprint Series, Vol. VIII, *Jet Transport Design*, John M. Swihart, editor, 1969.

[81] M. Leroy Spearman, "The Evolution of the High-Speed Civil Transport," NASA TM 109089, Feb., 1994

[82] Kumar G. Bhatia and Jin Wertheimer, "Aeroelastic Challenges for a High Speed Civil Transport," AIAA Paper 1993-1478.

[83] Eric M. Conway, *High-Speed Dreams*, "NASA and the Techopolitics of Supersonic Transportation, 1945-1999," The Johns Hopkins Press, Baltimore, 2005.

[84] W. H. Mason and David S. Miller, "Controlled Supercritical Cross-Flow on Supersonic Wings-An Experimental Validation," AIAA Paper 1980-1421, July 1980.

[85] Antonio Ferri, *Elements of Aerodynamics of Supersonic Flow*, The Macmillan Company, New York, 1949, pg. 237, eqn. 446.

[86] Clinton E. Brown, F. E. McLean and E. B. Klunker, "Theoretical and Experimental Studies of Cambered and Twisted Wings Optimized for Flight at Supersonic Speeds," Proc. of the 2nd International Congress of Aeronautical Sciences, *Adv. in Aero Sci*., Vol 3, ed T. von Karman, et al, Pergamon Press, Oxford, 1962.

[87] William H. Mason, Michael J. Siclari, David S. Miller and James L. Pittman, "A Supersonic Maneuver Wing Designed for Nonlinear attached Flow," AIAA Paper 1983-0425, Jan. 1983.

[88] A. Warner Robins, Samuel M. Dollyhigh, Fred L. Beissner, Jr., Karl Geiselhart, Glenn L. Martin, E.W. Shields, E.E. Swanson, Peter G. Coen, and Shelby J. Morris, Jr., "Concept Development of a Mach 3.0 High-Speed Civil Transport," NASA TM 4058, September 1988.

[89] Gloria Hernandez, Peter F. Covell, and Marvin E. McGraw, Jr., "An Experimental Investigation of a Mach 3.0 High-Speed Civil Transport at Supersonic Speeds," NASA TP 3365, November 1993.

[90] Boeing Commercial Airplanes, "High-Speed Civil Transport Study," NASA CR 4233, 1989.

[91] Douglas Aircraft Company, "Study of High-Speed Civil Transports," NASA CR 4235, December 1989.

[92] J. K. Ray, C. M. Carlin and A.A. Lambregts, "High-Speed Civil Transport Flight- and Propulsion Control Technological Issues," NASA CR 186015, March 1992 (Boeing)

[93] Craig A. McCarty, John B. Feather, John R. Dykman, Mark A. Page and John Hodgkinson, "Design and Analysis Issues of Integrated Control Systems for High-Speed Civil Transports," NASA CR 186022, May 1992. (Douglas)

[94] Guy T. Kemmerly, Bryan A. Campbell, David W. Banks and Steven F. Yaros, "Low-Speed Stability-and-Control and Ground-Effects Measurements on the Industry Reference High Speed Civil Transport," NASA /TM-1999-209702, December 1999.

[95] Raphael Haftka, Bernard Grossman and William Mason, "Multidisciplianry Optimization via Intelligent Response Surface Methodology," MAD Center White Paper No. 1, Sept. 1995.

[96] Chuck A. Baker, Bernard Grossman, Raphael T. Haftka, William H. Mason and Layne T. Watson, "High-Speed Civil Transport Design Space exploration Using Aerodynamic Response Surface Approximation," *Journal of Aircraft*, Vol. 39, No. 2, March-April 2002, pp. 215-220.

[97] Knill, D.L., Giunta, A.A., Baker, C.A., Grossman, B., Mason, W.H., Haftka, R.T. and Watson, L.T., "Response Surface Models Combining Linear and Euler Aerodynamics for Supersonic Transport Design," *Journal of Aircraft*, Vol. 36, No. 1, Jan-Feb 1999, pp. 75-86.

[98] Susan E. Cliff, James J. Reuther, David A. Saunders and Raymond M. Hicks, "Single-Point and Multipoint Aerodynamic Shape Optimization of High Speed Civil Transport," *Journal of Aircraft*, Vol. 38, No. 6, Nov-Dec 2001, pp. 997-1005.

[99] Seongim Choi, Juan J. Alonso and Ilan M. Kroo, "Two-Level Multifidelity Design Optimization Studies for Supersonic Jets," *Journal of Aircraft*, Vol. 46, No. 3, May-June 2009, pp. 776-790.

[100] Kathy Barnstorff, Jan Walker and Jim Hart, "NASA Opens New Chapter in Supersonic Flight," NASA News Release No. 03-060, Sept. 4, 2003.

[101] Wu Li and Sriram Rallabhandi, "Inverse Design of Low-Boom Supersonic Concepts Using Reversed Equivalent-Area Targets," *Journal of Aircraft*, Vol. 51, No. 1, Jan-Feb 2014, pp. 29-36.

[102] Sriram K. Rallabhandi, Eric J. Nielsen and Boris Diskin, "Sonic-Boom Mitigation Through Aircraft Design and Adjoint Technology," *Journal of Aircraft*, Vol. 51, No. 2, March-April 2014, pp, 502-510.

[103] David C. Aronstein and Kurt L. Schueler, "Conceptual Design of a Sonic Boom Constrained Supersonic Business Aircraft" AIAA Paper 2004-0697.

[104] Robbie Cowart and Tom Grindle, "An Overview of the Gulfstream/NASA Quiet Spike™ Flight Test Program," AIAA Paper 2008-0123, Jan. 2008.

[105] Peter Sturdza, "Extensive Supersonic Natural Laminar Flow on the Aerion Business Jet," AIAA Paper 2007-0685, Jan. 2007.

[106] Antonio Ferri, "Experimental Results with Airfoils Tested in the High-Speed Tunnel at Guidonia," NACA TM 946, July 1940.

[107] The Staff of the Ames 1- by 3-foot Supersonic Wind –Tunnel Section, "Notes and Tables for Use in the Analysis of Supersonic Flow," NACA TN 1428, Dec. 1947.

[108] Angelo Miele, Ed., *Theory of Optimum Aerodynamic Shapes*, Academic Press, New York, 1965.

[109] Carl S. Droste and James E. Walker, *The General Dynamics Case Study on the F-16 Fly-by-Wire Flight Control System*, AIAA Professional study series.
[110] Guy Norris, "Sonic QueSST," *Aviation Week and Space Technology*, June-20-July 3, 2016.pg. 38.